

Luigi Privitera

ON THE CONTRIBUTION OF
HIGH-FREQUENCY INPUTS TO THE
MUSCLES IN FORCE CONTROL



POLITECNICO
MILANO 1863

POLITECNICO DI MILANO

April 2021

POLITECNICO DI MILANO
Master of Science in Biomedical Engineering
Department Of Electronics, Information and Bioengineering



POLITECNICO
MILANO 1863

On the contribution of high-frequency inputs to the muscles in force control

In collaboration with the Faculty of Engineering - Department of
Bioengineering of the Imperial College London

Supervisor: Ing. Alessandra Laura Giulia PEDROCCHII

Co-supervisor: Dr. Jaime IBANEZ PEREDA

Co-supervisor: PhD Blanka ZICHER

Candidate: Luigi PRIVITERA

Identification number: 883877

Academic Year 2020-2021

Contents

Abstract	vii
Extended abstract	ix
0.1 Introduction	ix
0.2 Notes on anatomy	x
0.2.1 Motor Neurons	x
0.3 Proprioceptors	xii
0.4 Mathematical model of the neuromuscular system	xvi
0.4.1 Afferent run	xx
0.4.2 Tests run with the mdoels	xxv
0.4.3 Descending run model	xxv
0.4.4 Spindle model	xxv
0.4.5 Control cycle structure	xxv
0.5 Results	xxix
0.5.1 Descending model	xxix
0.5.2 Full spindle model results	xxx
0.5.3 Simplified spindle model results	xxx
0.5.4 Results of the simplified afferent feed-back model tests	xxxii
Introduction	xxxv
1 The movement	1
1.1 Organization of the movement	2
1.2 The motor program	2
1.3 Properties of the Motor Control system	3
1.4 Motor control models	4

1.4.1	Feed-forward Control	5
1.4.2	Feed-back Control	6
1.4.3	Feedback control with feedforward	6
2	Notes on anatomy	11
2.1	Structure of the nervous system	11
2.2	Central Nervous System	12
2.2.1	Cerebral cortex	12
2.2.2	Cortical organization of movement	13
2.2.3	Cerebellum	15
2.2.4	Spinal cord	16
2.3	Periferal Nervous System	16
2.3.1	Spinal nerves	17
2.4	Peripheral organization of movement	17
2.4.1	Motor Neurons	17
2.4.2	The motor units	18
3	Proprioceptors	23
3.1	Muscle spindle	24
3.1.1	Structure	24
3.1.2	Spindle Physiology	27
3.1.3	Spindle dynamics	29
3.2	Golgi Tendon Organ	31
3.3	Spindle reaction to contraction	31
4	Mathematical model of the neuromuscular system	33
4.1	Descending run model	34
4.2	Afferent run	43
4.2.1	Feed-back response	43
4.2.2	Full afferent model	45
4.2.3	Simplified mathematical model	53
4.3	Tests run with the mdoels	56
4.3.1	Descending run model	57
4.3.2	Spindle model	57
4.3.3	Control cycle structure	57

4.3.4	PID	59
4.3.5	Tuning	60
5	Results	63
5.1	Descending model	63
5.2	Afferent model analysis	67
5.2.1	Full spindle model results	67
5.2.2	Simplified spindle model results	70
5.3	Results of the simplified afferent feed-back model tests . . .	74
5.4	Conclusions	77
A	Appendix A	79
A.1	Motor neurons parameters	79
A.1.1	S-type	79
A.1.2	FR-type	80
A.1.3	FF-type	80
A.2	Afferent fibers parameters	81
A.2.1	Ia-type	81
A.2.2	II-type	81
A.2.3	Ib-type	82
A.3	Interneurons parameters	82
A.3.1	IIIN-type	82
A.3.2	IbIN-type	83
A.4	PID Ks paramters	83
A.4.1	Descending model	83
A.4.2	Full afferent model	83
A.4.3	Simplified afferent model	84
A.5	PSO parameters	84

List of Figures

1	Spindle	xv
2	GTO	xv
3	Descending run model	xvii
4	Spindle structure	xxii
5	Spindle behavior	xxii
6	Full model	xxiii
7	Simplified model	xxiv
8	Control cycle	xxvii
9	Descending model test results	xxix
10	Full spindle model afferent feed-back	xxxii
11	Simplified model afferent feed-back	xxxii
12	Simplified afferent feed-back model test results at 0Hz xxxiii	xxxiii
1.1	Feed-forward Control	6
1.2	Feed-back Control	7
1.3	Feed-back control with feed-forward	8
3.1	Structure of the muscle spindle	25
3.2	Muscle spindle - comparison between fibers Ia and II dynamics	27
3.3	Muscle spindle - comparison between fibers Ia and II dynamics	28
3.4	Muscle spindle - comparison between fibers Ia and II dynamics	30
3.5	Spindle reaction	32
3.6	GTO structure and reaction	32
4.1	Descending run model	37
4.2	DENDRITE	41

4.3	SOMA	41
4.4	Afferent run	42
4.5	Spindle structure	44
4.6	Spindle behavior	44
4.7	Simplified model	52
4.8	Control cycle	58
5.1	Average model error when no afferent inputs are used	64
5.2	Descending model test results	66
5.3	Full spindle model behavior	68
5.4	Full spindle model behavior	71
5.5	Full spindle model afferent feed-back	73
5.6	Simplified model afferent feed-back	73
5.7	Simplified afferent feed-back model test results at 0Hz	75
5.8	Simplified afferent feed-back model test results at 0Hz	76
5.9	Simplified afferent feed-back model test results with diffeent force traces	78

Abstract

Oscillations in the beta and gamma bands ($13\text{--}30\text{Hz}$; $37\text{--}70\text{Hz}$) have often been observed in motor cortical outputs that reach the spinal cord, acting on motor neurons and interneurons.

However, the frequencies of these oscillations are above the frequency range of muscle strength: the muscles in fact behave similar to low pass filters which are supposed to cut inputs with frequencies higher than 10 Hz.

The common view was that the transformation of the motoneuron pool inputs into force is linear, for this reason possible roles for these oscillations are unclear, since if this transformation is linear, the high frequencies in the motoneuron inputs (e.g., 20 Hz from pyramidal tract neurons) would be filtered out by the muscle and have no effect on force control.

Recent studies have demonstrated that a typical motor neuron pool has a non-linear behavior that enables the modulation of a high-frequency oscillatory input, suggesting a potential role in force control for cortical oscillations at frequencies at or above the beta band.

In this study, a mathematical model biologically inspired by the neuromuscular system was created.

The goal is to study how afferent inputs can change our interpretations regarding the controllability of muscle contractions, comparing the generation of force when high-frequency signals are input versus when signals are in the 0-5Hz band.

Extended abstract

0.1 Introduction

Oscillations in the beta and gamma bands ($13\text{--}30\text{Hz}$; $37\text{--}70\text{Hz}$) have often been observed in motor cortical outputs that reach the spinal cord, acting on motor neurons and interneurons.

How they are involved in controlling muscle contractions is still a mystery: muscles behave similarly to low-pass filters and should filter out high-frequency signals from higher systems. In recent years, however, research has gained strong momentum in this field.

In this study, a mathematical model biologically inspired by the neuromuscular system was created and two different representative models of the afferent system were connected to it:

- The first is a complete model that tries to be as realistic as possible in its structure, simulating the activity of the muscle spindle and the GTO, and of all the nerve connections and synapses that bring the signal back to the spine;
- The second model, on the other hand, is a simplified model of the first, which reduces the realism of the first model to mathematical formulas that are in any case able to represent the afferent system.

In this still open field of study, other studies have been carried out on the analysis of the contribution of high frequencies in muscle contraction, but few have implemented the afferents represented by the proprioceptive organs and even fewer have tried to implement a model for these so complex organs. With this thesis, we wanted to try to implement a model capable of closing

the control loop, comparing a more realistic model against a simpler and more generalized one.

0.2 Notes on anatomy

0.2.1 Motor Neurons

The neuron is the elemental nerve cell and together with the ganglia forms the basis of the nervous system.

A neuron is made up of *Dendrites*, *Soma* (central unit) and the *Axon and axonic arborescence* (system output). There are many studies done on neurons, in this thesis, the *Hodgkin and Huxley model (HH model)* will be used for the modeling of nerve fibers.

Motor neurons are particular types of neurons that arise from the anterior horns of the spinal cord.

The motor axon then enters the muscle and branches out into unmyelinated branches establishing numerous synaptic contacts. Each muscle fiber comes into contact with only one axon while a single axon innervates several muscle fibers.

The complex formed by the axon and the muscle fibers that it innervates constitutes a *motor unit*.

The motor units

A motor unit is made up of a group of fibers innervated by the *motor neuron* itself and therefore constitutes the functional unit of skeletal muscles.

There are three types of motor units depending on the muscle fibers of which they are composed: type *I (SO)*, type *IIA (FOG)* and type *IIB (FG)*.

The activation of the motor units follows the *Henemann's size principle* and the fibers belonging to the same motor unit obey the law of all or nothing: either they contract to the maximum, or they do not contract at all.

The force that a muscle is able to exert increases in proportion to the number of motor units recruited and the frequency of action potentials.

Muscle fibers

Each fiber is innervated by an axon belonging to a motor neuron which controls the behavior of the fiber itself.

The fiber becomes the seat of electrochemical phenomena as a result of the arrival of a nerve impulse (*spike*) which manifest themselves from a mechanical point of view with the generation of a force impulse (*twitch*).

The force twitch is characterized by three distinct phases:

- **Latency phase:** time between the arrival of the nerve stimulus and the beginning of the contraction phenomenon;
- **Strength Gain phase:** the main contraction phase;
- **Strength Decrease phase:** also called the relaxation phase

Fibers types Depending on the system used and the speed with which energy is made available to the contractile system of the sarcomere, three types of muscle fibers can be classified:

- **Slow Oxidative** fibers (**SO**) called type **I**: they use the aerobic energy system, contract slowly and are able to respond to repeated stimulations for a long time;
- **Fast Glycolic** fibers (**FG**) called type **IIB**: they use the anaerobic glycolytic system, contract very quickly but are unable to repeat the same force twitch for long times, they provide the so-called "*explosive power*";
- **Fast Oxidative-Glycolic** fibers (**FOG**) called type **IIA**: they utilize both aerobic and anaerobic energy systems, they contract quickly and can maintain the contraction for relatively long periods of time.

Recruitment and Contraction

Contraction When the same fiber is repeatedly stimulated, there is a temporal summation effect of the force twitches which can lead to the so-called "*fusion*", a situation in which the individual twitches are no longer distinguishable.

Given the different speeds with which the force twitch is generated in the two types of fibers (slow and fast), the frequency at which this phenomenon occurs (*fusion frequency*), is low for slow fibers, and high for fast fibers.

Henneman Recruiting Principle The value of force above which a certain type of motor unit is called into action is called "*recruitment threshold*", the initial frequency at which the motor unit begins to be activated is called "*recruitment frequency*".

As muscle strength increases, the frequency of each motor unit increases to a maximum characteristic of the same MU and new MUs are recruited starting from the smallest to the largest. This criterion never seems to have been contradicted by experimental evidence, and goes by the name of ***Henemann's size principle***.

0.3 Proprioceptors

Proprioception (or kinaesthesia) the sense of static position and movement of the limbs and body.

It is made possible by the presence of specific receptors, called proprioceptive or kinesthetic receptors, sensitive to changes in body postures and body segments.

In this thesis the main ones will be examined:

- Muscle spindles: it responds to the speed and different length of muscle fibers;
- Golgi tendon organs: it is placed at the muscle-tendon junction and it is sensitive to variations in tension.

Muscle spindle

The muscle spindle is inserted into the muscle in parallel to the muscle fibers; from this position it is stressed to lengthen or shorten according to the movement made by the extrafusal fibers, therefore being able to produce information related to the length or variation in length of the muscle fibers. The information thus generated will be conveyed by the afferent fibers to

the spinal level where, through neuronic connections in the spinal cord, they will be transported to the competent areas of the brain.

There is also an efferent system, the purpose of which is to vary the sensitivity or the intervention threshold of the spindle, modifying its behavioral characteristics, automatically or depending on voluntary orders.

Structure It is essentially a bundle of fibers wrapped in a sheath that has a central swelling (capsule) and contains interstitial fluid.

This bundle consists of three types of intrafusal muscle fibers:

- **Nuclear Bag fibers (NB)**, usually divided in 1 bag1 and 1 bag2: they are divided into a central "non-contractile" area called the "nuclear bag", and the external "polar" regions, which are contractile in a similar way to the extrafusal fibers of the muscle;
- **Nuclear Chain fibers (NC)**, ranging from 4 to 11 fibers: nuclei and myofibrils are distributed throughout their length making them more uniform in terms of elasticity.

Innervation The system consisting of muscle and spindles is innervated by two types of nerve fibers: afferent fibers (**afferents**) and efferent fibers (**efferents**).

The **afferents** are divided according to their diameter into fibers of type I, II, III:

- Type I come from both the spindle (Ia) and the Golgi tendon organ (Ib);
- Type II come only from the spindle;
- Type III originate from other receptors, cutaneous and articular.

The **efferences** that reach the spindle are also divided into two large categories:

- Alpha: they innervate the muscle directly (also called "extrafusal" muscle fibers);

- Gamma: they innervate the spindle inside the muscle (also called "intrafusal" fibers).

The efferences innervating the spindle are the gamma efferences (γ). Also in this case they can be divided into two categories according to their diameter and precisely in $\gamma_{Dynamic}$ and γ_{Static} .

Spindle Physiology The numerous physiological experiments on the neuromuscular spindle mainly concern its response to both mechanical (stretching) and nervous (stimulation of the efference) external stimuli.

The output of the spindle consists of a series of impulses (spikes) on the primary and secondary afferents and as a response the trend of the impulses (spikes) generated by the spindle and recorded on the afferents is considered significant.

The typical behavior of the Ia response to an elongation ramp can be schematized as follows:

- **Dynamic index:** the difference between the firing frequency at the end of the ramp and that at which it settles in steady state;
- **Static sensitivity:** the ratio between the frequency variations before and after the elongation and the elongation itself;
- **Dynamic sensitivity:** the relationship between the dynamic index and the elongation speed
- **Polarization:** the initial frequency.

It can therefore be concluded that qualitatively the fibers γ_D influence the response of Ia to elongation, such as to enhance the dynamic characteristics (depending on the elongation speed), while they have no influence on the static ones (depending on the elongation).

The γ_S fibers, on the other hand, have a depressing effect on the sensitivity to the stretching speed, but exhilarating on the sensitivity to the stretch.

On the other hand, studying the influence of stimulation γ on afferent fibers II, it is noted that the γ_S have an effect similar to that which they have on Ia, while the γ_D have absolutely no effect.

Golgi Tendon Organ

Given the arrangement in series with the muscle fibers, in the muscle-tendon junction, the Golgi Tendon Organ (GTO) is subjected to a portion of the force generated by the entire muscle, and can therefore detect its extent. The afferent fibers Ib encode the force applied to the muscle in firing frequency, and have an inhibitory effect on the alpha motor neuron, especially in the presence of high forces. It therefore has a protective function for the muscle.

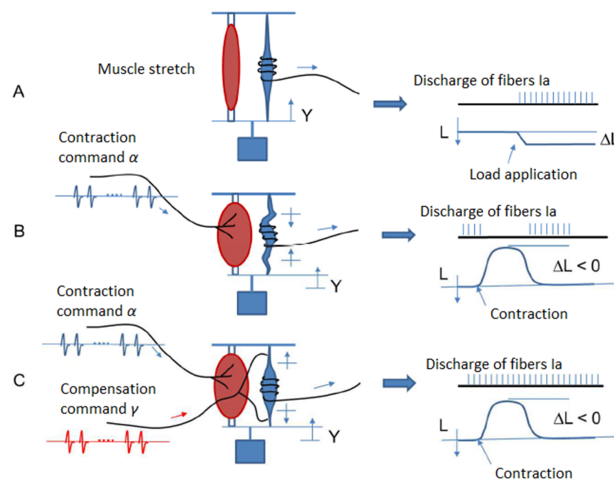


Fig. 1. Spindle

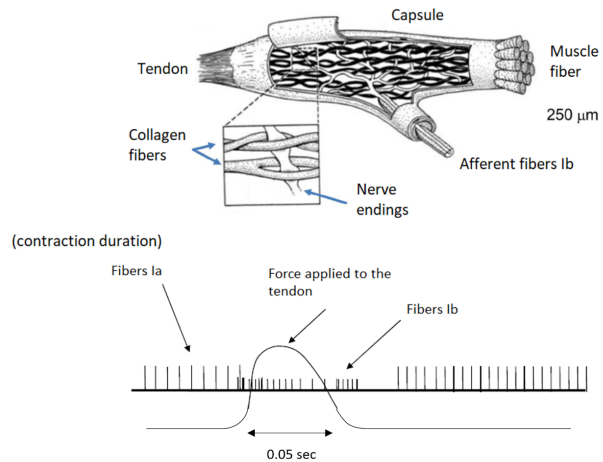


Fig. 2. GTO

0.4 Mathematical model of the neuromuscular system

The objective of the proposed model, consisting of a mathematical model biologically inspired by the neuromuscular system and a representative model of the afferent system, is to:

- Simulate the behavior of motor neurons in the presence of a command from higher levels expressed as a high frequency signal and study if the modulation of certain types of inputs to the MNs can be used to control force;
- Simulate the behavior of the proprioceptive organs, in particular the muscle spindle and the Golgi tendon organ (GTO) and how the afferent circuit reports the information of the muscular contraction back to the controller, simulated by a PID;
- How the contribution of the afferent response contributes to the control of the PID on the contraction under consideration.

In order to do so, a mathematical model biologically inspired by the neuromuscular system was created and two different representative models of the afferent system were connected to it:

- The first is a complete model that tries to be as realistic as possible in its structure, simulating the activity of the muscle spindle and the GTO, and of all the nerve connections and synapses that bring the signal back to the spine;
- The second model, on the other hand, is a simplified model of the first, which reduces the realism of the first model to mathematical formulas that are in any case able to represent the afferent system.

The behavior of the models for sinusoidal inputs at 5Hz and 20Hz is analyzed.

The structure of the model that simulates the descending run is well described in (Watanabe, Kohn; 2015) and is shown in the fig.3a, while the modeling of the motoneurons can be seen in the fig.3b.

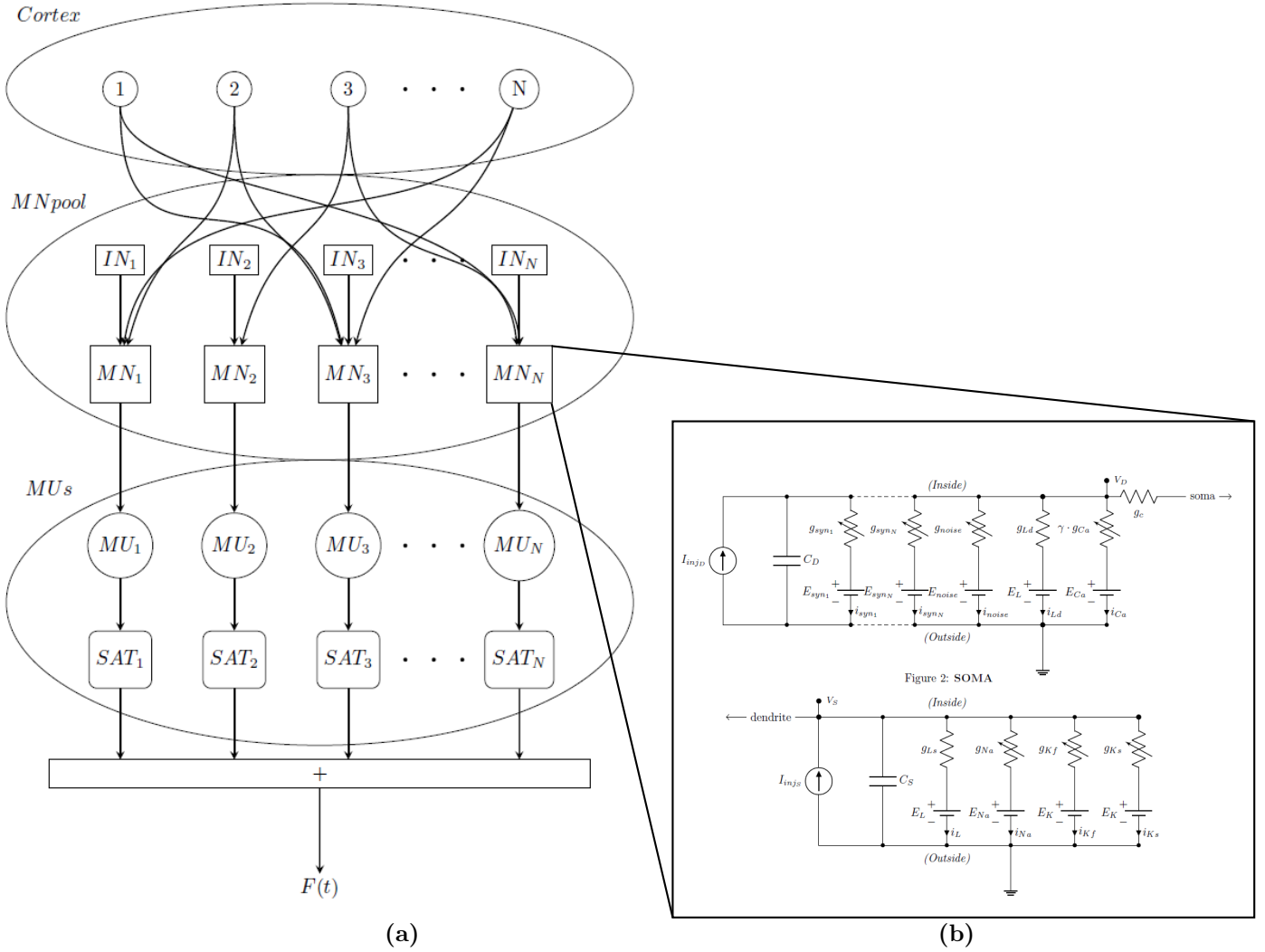


Fig. 3. Descending run model

(a) Schematic view of the overall model.

Cortical common input: the input from the cortex is described by 4000 descending axons; each of these 4000 axons connect to $\sim 30\%$ of the MNs, randomly chosen for each simulation run (each MN will roughly receive a similar number of synaptic inputs).

Motoneuron Pool: each motor unit encompasses a MN and a muscle unit (MU). The input to the MN pool is the combination of the descending signal from the cortex and a different independent noise (IN) source input in the form of a Poisson point process, with the ISIs following a Poisson distribution. The MN pool used in this study is composed of 10 slow MNs, 10 fatigue resistant MNs, and 5 fast-fatiguing MNs (Watanabe et al., 2013).

Contraction: following (Cici, Khon - 2008), the force produced by a given MU is obtained by the convolution of the respective MN spikes with the impulse response of a second-order critically damped system.

(b) Equivalent circuit used to represent each MN model.

Contraction Following (Cici-Khon), the force produced by a given MU is obtained by the convolution of the respective MN spikes with the impulse response of a second-order critically damped system.

This force signal is then passed through a nonlinear saturation (Watanabe et al., 2013) and summed to the force signals of the other MUs, resulting in the muscle force $F(t)$.

$$a(t) = A_{peak} \frac{t}{t_{peak}} \exp\left(1 - \frac{t}{t_{peak}}\right) u(t) \quad (1)$$

$$e(t) = \sum \delta(t - t_{APi}) \quad (2)$$

$$f(t) = e(t) \cdot a(t) \quad (3)$$

Where $a(t)$ is the function that models one twitch; A_{peak} and t_{peak} are the peak and time-to-peak (or contraction time) of the twitch; $u(t)$ is the Heaviside step function; $f(t)$ is the force developed by one MU; $e(t)$ is the system input, i.e., the superposition of all MU action potentials occurring at times t_{APi} .

During the contraction the Henneman's size principle is used, for the recruitment of different types of muscle fibers.

Neural fibers modeling All the neural fibers are modeled following the studies by Cisi and Kohn (2008), Watanabe et al. (2013), and Elias et al. (2014). and Kohn (2008), Watanabe et al. (2013), and Elias et al. (2014).

The parameters are randomly generated for each fibers, making each fiber unique and resulting in different pools every time they are generated.

All the differential equations were solved using a fourth-order Runge-Kutta method with fixed step of 0.05 ms.

The model used the Hodgkin-Huxley equations to calculate the voltage-dependent ionic currents through channels [1].

Figure 3b shows the equivalent circuit used to represent each MN model: g_{syn1} to g_{synM} , synaptic conductances of a dendrite activated by synapses

1 to M, respectively; g_c , coupling conductance; g_{Ld} and g_{Ls} , dendritic and somatic leakage conductances, respectively; g_{Na} , g_{Kf} , and g_{Ks} , conductances of $Na+$, fast $K+$, and slow $K+$, respectively; E_L , leakage potential; E_{Na} and E_K , $Na+$ and $K+$ equilibrium potentials, respectively; E_{syn_1} to E_{syn_M} , reversal potentials for synapses 1 to M, respectively; C_S and C_D , somatic and dendritic capacitances, respectively; V_S and V_D , somatic and dendritic membrane potentials, respectively.

$$C_d \frac{dV_d(t)}{dt} = -I_{syn_d}(t) - g_{ld}(V_d(t) - E_l) - g_c(V_d(t) - V_S(t)) + I_{inj_d}(t) \quad (4)$$

$$C_s \frac{dV_s(t)}{dt} = -I_{syn_s}(t) - g_{ls}(V_s(t) - E_l) - g_c(V_s(t) - V_d(t)) + I_{inj_s}(t) \quad (5)$$

$$I_{ion}(t) = \bar{g}_{Na} m^3 h (V_s(t) - E_{Na}) + \bar{g}_{Kf} n^4 (V_s(t) - E_K) + \bar{g}_{Ks} q^2 (V_s(t) - E_K) \quad (6)$$

$$C_s = 2 \cdot \pi \cdot l_s \cdot r_s \quad (7)$$

$$C_s = 2 \cdot \pi \cdot l_s \cdot r_s \quad (8)$$

$$C_d = 2 \cdot \pi \cdot l_d \cdot r_d \quad (9)$$

$$g_c = \frac{2}{\frac{R_i \cdot l_d}{\pi \cdot r_d^2} + \frac{(R_i \cdot l_s)}{\pi \cdot r_s^2}} \quad (10)$$

$$g_{ls} = \frac{2 \cdot \pi \cdot r_s \cdot l_s}{Rm_s} \quad (11)$$

$$g_{ld} = \frac{2 \cdot \pi \cdot r_d \cdot l_d}{Rm_d} \quad (12)$$

$$Rn = \frac{1}{g_{ls} + \frac{g_{ld} \cdot g_c}{g_{ld} + g_c}} \quad (13)$$

$$V_{th} = Rn \cdot I_{rh} \quad (14)$$

0.4.1 Afferent run

Once the force generated by the MN pool during contraction has been calculated, we move on to the analysis of the afferent signal that reports the feedback to the spine and, in turn, to the cortex.

The afferent signals are generated by the proprioceptors, the muscle spindles and the Golgi tendon organs (GTO).

There are two model for the afferent signal generation, a full one (fig.6), which tries to faithfully follow that of the corresponding anatomical system (fig.5), and a simplified one (fig.7).

Response to force

Newton's second law of motion is used to calculate the speed of contraction. By dividing the force $F(t)$ by the mass m , the acceleration $a(t)$ is obtained. By integrating the acceleration, just found, over time, we obtain the displacement speed $v(t) - v(t_0)$ and by integrating again we obtain the displacement $x(t) - x(t_0)$:

$$F(t) = m \cdot a(t) \quad (15)$$

$$\int_{t_0}^t \frac{F(t)}{m} dt = \int_{t_0}^t a(t) dt = v(t) - v(t_0) \quad (16)$$

$$\int_{t_0}^t \left(\int_{t_0}^t \frac{F(t)}{m} dt \right) dt = \int_{t_0}^t (v(t) - v(t_0)) dt = x(t) - x(t_0) - v(t_0)(x - x_0) \quad (17)$$

$$\text{Assuming } v(t_0) = 0 \rightarrow v(t_0)(x - x_0) = 0 \quad (18)$$

$$\int_{t_0}^t \left(\int_{t_0}^t \frac{F(t)}{m} dt \right) dt = \int_{t_0}^t (v(t) - v(t_0)) dt = x(t) - x(t_0) \quad (19)$$

Newton's law and Hill model Newton's law, however, is not suitable for fully representing the behavior of the muscle, resulting in speeds and lengths

well above those physiologically possible: Newton's law $F(t) = m \cdot a(t)$ is a linear formula where as the parameters increase, the force involved increases, even at infinite levels.

This cannot happen in the muscle, for obvious reasons: the muscle force does not have a linear trend while in fact, following the Hill model, it has a paraboloid trend with concavitus downwards, with asymptotes representing the maximum force and speed that it can achieve.

Hill's model, however, is based on the length of the fibers and how they are lengthened or shortened during muscle activity: in order to use this model it would have been necessary to build a muscle model that simulates the contraction with mechanical displacement of the fibers; instead a time window is used within which the integrals used for the force analysis are carried out. To overcome this problem, limits have been imposed on the maximum possible speed and the maximum length of the fibers.

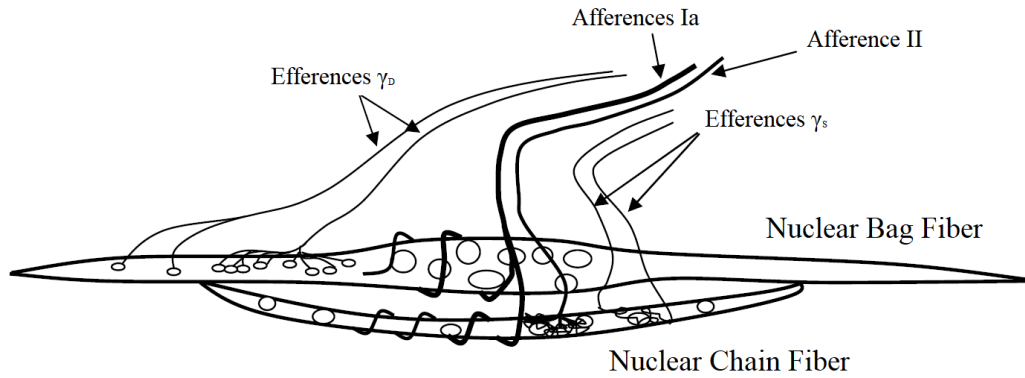


Fig. 4. Spindle structure

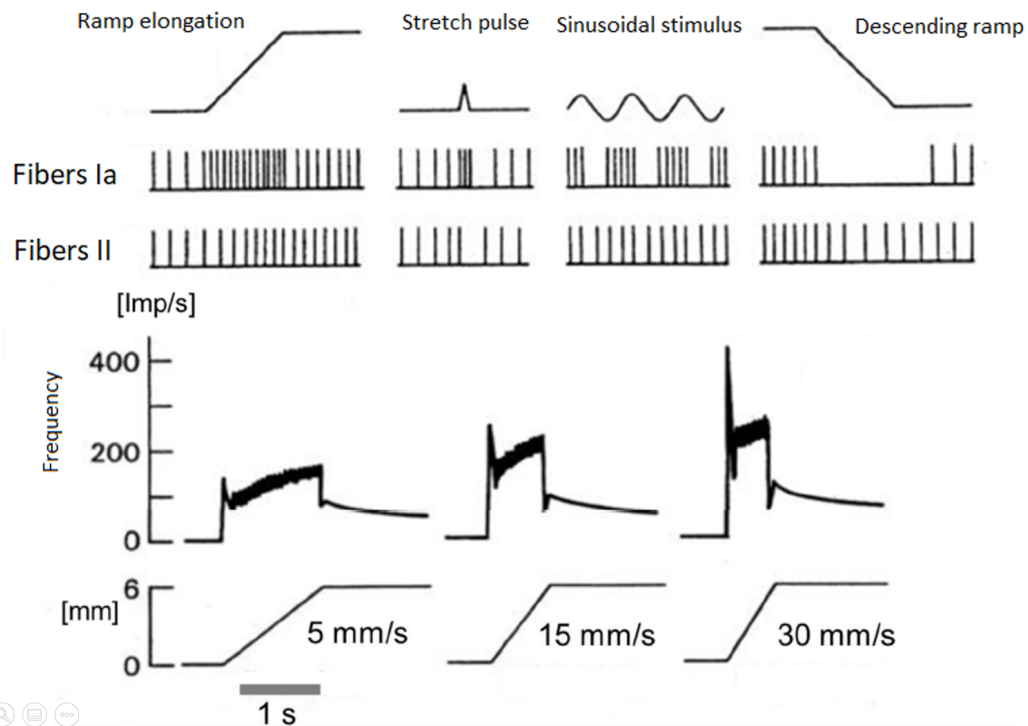


Fig. 5. Spindle behavior

Structure of a spindle taken as a basis for the model used: Ia fibers bind to both Nuclear Bag and Nuclear Chain fibers, II fibers only bind to Nuclear Chain fibers; the γ_D fibers bind to the Nuclear Bag fibers, the γ_S fibers bind to the nuclear chain fibers.
 Images taken from "BIOINGEGNERIA DEL SISTEMA MOTORIO"

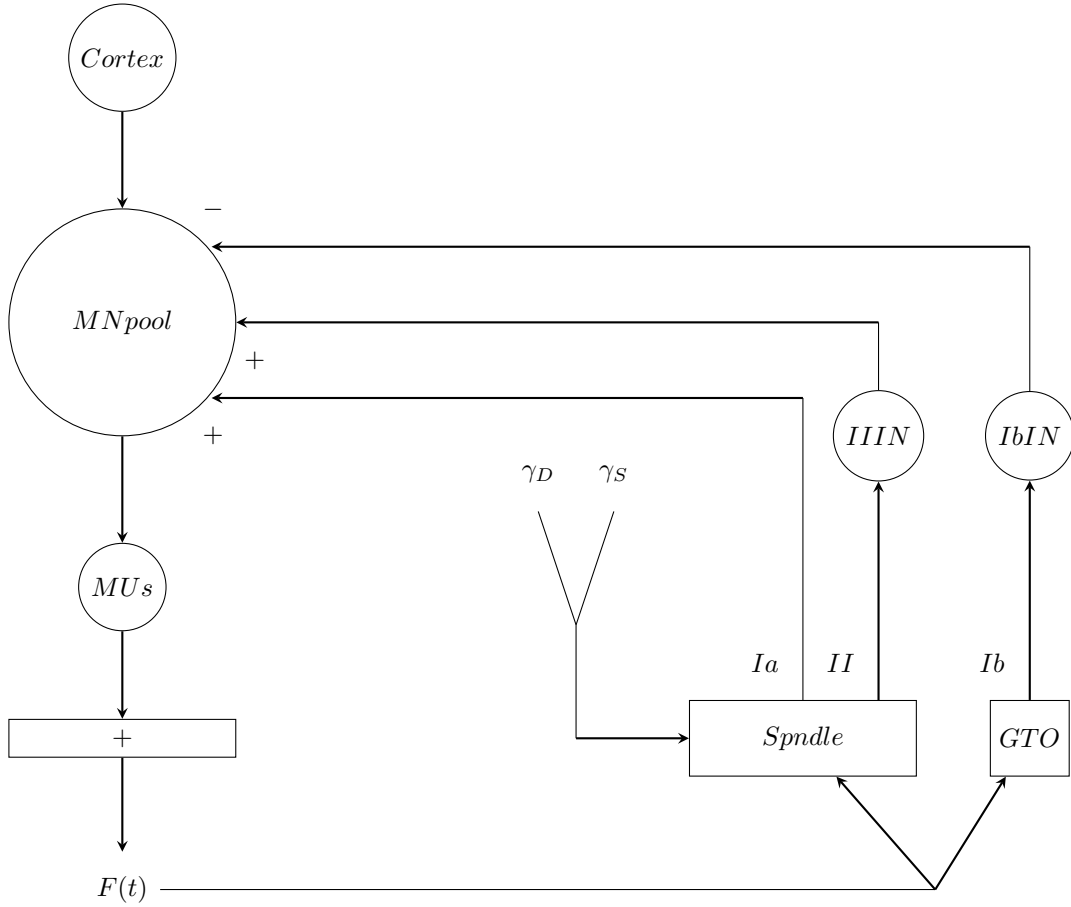


Fig. 6. Full model

Response to force:

$$\begin{aligned} \text{contraction speed}(t) &= \int_{t_0}^t \frac{F_{\text{mean}}(t) - F(t)}{m} dt \\ \text{fibers displacement}(t) &= \int_{t_0}^t \left(\int_{t_0}^t \frac{F_{\text{mean}}(t) - F(t)}{m} dt \right) dt \\ AS(t) &= \sum \frac{\text{contraction speed}(t)}{T} \\ AD(t) &= \sum \frac{\text{fibers displacement}(t)}{T} \end{aligned}$$

(20)

Impulse trains generation:

$$\begin{aligned} \gamma_D &= \omega \cdot AS(t) \\ \gamma_S &= \omega \cdot AD(t) \\ f_{\text{dynamic}} &= \left[1 - \exp\left(\frac{t_{\text{dynamic}}}{\tau_{\text{bag1}}}\right) \cdot \frac{\gamma_{\text{dynamic}}}{\gamma_{\text{dynamic}} + \text{freq}_{\text{bag1}}} \right] \\ f_{\text{static}} &= \left[1 - \exp\left(\frac{t_{\text{static}}}{\tau_{\text{bag2}}}\right) \cdot \frac{\gamma_{\text{static}}}{\gamma_{\text{static}} + \text{freq}_{\text{bag2}}} \right] \end{aligned}$$

(21)

At this point, two conditions must be guaranteed for the pulse train generation: $\rho < \delta t \cdot f_{\text{dynamic}/\text{static}}$ and at least 1ms has passed since the previous pulse; ρ is a randomly generated decimal number. When the conditions are met, a pulse is generated for that particular fiber (or fibers), the pulses last 1ms and have a refractory period of 1ms.

Due to the non-linear behavior of the spindle [2], a check is made on the response level of fibers Ia and II to see which of the two generates the greater response: the response of the fiber with the lower response is set to 0.

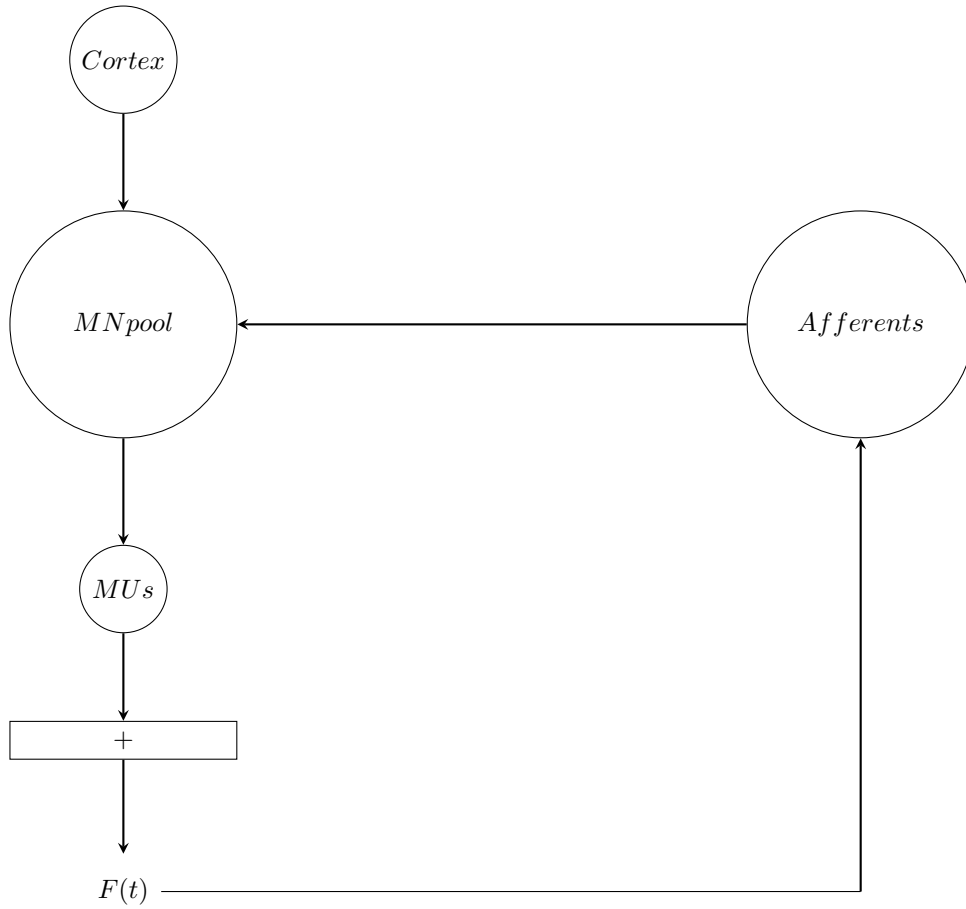


Fig. 7. Simplified model

Response to force:

$$\begin{aligned}
 \text{Spindle output Ia} &= f_{dynamic} \cdot \left(\int_{t_0}^t \frac{F_{mean}(t) - F(t)}{m} dt - \int_{t_0}^t \left(\int_{t_0}^t \frac{F_{mean}(t) - F(t)}{m} dt \right) dt \right) = \\
 &= f_{dynamic} \cdot (AS(t) - AD(t)) \\
 \text{Spindle output II} &= f_{static} \cdot \left(\int_{t_0}^t \frac{F_{mean}(t) - F(t)}{m} dt \right) = \gamma_{static} \cdot AD(t) \\
 \text{GTO output Ib} &= \int_{t_0}^t \frac{F(t) - F_{mean}(t)}{m} dt = GTO_{AD}(t) \\
 \gamma_D &= \omega \cdot AS(t) \\
 \gamma_S &= \omega \cdot AD(t) \\
 f_{dynamic} &= \left[1 - \exp\left(\frac{t_{dynamic}}{\tau_{bag1}}\right) \cdot \frac{\gamma_{dynamic}}{\gamma_{dynamic} + freq_{bag1}} \right] \\
 f_{static} &= \left[1 - \exp\left(\frac{t_{static}}{\tau_{bag2}}\right) \cdot \frac{\gamma_{static}}{\gamma_{static} + freq_{bag2}} \right]
 \end{aligned} \tag{22}$$

Feedback transport:

$$\begin{aligned}
 Ia &= \frac{d\text{Spindle output Ia}}{dt} \\
 II &= \frac{d\text{Spindle output II}}{dt} \\
 Ib &= \frac{d\text{GTO output Ib}}{dt} \\
 IIN_{output} &= \frac{dII}{dt} \\
 IbIN_{output} &= \frac{dIb}{dt} \\
 Afferents &= Ia - IbIN_{output} + IIN_{output} \\
 \text{Afferent Feedback} &= \frac{Afferents(t) - Afferents_{min}}{Afferents_{max} - Afferents_{min}}
 \end{aligned} \tag{23}$$

0.4.2 Tests run with the mdoels

0.4.3 Descending run model

We start by testing the descending model for proper functioning. The tests carried out were:

- Force generation from input signals at different frequencies: with this tests we want to check the correct functioning of the MUs; the inputs used are signals in which the first half of the time series does not contain the sinusoid, the second half contains sinusoids at different frequencies, namely $0Hz$, $5Hz$, $15Hz$ and $20Hz$;
- Force controlled with the PID directly driving the conductance of the MNs without sinusoid modulation: this is done to better compare the effect of sinusoidal input at different frequencies.
- Force controlled with the PID directly driving the conductance of the MNs without the contribution of the afferents: this is done to better compare the results of the two afferent models.

0.4.4 Spindle model

With this tests we want to check the correct functioning of the spindle model for both the full and the simplified model: The tests used are:

- sinusoidal stimuli with different frequencies, namely $0Hz$, $5Hz$, $15Hz$ and $20Hz$;
- ramp elongation;
- stretch pulse;
- descending ramp;

0.4.5 Control cycle structure

The control unit of the model is a PID controller which compares the force generated to the chosen target force and la cui uscita viene usata per modulare il segnale in ingresso alla MN pool.

The control structure can be seen in fig.8. The full simulation duration is 10s, the sampling time is 50ms, for a total of 200 cycles.

The choice of the sampling time is due to the fact that, for a correct use of the controller in the analysis of the input signal and in the generation of the correction signal, it is necessary to take the complete cycle of the input signal: in the case of a sinusoidal input at 20Hz, the cycle is completed every 50ms.

The input signal is given by the target force the system must reach. The target force is $F_{target}(t) = 210gf$, which represent 10% of the maximal voluntary contraction (MVC) and is expressed in gram-force (gf), defined as the force per unit mass due to gravity at the Earth's surface and representing the standard gravity.

In order to reach the target, a sinusoid, which enters the MN pool, is modulated at each cycle: the sinusoid used for the tests has different frequencies, so to see how these affect the generation of the force, the frequencies suate are again: 0Hz, 5Hz, 15Hz and 20Hz.

PSO

The algorithm iteratively tries to improve a candidate solution with regard to a given measure of quality. It solves a problem by having a population of particles, chosen by the user, moving around in the search-space according to the particle's position and velocity. Each particle's movement is influenced by its local best known position, but is also guided toward the best known positions in the search-space, which are updated as better positions are found by other particles.

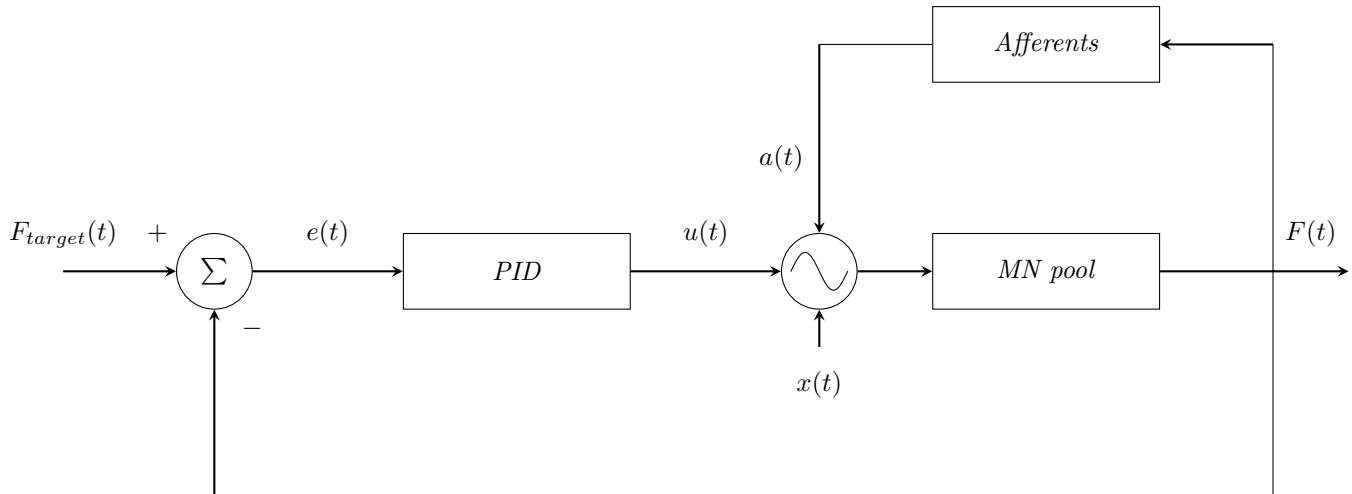
At each cycle the swarm moves towards the new global minimum and updates the values of the Ks parameters used by the PID:

$$v_k^{t+1} = \omega v_k^t + \phi_1 \beta_1 (pbest_k^t - x_k^t) + \phi_2 \beta_2 (gbest_k^t - x_k^t) \quad (24)$$

for each condition, individually using the linearly decreasing inertia weight approach:

$$\omega = \frac{0.9 - 0.4}{T} t \quad (25)$$

Fig. 8. Control cycle



Cycle structure: $F_{target}(t)$ represents the target force, $e(t)$ is the error between the target force and the force $F(t)$ generated at each cycle, $x(t)$ is the descending command, $u(t)$ is the output signal of the PID controller, $a(t)$ is the afferent feed-back signal.

$u(t)$ and $a(t)$ modulate $x(t)$ and the new signal is used as input of the MN pool for the generation of the force $F(t)$.

At each cycle I have the following steps:

1. target force sampling;
2. modulation of the input sine wave based on the PID output of previous cycle;
3. generation of the afferent response based on the force generated in the previous cycle;
4. combination of the sine wave and afferent feedback as input for the MN pool;
 - Full model: the responses of the single fibers, together with the sinusoid in input, are inserted separately, each with its own synapse, and separately pass through the respective connectivity matrices;
 - Simplified model: the complete response of the afferent circuit is added to the input sinusoid and it is only this sum that enters the MN pool as input.
5. simulation of the MN pool reaction to the new input;
6. force calculation starting from the generated spikes;
7. calculation of the error as the difference between the generated force and the target force;
8. generation of the new amplitude of the input sine wave using the PID.

introduced by Shi and Eberhart [3].

This was combined with time-varying acceleration coefficients (TVAC):

$$\phi_1 = \frac{2.5 - 0.5}{T}t + 0.5 \quad (26)$$

$$\phi_2 = \frac{0.5 - 2.5}{T}t + 2.5 \quad (27)$$

$$(28)$$

It starts with a high ϕ_1 cognitive weight, so it can focus on a local area, then the social weight increases ϕ_2 [4], [5]. β_1 and β_2 represent random numbers which are used in the computation to update the velocity v of each particle, p_{best} (the best position of the particle), g_{best} (the best global position) and to calculate the integral of time-weighted absolute error (ITAE) $e(t)$, which reflect the degree to which absolute error and steady-state error effect performance assessment [6]. For the high-pass filters, a third-order Butterworth filter was used for four different bandwidths: one with no cut-off and the others with a cut-off frequency of $5Hz$, $15Hz$, $20Hz$.

0.5 Results

0.5.1 Descending model

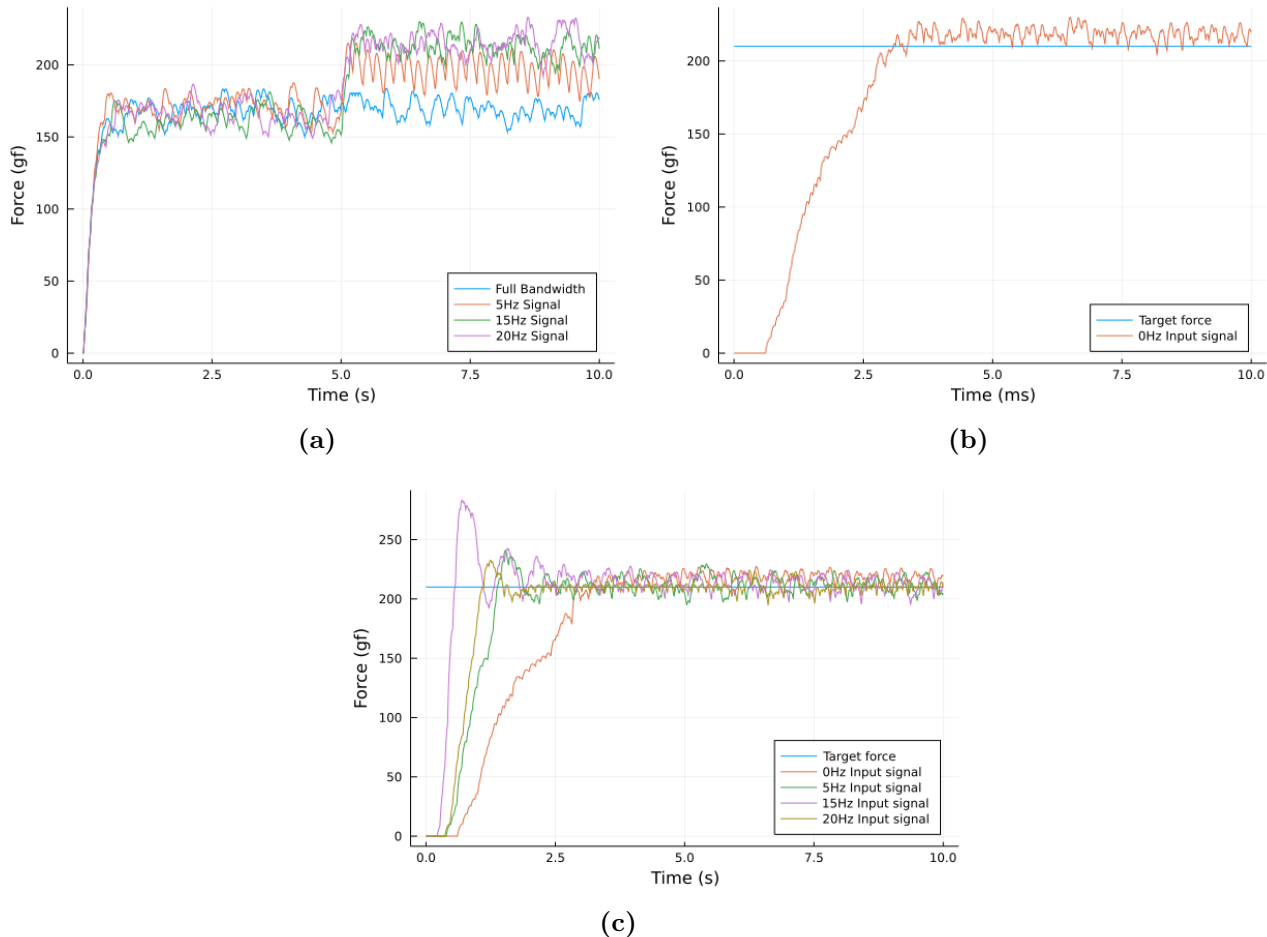


Fig. 9. Descending model test results

Results for different tests on the descending run model: **a)** Force generated by the descending run model when the inputs are signals in which the first half of the time series does not contain the sinusoid, the second half contains sinusoids at different frequencies, namely $0Hz$, $5Hz$, $15Hz$ and $20Hz$; **b)** Behavior of the model while being controlled by the PID directly driving the conductance of the MNs without any sinusoid modulation; **c)** Behavior of the model while being controlled by the PID directly driving the conductance of the MNs, without the contribution of the afferents, with a sinusoid at different frequencies, namely $0Hz$, $5Hz$, $15Hz$ and $20Hz$.

This results are perfectly in line with the ones seen in [7] and [8], they shows the nonlinear behavior of the MN pool and how high frequencies actively contributes to the generation of forces.

Fig.9b shows the behavior of the model while being controlled by the PID directly driving the conductance of the MNs without any sinusoid modulation, at different values of the K s parameters.

0.5.2 Full spindle model results

The problem of the time window: The consequence of using the force with respect to the instantaneous elongation is that, to analyze the response, it is necessary to use a predetermined time window, in our case $50ms$, thus losing the memory of which is the "rest" length of the fibers with respect to when they are stretched or contracted and the instantaneity of the response. To overcome the memory problem, the time window of $50ms$ is analyzed $1ms$ at a time and the average of the force is calculated and updated with each new $1ms$ examined up to $10ms$: in this way a sort of fictitious "memory" is created inside the window itself.

Analysis of the spindle reaction of to high frequency stimuli: The ability to respond to different inputs depends on the frequency with which the oscillations occur, if too high, therefore too narrow, the model is not able to follow them adequately; this is mainly noticeable in the response to the $20Hz$ sinusoid signal.

The cause of this is the use of the time window to analyze the force response: the time available to the spindle is limited to $50ms$ and each pulse lasts $1ms$ with a subsequent wait of $1ms$; if the peaks of the sine wave are within the $2ms$ already used by a spike, that peak is lost.

Fibers II, on the other hand, are unable to follow the trend of the force in the same way as fibers Ia, this is an expected result of this model, in fact the action of fibers II is very limited by the presence of Ia, as explained for both models, due to the non linearity of the spindle, when the response of Ia is higher than that of II, the response of the latter is reset to 0 and vice versa.

0.5.3 Simplified spindle model results

The simplified model is able to bypass the complexity of the afferent nervous system using mathematical formulas that are still able to represent the "essence" of afferences in the motor neuron loop: it reacts to changes in muscle dynamics and modulates excitability of MNs accordingly using physiologically-inspired positive and negative feedback loops.

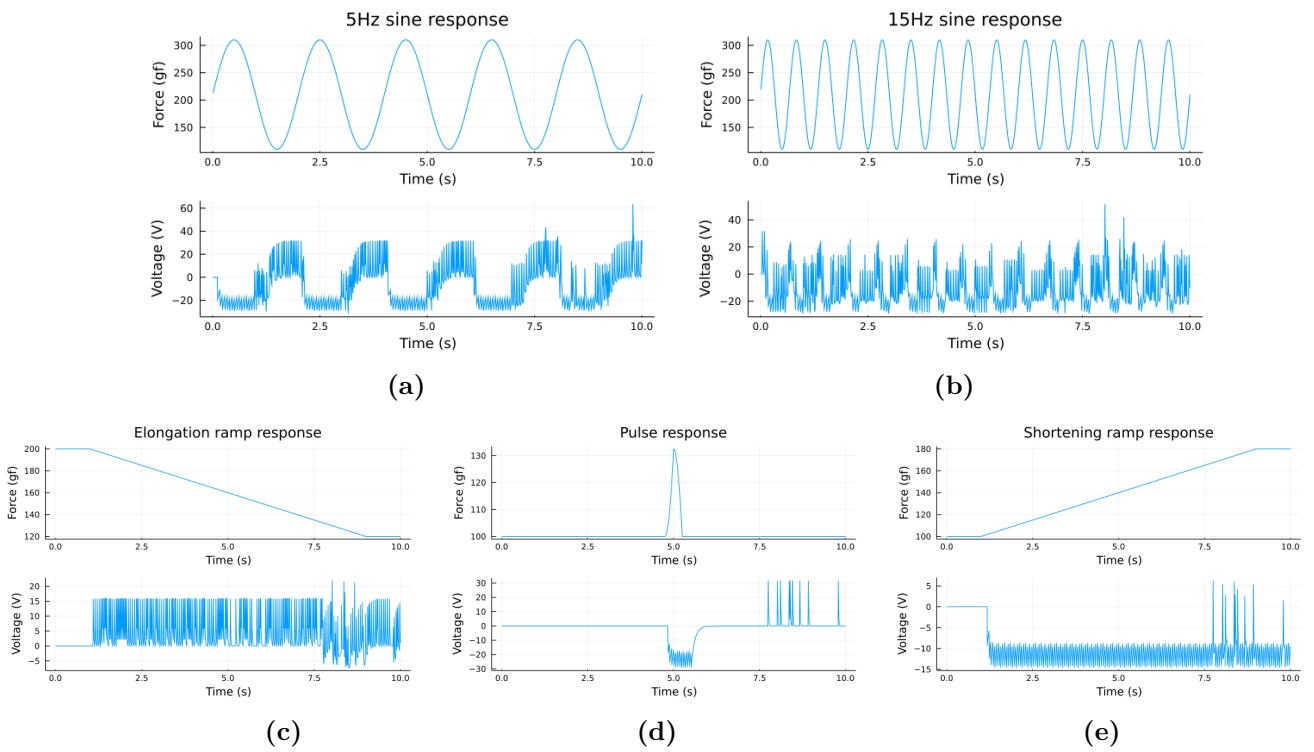


Fig. 10. Full spindle model afferent feed-back

Complete afferent feed-back of the full spindle model for: (a) Sinusoidal stimulus at 5Hz, (b) Sinusoidal stimulus at 15Hz, (c) Ramp down, (d) Stretch pulse, (e) Ramp up.

For each panel the force trace and the voltage (V) generated by the afferents are shown.

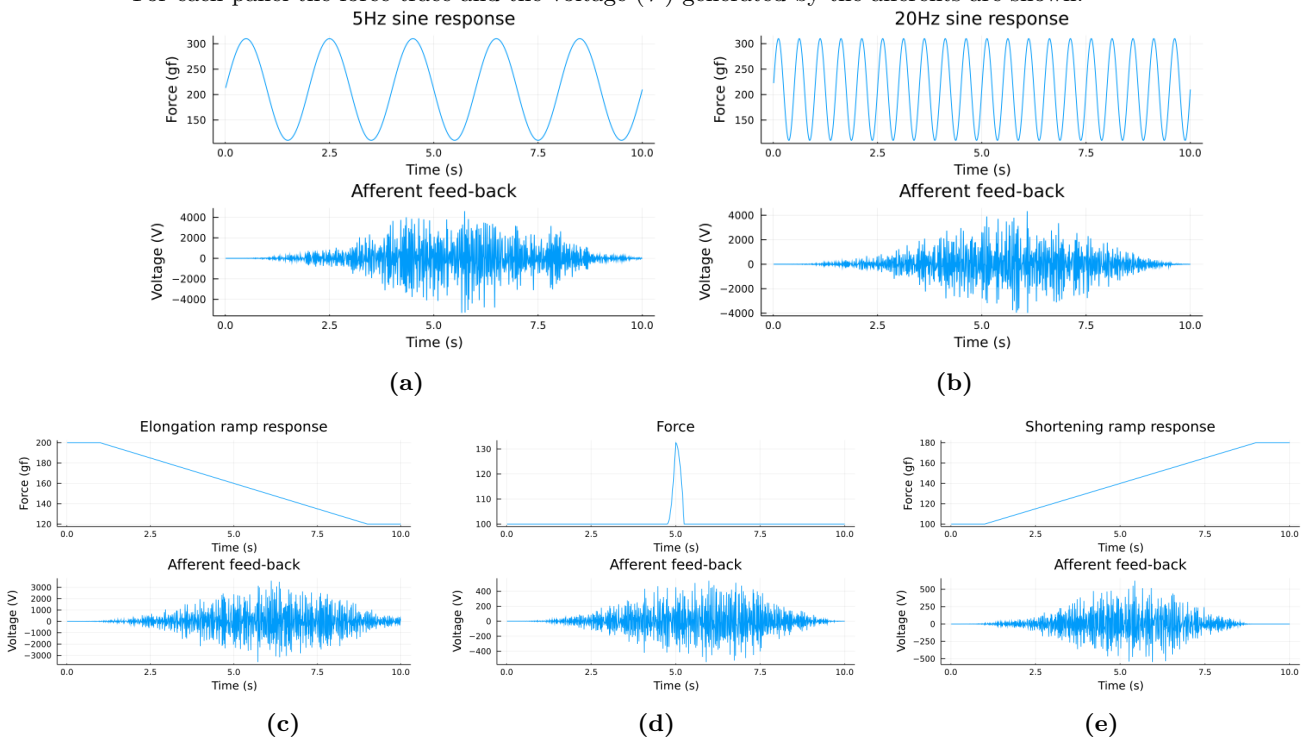


Fig. 11. Simplified model afferent feed-back

Complete afferent feed-back of the simplified model for: (a) Sinusoidal stimulus at 5Hz, (b) Sinusoidal stimulus at 15Hz, (c) Ramp down, (d) Stretch pulse, (e) Ramp up.

For each panel the force trace and the voltage (V) generated by the afferents are shown.

0.5.4 Results of the simplified afferent feed-back model tests

Results Fig.12 shows the results of the tests made with the model, when in input it has a signal modulated by the PID at frequencies 5, 15 and 20.

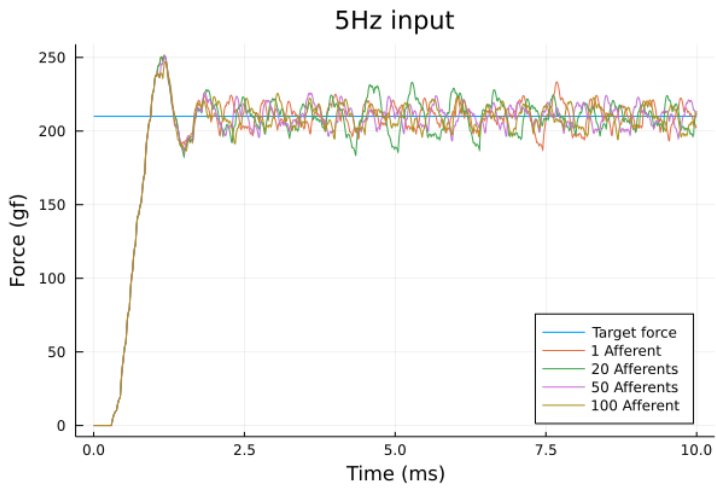
Conclusions

The goal of the thesis was to build two possible models for afferent feed-back in motor control and compare them to see which of the two best suited the study of the contribution of high frequencies in motor control.

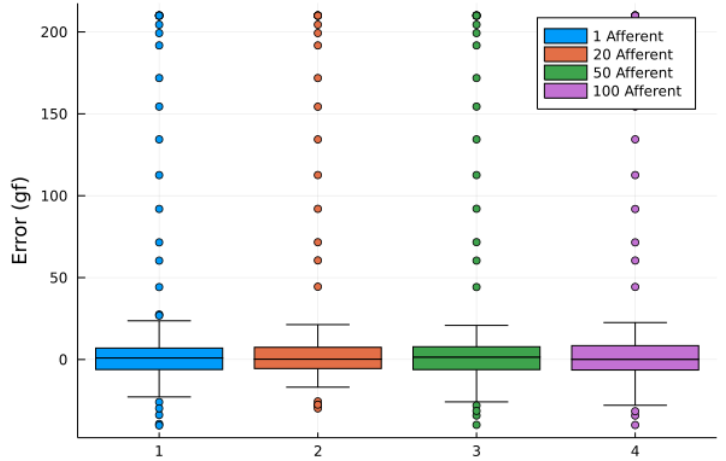
The results obtained show how the complete model tries to play its role but is limited by the above problems.

On the contrary, the simplified model, although much more generic in its function, is able to perfectly follow the control command, adapting to the force generated at all the frequencies considered.

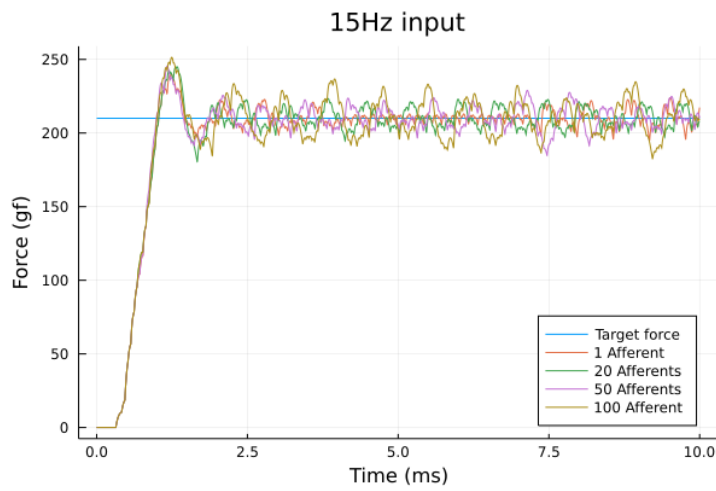
Following are some tests that test the model used as it tries to follow different force trace to see if it is able to follow them or it becomes unstable.



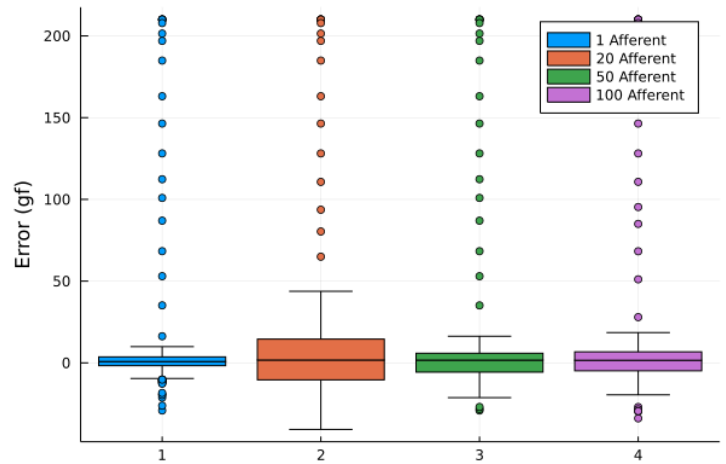
(a)



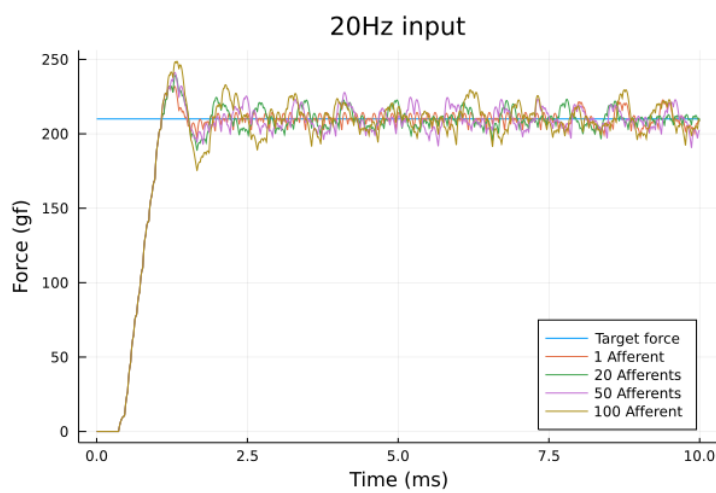
(b)



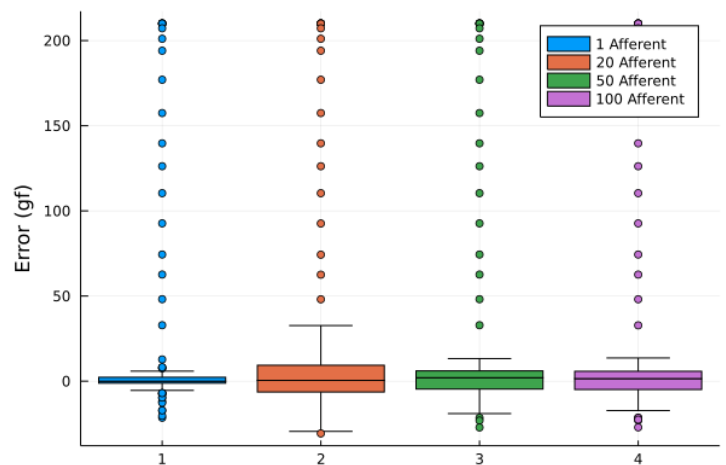
(c)



(d)



(e)



(f)

Fig. 12. Simplified afferent feed-back model test results at 0Hz

Results for the simplified afferent feed-back model when the input signal is modulated by the PID with different frequencies: **a - b)** input signal modulated at a frequency equal to $5Hz$, with different numbers of afferent fibers and boxplots of the average errors; **c - d)** input signal modulated at a frequency equal to $15Hz$, with different numbers of afferent fibers and boxplots of the average errors; **e - f)** input signal modulated at a frequency equal to $20Hz$, with different numbers of afferent fibers and boxplots of the average errors;

Introduction

Oscillations in the beta and gamma bands ($13\text{--}30\text{Hz}$; $37\text{--}70\text{Hz}$) have often been observed in motor cortical outputs that reach the spinal cord, acting on motor neurons and interneurons.

How they are involved in controlling muscle contractions is still a mystery: muscles behave similarly to low-pass filters and should filter out high-frequency signals from higher systems. In recent years, however, research has gained strong momentum in this field.

In this study, a mathematical model biologically inspired by the neuromuscular system was created and two different representative models of the afferent system were connected to it:

- The first is a complete model that tries to be as realistic as possible in its structure, simulating the activity of the muscle spindle and the GTO, and of all the nerve connections and synapses that bring the signal back to the spine;
- The second model, on the other hand, is a simplified model of the first, which reduces the realism of the first model to mathematical formulas that are in any case able to represent the afferent system.

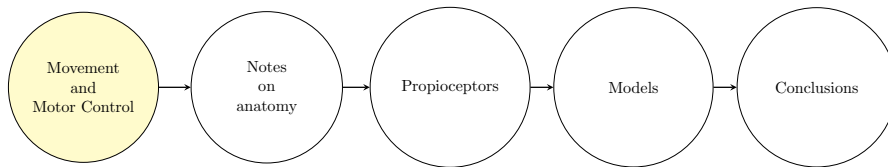
In this still open field of study, other studies have been carried out on the analysis of the contribution of high frequencies in muscle contraction, but few have implemented the afferents represented by the proprioceptive organs and even fewer have tried to implement a model for these so complex organs. With this thesis, we wanted to try to implement a model capable of closing the control loop, comparing a more realistic model against a simpler and more generalized one.

In the following chapters we will analyze which processes are involved in the generation of the movement, following the following structure:

1. In the first chapter we will see what movement is, how the planning and execution of complex movements is organized and which neurophysiological processes are involved in its realization;
2. In the second chapter we will go into more detail of which organs and systems are involved in motor control, giving an outline of the anatomy of the central and peripheral nervous system;
3. The third chapter is dedicated to proprioceptors, how they are structured and what their functioning is, given their importance in the main model built for this thesis;
4. The fourth chapter describes the mathematical model biologically inspired by the neuromuscular system and two different representative models of the afferent system built for this thesis, starting from the complete model and then moving on to the simplified one;
5. In the conclusions we will see the results of the two models used and their differences

Chapter 1

The movement



Movement is one of the most important relational functions for humans. It is our only instrument for active interaction with the external world. Obvious examples range from expression of complex thoughts (writing, reading, talking, communication) to sportive activities, interpersonal relationships and more.

It is performed by modifying the system of forces that previously maintained the static balance of the body or part of it (first principle of dynamics).

The organs capable of modifying these forces in a short time are the muscles which, through the nervous system, generally act under the action of motor commands and, thanks to the presence of receptors placed inside them, are also able to send back signals relating to their status: mainly relating to the force generated, the variation in length suffered and the speed of variation of this length [9].

The nervous system also collects signals from other parts of the body relating to different physical quantities: contact forces with the ground or with objects external to the body, load and movement of the joints, orientation and speed of movement (rotation) of the head, visual information and auditory. Based on this information, motor commands suitable for carrying out

the *motor acts* are produced and sent to the muscles.

1.1 Organization of the movement

What we call *action* is defined as a sequence of movements that allow the individual to reach a goal: any action, even the simplest, is the result of a complex series of events linked to different levels of the psyche and body systems. The need for action arises from the psychological sphere or from a more automatic event, such as the reaction to a danger or a stimulus.

If we consider an individual who wants to drink a glass of water, the series of movements that allow him to grasp the glass and drink is, in its entirety, an action. If we analyze this action over time, step by step, it can be divided into a series of motor segments, called *motor acts*, each of which has its own purpose: to approach the glass, reach it with the arm, take it, bring it to the mouth and drinking.

Each motor act is constituted, in turn, by an ordered series of movements which, carried out in succession, carry out that specific motor act. For example: grasping involves the extension and subsequent flexion of the wrist and fingers.

In the organization of the action, it is necessary to consider the relative parameters of the movement such as speed, acceleration and force, therefore what we call a *motor program* is necessary.

1.2 The motor program

The need for action is processed by the nervous system, with or without brain intervention, which generates the motor program which, in turn, is transmitted to the musculoskeletal actuators through the efferent nerve pathways.

The drafting of a motor program requires detailed information on the spatial position of the body and of the objects with which it must or intends to interact; this information comes from the *sensory systems* and *proprioceptors* that control the correct execution of the program: they are processed centrally to derive the laws of motion, estimate the state of the

various parts of the body and surrounding objects and, if necessary, modify and re-elaborate the motor program to following any environmental disturbances.

The control of the action obviously cannot be entirely delegated to the central level, the speed of reaction to external stimuli could in fact be too low; to overcome this problem there are local monosynaptic circuits capable of providing almost immediate reactions in case of need.

However, not all actions are performed in a closed loop, but there are some, such as very fast gymnastic performances, which require careful pre-programming as, once started, they can only be corrected locally and even the slightest disturbance cause an irremediable deviation from the intended purposes.

1.3 Properties of the Motor Control system

First of all, there are several features of the human motor system that significantly complicate motor control:

- Delays: there are delays both in the transmission of motor commands from the CNS to the muscular system and, vice versa, in the communication of sensory information to the CNS, making the sensorial information unusable to guide at least the initial part of the movement;
- Noise: both sensorial inputs and motor control signals are subject to intrinsic neural noise that limits the motor system ability to simultaneously execute fast and accurate movements.;
- Non stationarity: the relation between motor commands and movement changes over time by two different factors:
 - Ontogenetic: living subjects grow up, training as well as pathologies continuously modify our actuation system and also the controlling neural mechanisms;
 - Task dependant: motor task actuation changes with respect to different objects and different environments;

- Non linearity: Motor Control works in a non-linear environment, this can be seen from:
 - Gravitational force (external non linearity);
 - Joint range of motion (internal non linearity);
- Multidimensionality: from the computational point of view, the brain is a processing system that converts inputs into outputs; inputs are movement commands and feedback signals from our sensory system, outputs are motor commands that act on our muscles.

In order to make the muscles contract and relax, to obtain the desired act of motion, the control system must send accurately timed commands (*problem of temporal distribution*) not only to a muscle group but to numerous groups of muscle agonists and antagonists (*problem of spatial distribution*) (even very simple movements, such as lifting an arm, involve the control action of multiple joints (wrist, elbow, shoulder).

Moreover the control system must take into account the functional characteristics of the various components of the structure and create the postural conditions for which the movement can be carried out correctly, without loss of balance, according to the desired trajectories, despite the mass displacements of the moving parts. These preparatory actions, which often occur in advance of the desired movement, are called *Anticipatory Postural Adjustments* (APA).

1.4 Motor control models

The systems used by our body for motor control are very complex to study.

In this section we will see some examples of control models that try to explain, in a simplified way, how motor control works.

In general, a command sent to a lower level system with the aim of obtaining a certain result will be effective if there is the possibility to verify the effect obtained and to modify the command itself if the result is different from the desired one. This is the concept of a retro-operated or feedback system.

Applying this concept to our body, the physiological control systems are all those systems that regulate our physiological functions (such as metabolic activity, temperature and chemical concentrations), the actuators carry out their activity through contraction/distension, excretion, conduction time modulations, fluid/gas exchange and more and the desired result is homeostasis.

For this thesis we will focus exclusively on the motor control system in which the actuators are the muscles, the desired result is the movement according to a certain trajectory.

Once the desired movement is established to achieve a goal, a trajectory is drawn that the limbs must follow, the muscles (actuators) take care of carrying out the action. The verification of the correct execution is carried out through the detection of quantities relating to the movement carried out by suitable sensors (feed-back signals), represented by the *proprioceptors*, and the comparison of these quantities with those corresponding to the desired movement. The difference found will allow to activate a *controller* which will increase or decrease the motor command accordingly and obtain the desired output.

This scheme also allows us to automatically respond to perturbations applied to the controlled system, whether they are variations of external forces (sudden loads) or changes in the force generation properties by the actuators (for example muscle fatigue).

1.4.1 Feed-forward Control

Open loop regulation may perform complex behaviours but can not compensate disturbances that are a-priori unknown.

For most natural movements, open loop control is essential where the eventual timing of closed loop control would be available too late to effectively guide the movement.

This type of control, called *feed-forward* figure (1.1), is essential for the execution of a great variety of motor acts.

In the case of catching a ball, the feed-forward control interprets the visual information so as to put tension on the muscles in advance of the moment of

impact and adjust the characteristics of the *feed-back* controller correctly.

1.4.2 Feed-back Control

The feedback is used to maintain or modulate quantities such as position or strength in postural situations.

With this system the error signal is continuously calculated and serves to control the movement during its development, instant by instant, figure (1.2).

As a result of the long delay in the conduction of nerve signals, feedback processes are generally relatively slow and are mainly used for maintaining posture and regulating slow movements.

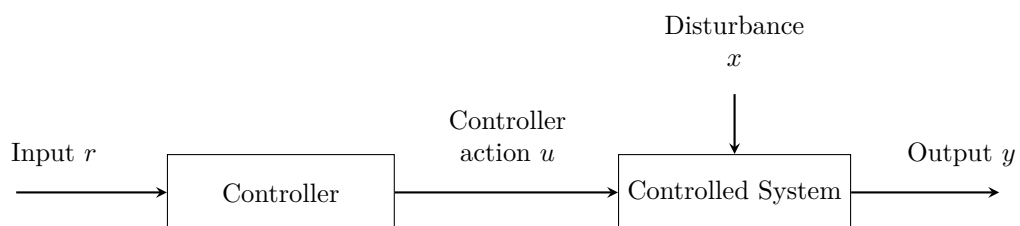
1.4.3 Feedback control with feedforward

The feed-forward control is essential for rapid movements, and is based on advance information to adjust the controlled variables, the feed-back system is essential for movements that require precision and, as seen in figure (1.3), both systems play an important role in motor control.

Taking the example of catching a ball on the fly:

1. Advance knowledge of the trajectory of the ball and the position of the hand are prepaid information received by the sensors and sent to the feed-forward controller;
2. on the basis of this information, the feed-forward controller adjusts the gain of the feed-back controller and sends additional signals to the

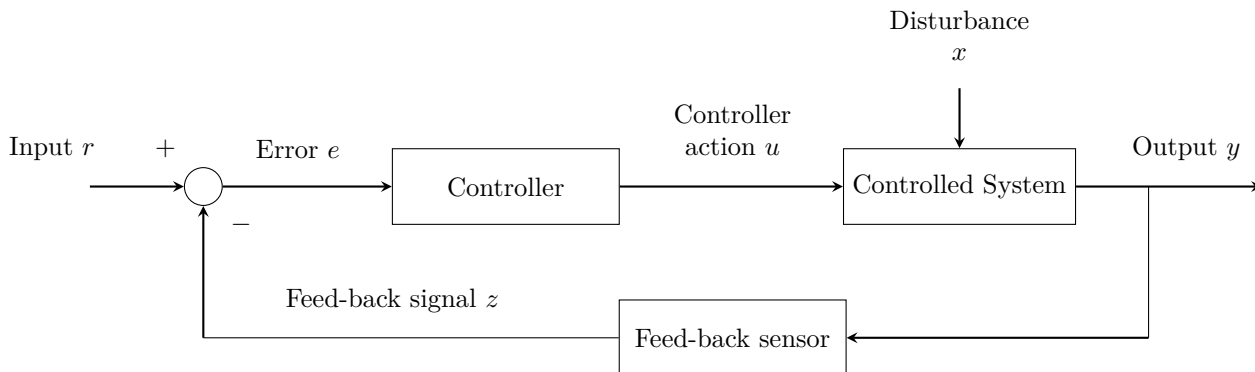
Fig. 1.1. Feed-foreward Control



Example block diagra of an open loop system: rising an object supposed heavy but which was light instead and consequently doing a completely wrong gesture.

Input r represents the force impressed in the movement initially while Output y represents the desired movement.

Fig. 1.2. Feed-back Control



Example block diagram of a closed loop system: a thermostat that regulates the temperature of a room (input r), using a temperature sensor and controlling a fan/heater to minimize the error between the desired temperature and the actual temperature in the room (Output y)

system to anticipate muscle activities capable of reducing perturbations and deviations from the desired trajectory or position of the hand;

3. The feed-back kicks in to position the hand appropriately after the ball has been captured. The feed-forward control also monitors the system for property changes that may occur over time, such as fatigue, through adaptive control mechanisms.

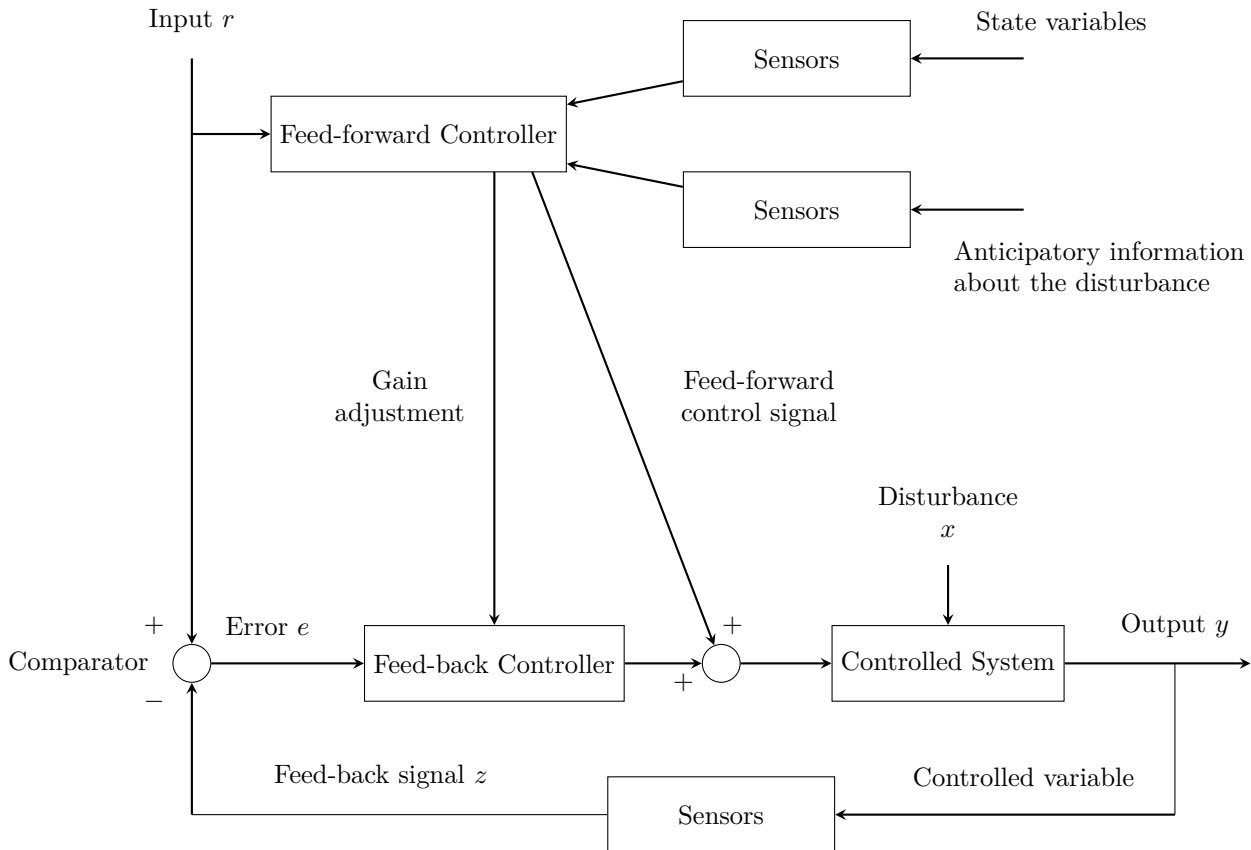
To do this, the feed-forward controller must know how to interpret anticipated information (such as visual information) to predict the muscle strength required to sustain the impact of the ball.

This requires an internal representation of the dynamics of the ball and the characteristics of the musculoskeletal system, what is called: internal model of the system.

The importance of proprioceptive input in the control of posture and movement, be it feed-back or feed-forward, is demonstrated by the motor deficits that appear in patients with damage to the proprioceptive system, in particular in the so-called neuropathy conditions of the large afferent fibers.

Although these patients can see their limbs, they do not have the perception of the position and movement of the joints: when they close their eyes, the limb, which should be kept in position, slowly begins to move unpredictably. Movement defects are also observed in pointing the finger towards a position, and as regards the lower limbs, in the instability of posture and walking.

Fig. 1.3. Feed-back control with feed-forward



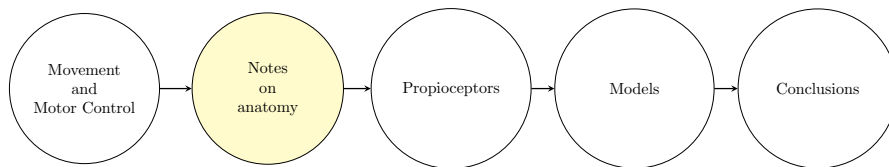
A block diagram of the full scheme of motor control with synergistic action of feed-back and feed-forward systems, with Input r representing the kinematics of the movement while Output y represents the desired trajectory.

The feed-forward controller, on the basis of the information received by sensors, adjusts the gain of the feed-back controller and sends additional signals to the system to anticipate muscle activities capable of reducing perturbations and deviations from the desired trajectory;

For this thesis, to theoretically evaluate whether the modulation of some types of input to the NMs can be used to control the force, the control of muscle force is entrusted to a *PID* controller.

Chapter 2

Notes on anatomy



In this chapter we will take a closer look at the organs and systems involved in the generation and implementation of the motor program.

The individual is ideally able to control any variable related to movement: joint angles, moments (forces), speed, accuracy, etc ...

There have been many studies that try to find a one-to-one correspondence between the various organs and levels of the central nervous system and the various steps that allow us to design and carry out the desired movement.

Until now, however, it is still a mystery how this process is carried out, we only know which areas are used but the details still elude us.

In this chapter we will go into more detail what these areas are and why their complexity is a problem for this type of study.

2.1 Structure of the nervous system

The entire nervous system is conventionally divided into:

- **Central Nervous System** (CNS), consisting of the brain (cerebrum and cerebellum) and spinal cord;

- **Peripheral Nervous System (PNS)**, composed of those parts (nerve fibers, receptors and synapses) mainly responsible for the collection and transmission of information and commands from/to the periphery;
- **Autonomous Nervous System (ANS)**, consisting of those nervous structures connected with the activation of smooth muscle (heart muscle and glands), which in fact is identified more for characteristic functional aspects than for the structure.

The organization of these systems is extremely complex, and it can be studied both at macrostructure and microstructure levels. In addition, cross-talks and feedbacks within and across parts of the systems are crucial in order to perform higher-level functions.

2.2 Central Nervous System

2.2.1 Cerebral cortex

The outer surface of the cerebral hemisphere is made up of a thin layer of gray matter called *cortex*. Its thickness is about 3 millimeters and is mainly made up of cell bodies whose axons run in the underlying white matter.

The cortex appears abundantly variegated with folds and fissures, which considerably increases the total surface area without requiring a greater brain volume: each fold, consisting of a rounded relief, is defined as *gyrus* or *convolution*; the groove that is formed, of varying depth, is called *groove* or *sulcus*.

The gyri and sulci, although they may vary in detail from one brain to another, follow a recognizable pattern, so they are taken as a reference for topographically identifying the main areas of known functional significance.

Internal structure

The cerebral cortex is divided in two main different sections and it is possible to classify the brain according to the color and the threshold between these two parts:

- Grey matter: composed of cell bodies and unmyelinated fibers;

- White matter: composed by myelinated axons interconnecting different regions.

The myriads of nerve fibers (axons) that make up the white matter of the cerebral hemisphere connect the different sections of the brain both within the same hemisphere and cross the two hemispheres. There are three main connection in the brain:

- **Association fibers:** they connect cortical areas within the same cerebral hemisphere;
- **Commissural fibers:** cross the median plane connecting the two hemispheres;
- **Projection fiber:** they start from the cortex directed towards lower centers or go up to the cortex from lower centers; they are "*projections*" from/to the cortex, and therefore divided in:
 - **Afferent fibers:** they go from the encephalic nuclei up to the cortex (sensory system);
 - **Efferent fibers:** they go from the cortex down to the encephalic nuclei (motor system, sensory system - efferent part);

During our life we constantly build connections according to the stimuli and our experiences, constantly adapting and allowing us to learn.

2.2.2 Cortical organization of movement

Given the anatomical and functional complexity of the human machine, it is certainly not easy to find, nor to affirm, that there is a unique physiological correspondence between the morphological levels of organization of voluntary movement and the cortical motor areas.

Homunculus

Woolsey et al. (1952) are responsible for the description of the *homunculus* in which the representation of the distal musculature is located in the depth and convexity of the central sulcus.

The motor program arises from the areas assigned to this task, namely the motor and pre-motor cortex.

Although the organization of the movement is not carried out in specific areas, but it arises from the interaction of different areas, the main ones involved are 4 and 6.

The neurons belonging to area 4 do not seem to be individually responsible for the contraction of a single muscle, but rather govern muscle fields completely analogous to the sensory fields; moreover, they also encode the movement parameters or have the function of controlling complex programs already present at the subcortical level.

Brain's sections

Before a movement can be made, the cortex receives information from the different lobes. The cortex can in fact be divided, from the anatomic point of view, into four main regions: ***Frontal***, ***Temporal***, ***Parietal*** and ***Occipital***.

Each area is anatomically different from the others but it has also different functionalities:

- ***Frontal cortex*** includes the premotor cortex and the primary motor cortex: from the anterior portion of the frontal lobe, information about the goal to be achieved and the appropriate strategy to achieve it are obtained;
- ***Parietal lobe*** integrates many sensory information, including spatial sense, navigation (proprioception), somatosensory features, taste and touch;
- ***Temporal lobe*** is involved in visual memory, language comprehension, and emotion association: here the memorization of past strategies takes place;
- ***Occipital lobe*** incorporates the visual cortex and is the visual processing center.

For this thesis we will mainly focus on the synergy between the motor cortex and the parietal lobe.

Sensory hierarchy There is a succession of commands sent by the different areas that constitutes the sensory hierarchy for the execution of the movement: the primary sensory area sends information to higher order areas and subsequently to associative areas; The primary motor area receives information from the premotor area which in turn receives information from the prefrontal associative areas. Below is a simplified scheme:

1. Primary somatosensory cortex;
2. Higher order somatosensory cortex;
3. Parietal associative areas;
4. Prefrontal associative areas;
5. Premotor area;
6. Primary motor area;

2.2.3 Cerebellum

The cerebellum is located behind the pons and medulla oblongata and has a particular appearance characterized by lobes (anterior, middle, posterior) engraved with thin, transverse and numerous folds, called 'folia cerebelli'. Although the cerebellum constitutes about 10% of the brain mass in 'homo sapiens', it contains approximately 80% of the total brain neurons.

Structure As in the brain, it has a thin outer cortex of gray matter, and in depth we find the white matter: in the sagittal sections, the branched aspect of the white matter that pushes into the folds of the gray matter has inspired the fanciful name of *arbor vitae* (tree of life).

Deep in the white matter, near the roof of the fourth ventricle, there are the *central nuclei* of gray matter from which all the cerebellar pathways exit. The most conspicuous of the central nuclei is the *dentate nucleus*, so called because of its shape and size. In addition to the middle cerebral peduncle, the cerebellum has a *superior cerebellar peduncle* which goes upwards, and connects it with the midbrain, and a *inferior cerebellar peduncle* which enters the cerebellum from the spinal cord.

Functions The cerebellum plays an important role in the control of movements and is involved in various cognitive functions, such as attention, memory and language. By itself, the human cerebellum does not initiate movement, but contributes to its coordination, precision and accurate timing: it receives input from the sensory systems of the spinal cord and other areas of the brain and integrates these signals. in the optimization of motor activity.

2.2.4 Spinal cord

The spinal cord is the main communication route between the brain and the peripheral nervous system and, through the spinal nerves, carries motor, sensory, and autonomic signals between the brain and the body.

The human spinal cord is contained and protected by the spinal column, lodged in the vertebral foramina it consists of 31 segments: 8 *cervical*, 12 *thoracic*, 5 *lumbar*, 5 *sacral* and 1 *coccygeal*.

The *spinal cord*, seen in cross section, has different shapes and sizes at different levels of its length, but the shape of the central gray matter resembling the letter H remains constant. The gray matter contains the cell bodies of neurons and around it is the white matter, occupied by the fibers that run into the spinal cord.

The various sensory receptors distributed throughout the body send information to the spinal cord via the *spinal nerves*.

Nerve fibers enter the spinal cord through the dorsal root: some fibers synapse with neurons found in the dorsal horn, while others go up to the brain.

Many cell bodies of the ventral horn, on the other hand, send axons up to the muscles, through the ventral root, to control movement.

2.3 Peripheral Nervous System

The PNS consists of nerve fibers, receptors and synapses mainly responsible for the collection and transmission of information and commands from/to the periphery.

2.3.1 Spinal nerves

A spinal nerve is a mixed nerve, which carries motor, sensory, and autonomic signals between the spinal cord and the body.

It is formed from the combination of nerve fibers from:

- **Dorsal root:** is the afferent sensory root and carries sensory information to the brain.
- **Ventral root:** is the efferent motor root and carries motor information from the brain.

The spinal nerves emerge from the spinal column through an opening between adjacent vertebrae at different levels and innervate different (partially overlapping) areas of the body arranged in a longitudinal progression that reflects the different levels of origin of the same spinal nerves. This correspondence is called *somatotopic organization*.

In the next chapter we will see the peripheral organization of movement, looking in more detail at the structure of the motor unit, composed of muscles and motor neurons.

2.4 Peripheral organization of movement

In this chapter we will see in more detail how a motor act takes place. More specifically we will analyze the element that, in the kinematic chain, is the one whose structure and functioning are the best known, that is the motor unit.

2.4.1 Motor Neurons

The neuron is the elemental nerve cell and together with the ganglia forms the basis of the nervous system.

A neuron is made up of:

- **Dendrites:** input of the neuron system: they collect the signal coming from other neurons and transmit it to the soma;

- **Soma** (central unit): integrates the signal (potentials) and generates the action potential
- **Axon and axonic arborescence** (system output): transmits the signal (action potential) to other neurons

Motor neurons are particular types of neurons that arise from the anterior horns of the spinal cord. Motor neurons [10] have cell bodies of considerable size and possess a nucleus characterized by a large clearly evident nucleolus; they have several dendritic branches that arise directly in the cell body but each motor neuron gives rise to only one axon.

Each somatic motor neuron that leaves the medulla to go towards the relative muscle emits a recurrent axon which, returning to the medulla, enters into synapse with an inhibitory interneuron.

This inhibition system eliminates the possibility of overstimulation of a muscle, called tetanic stimulation, which can be physiological (for example the maximal isometric contraction) or pathological: the pathological tetanic contraction is a symptom of the homonymous disease and is caused by the destruction of these inhibitory neurons collateral caused by the tetanus clostridia.

The motor axon then enters the muscle and branches into unmyelinated branches; these terminal fibers run on the surface of a muscle fiber and establish numerous synaptic contacts, called neuromuscular junctions.

Each muscle fiber comes into contact with only one axon while a single axon innervates several muscle fibers.

The complex formed by the axon and the muscle fibers that it innervates constitutes a **motor unit**.

2.4.2 The motor units

A motor unit [9] is made up of a group of fibers innervated by the **motor neuron** itself and therefore constitutes the functional unit of skeletal muscles.

The fibers belonging to the same motor unit are generally not contiguous but are scattered in the section of the muscle; so if a motor neuron is stimulated, a large portion of the muscle appears to contract.

The number of fibers that make up a motor unit can vary from 3 to 2000, depending on the precision of the movement to which the muscle is responsible; the ratio between the number of muscle fibers and the number of nerve fibers in a muscle is called the *innervation ratio*.

A muscle composed of all three types of muscle fibers will have different motor units for all three types of fibers: for low muscle tension only the motor units composed of type **I** (Slow Oxidative, **SO**) fibers are contracted (recruited); as the tension increases, the motor units composed of type **IIA** (Fast Oxidative-Glycolytic, **FOG**) fibers are recruited first and then those of type **IIB** (Fast Glycolytic, **FG**).

The activation of the motor units follows the *Henemann's size principle* and the fibers belonging to the same motor unit obey the law of all or nothing: either they contract to the maximum, or they do not contract at all.

The force that a muscle is able to exert increases in proportion to the number of motor units recruited and the frequency of action potentials.

Muscle fibers

Each fiber is innervated by an axon belonging to a motor neuron which controls the behavior of the fiber itself.

The fiber becomes the seat of electrochemical phenomena as a result of the arrival of a nerve impulse (*spike*) which manifest themselves from a mechanical point of view with the generation of a force impulse (*twitch*).

The fiber then begins to contract generating force based on the length of the fiber and the speed of contraction: if the fiber is allowed to shorten (*concentric contraction*) the force generated will be less than when the fiber is kept at a constant length (isometric condition) and this it will, in turn, be less than when the fiber is stretched by external forces (*eccentric contraction*).

The force twitch is characterized by three distinct phases:

- **Latency phase**: time between the arrival of the nerve stimulus and the beginning of the contraction phenomenon;
- **Strength Gain phase**: the main contraction phase;
- **Strength Decrease phase**: also called the relaxation phase

These various temporal phases and the amplitude of the generated force peak are characterized by parameters that vary according to the kinematic conditions, the geometric dimensions of the various components of the motor unit (nerve termination, motor plate, muscle fiber) and the conversion mechanism of metabolic to mechanical energy.

Fibers types

Depending on the system used and the speed with which energy is made available to the contractile system of the sarcomere, three types of muscle fibers can be classified:

- **Slow Oxidative** fibers (**SO**) called type **I**: are supplied with a dense network of blood vessels that supply oxygen and nourishment and contain many mitochondria; they mainly use the aerobic energy system, contract slowly and are able to respond to repeated stimulations for a long time (they are mostly present in the antigravity muscles);
- **Fast Glycolic** fibers (**FG**) called type **IIB**: they mainly use the anaerobic glycolytic system: they are supplied with a few blood vessels and contract very quickly but are unable to repeat the same force twitch for long times, they provide the so-called "*explosive power*";
- **Fast Oxidative-Glycolic** fibers (**FOG**) called type **IIA**: they utilize both aerobic and anaerobic energy systems. They contract quickly and are well perfused by the capillaries, so they can maintain the contraction for relatively long periods of time.

Type I and IIA fibers are also called *red fibers*; the red color is due to the massive presence of myoglobin inside them. Type IIB fibers are also called *white fibers*, given the almost total absence of myoglobin inside them. The force twitches of slow and fast fibers are characterized by a different duration of the contraction phenomenon.

Recruitment and Contraction

Contraction When the same fiber is repeatedly stimulated, there is a temporal summation effect of the force twitches which can lead to the so-called "*fusion*", a situation in which the individual twitches are no longer distinguishable.

Given the different speeds with which the force twitch is generated in the two types of fibers (slow and fast), the frequency at which this phenomenon occurs (*fusion frequency*), is low for slow fibers, and high for fast fibers.

The same phenomena that are generated in a single muscle fiber occur with similar characteristics in all the muscle fibers belonging to the same motor unit, ie innervated by the same motor neuron.

The force twitch of the motor unit will therefore have approximately the same temporal trend as the twitches of the individual fibers that compose it, and an amplitude equal to the sum of the amplitudes of the individual twitches, will therefore depend on the number of muscle fibers that compose it.

Henneman Recruiting Principle In general, there is a correspondence between the characteristics of motor neurons and those of the muscle fibers innervated by them:

- ***Small muscle fibers*** (slow, oxidative, resistant to fatigue): they make up motor units with a low innervation ratio and receive small diameter axons from small motor neurons; they are characterized by low conduction speed and are the first to be activated for low values of force required by the muscle;
- ***Larger diameter muscle fibers*** (fast, glycolytic, easily fatigued): they make up motor units with a high innervation ratio and are innervated by large diameter axons; they are characterized by high conduction speeds and are activated only when it is required to produce high forces.

The value of force above which a certain type of motor unit is called into action is called "*recruitment threshold*", the initial frequency at which the

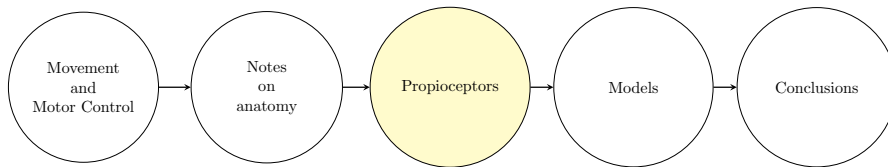
motor unit begins to be activated is called "*recruitment frequency*".

As muscle strength increases, the frequency of each motor unit increases to a maximum characteristic of the same MU and new MUs are recruited starting from the smallest to the largest. This criterion never seems to have been contradicted by experimental evidence, and goes by the name of ***Henemann's size principle***.

As the force required by the muscle decreases, de-recruitment occurs in the opposite direction: the larger MUs stop contracting earlier than the small ones, so that the latter remain active for the entire duration of the muscle contraction.

Chapter 3

Proprioceptors



An independent chapter is intended to be dedicated to the proprioceptive organs given their importance in the model constructed for this thesis [9].

Proprioception (or kinaesthesia) the sense of static position and movement of the limbs and body, it is the ability to perceive and recognize the position of one's body in space and the state of contraction of one's muscles without the support of sight.

Proprioception, sometimes is referred to as the "sixth sense", is of fundamental importance in the complex mechanism of movement control through sensory feedback neurons.

It is made possible by the presence of specific receptors, called proprioceptive or kinesthetic receptors, sensitive to changes in body postures and body segments, which send their signals through the spinal cord, up to the brain areas responsible for processing information on position and movement, necessary for the correct execution of the movement itself.

In this thesis the main ones will be examined:

- Muscle spindles: it responds to the speed and different length of muscle fibers;

- Golgi tendon organs: it is placed at the muscle-tendon junction and it is sensitive to variations in tension.

3.1 Muscle spindle

The muscle spindle is a proprioceptor which is inserted into the muscle in parallel to the muscle fibers; from this position it is stressed to lengthen or shorten according to the movement made by the extrafusal fibers, therefore being able to produce information related to the length or variation in length of the muscle fibers.

The information thus generated will be conveyed by the afferent fibers to the spinal level where, through neuron connections in the spinal cord, they will be transported to the competent areas of the brain.

There is also an efferent system, the purpose of which is to vary the sensitivity or the intervention threshold of the spindle, modifying its behavioral characteristics, automatically or depending on voluntary orders.

3.1.1 Structure

It is essentially a bundle of fibers (fig.3.1) wrapped in a sheath that has a central swelling (capsule) and contains interstitial fluid.

This bundle consists of three types of intrafusal muscle fibers:

- ***Nuclear Bag fibers (NB)***, usually divided in 1 bag1 and 1 bag2: they are the longest fibers (about the same length as the spindle), with a section of about $2\mu m$; they are divided into a central "non-contractile" area called the "nuclear bag", where the nuclei of the cells and a few myofibrils thicken, and the external "polar" regions, which are contractile in a similar way to the extrafusal fibers of the muscle;
- ***Nuclear Chain fibers (NC)***, ranging from 4 to 11 fibers: they are about half the length of those with a nuclear bag, and have a diameter of about $12\mu m$; nuclei and myofibrils are distributed throughout their length making them more uniform in terms of elasticity.

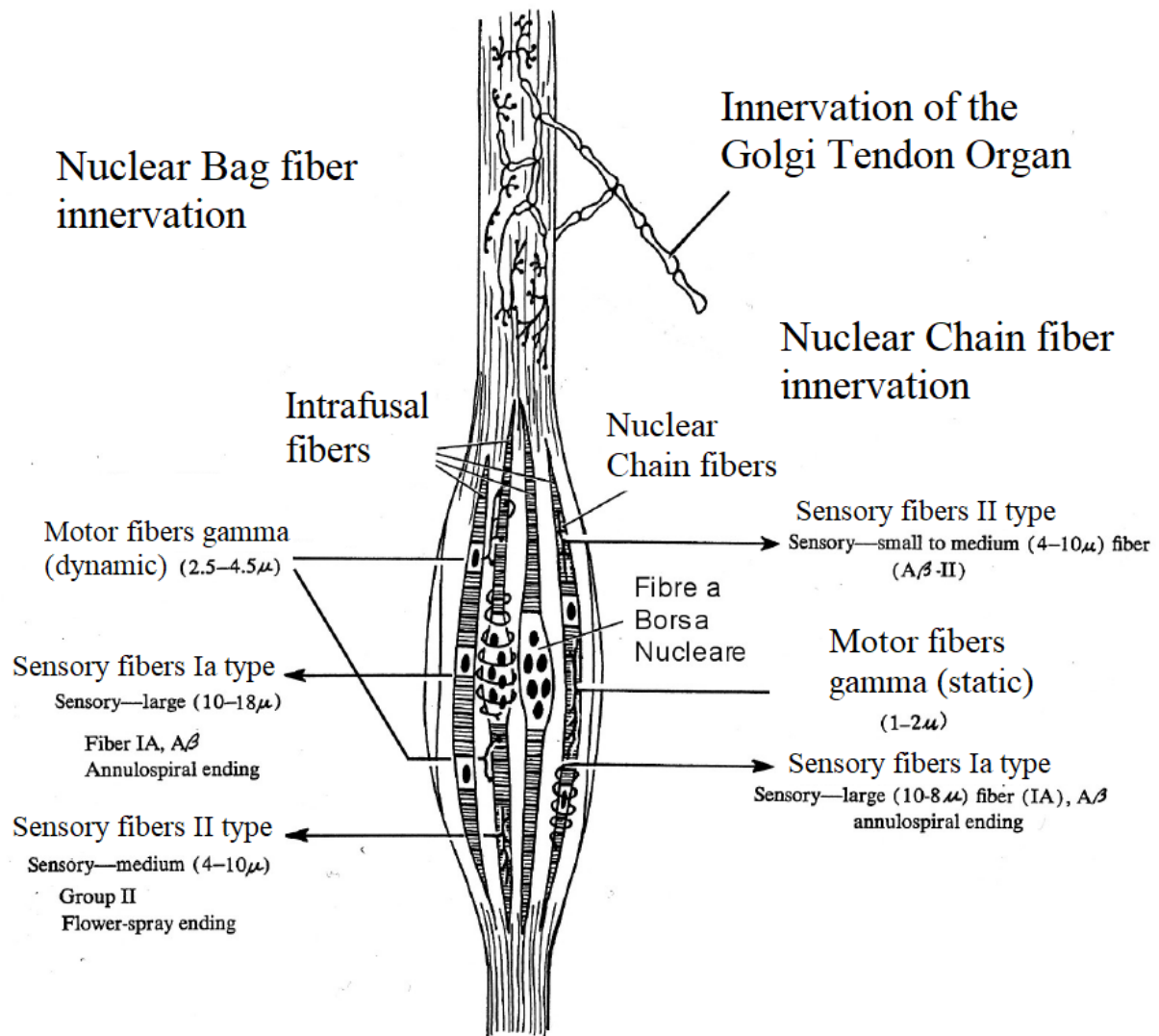


Fig. 3.1. Structure of the muscle spindle

Image taken from "BIOINGEGNERIA DEL SISTEMA MOTORIO"

Innervation

The system consisting of muscle and spindles is innervated by two types of nerve fibers: afferent fibers (*afferents*) and efferent fibers (*efferents*). The **afferents** are divided according to their diameter into fibers of type I, II, III:

- Type I come from both the spindle (Ia) and the Golgi tendon organ (Ib);

- Type II come only from the spindle;
- Type III originate from other receptors, cutaneous and articular.

The **efferences** that reach the spindle are also divided into two large categories:

- Alpha: they innervate the muscle directly (also called "extrafusal" muscle fibers);
- Gamma: they innervate the spindle inside the muscle (also called "intrafusal" fibers).

Afferents

The afferents coming from the spindle are divided into primary (*type Ia*) and secondary (*type II*).

For each spindle there is generally only one primary afferent while the secondary ones are present in a variable number from 0 to 6, but generally they are 1 or 2.

The primary afferents spiral on the central part of both the nuclear bag fibers and the nuclear chain fibers; the secondary afferents, on the other hand, are wound only on the nuclear chain fibers in regions a little more peripheral than the central area.

A schematic of the innervations of these fibers is shown in figure (fig.3.1).

Efferents

The efferences innervating the spindle are the gamma efferences (γ). Also in this case they can be divided into two categories according to their diameter and precisely in $\gamma_{Dynamic}$ and γ_{Static} .

The γ_D efferences innervate the polar regions of the nuclear bag fibers, and their terminations are of the plate type, that is, of the innervations that occur on the muscle fibers.

The γ_D efferences, on the other hand, end with innervations spread only on the nuclear chain fibers and are distributed along the entire fiber.

A summary scheme that recalls the links between the fibers of the spindle and its afferent and efferent fibers is shown in figure (fig.3.1).

3.1.2 Spindle Physiology

The numerous physiological experiments on the neuromuscular spindle mainly concern its response to both mechanical (stretching) and nervous (stimulation of the efference) external stimuli.

For responses to mechanical stimuli, the first experiments were carried out on deafferented spindles, or rendered so by means that inhibit the transmission of nerve impulses along the γ fibers.

According to the terminology of Katz (1950), two response phases can be identified: during the first there is an increase in the firing frequency due to the variation in length and is called 'dynamic', the second, during which the frequency is established at a value dependent on the elongation undergone is called 'static'.

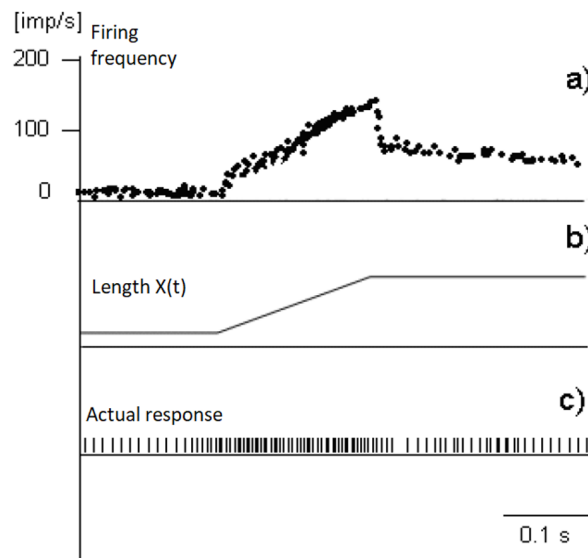


Fig. 3.2. Muscle spindle - comparison between fibers Ia and II dynamics

The spindle is subjected to a classic elongation in physiology tests: **b)** ramp elongation, that is, an elongation at a constant speed, time is represented on the abscissa and the elongation on the ordinate; **a)** response frequency chart, with the time on the abscissa and the instantaneous frequency of the output pulses on the ordinate; **c)** sequence of impulses showing the response of the primaries as a function of time.

Image taken from "BIOINGEGNERIA DEL SISTEMA MOTORIO"

By lengthening the spindle, an increase in the response frequency is obtained; instead, by causing a shortening, a decrease in frequency is obtained and in some cases even complete silence, that is, the absolute lack of output pulses. To simplify the problem, we begin to examine the system in the absence of gamma stimulation and neglecting the secondary afferents.

The spindle is subjected to a classic elongation in physiology tests: a ramp elongation, that is, an elongation, at a constant speed. Figure (3.4b) shows the time on the abscissa and the elongation to which the spindle is subjected on the ordinate; Figure (3.4a) shows the response frequency chart, with the time on the abscissa and the instantaneous frequency of the output pulses on the ordinate.

Fig.3.4c) shows the actual response of the primaries as a function of time, which is given by a sequence of impulses. From this we obtain the frequency chart of figure Figure (3.4) , measuring the time elapsed between the impulse under examination and the previous one: the inverse of the measured time

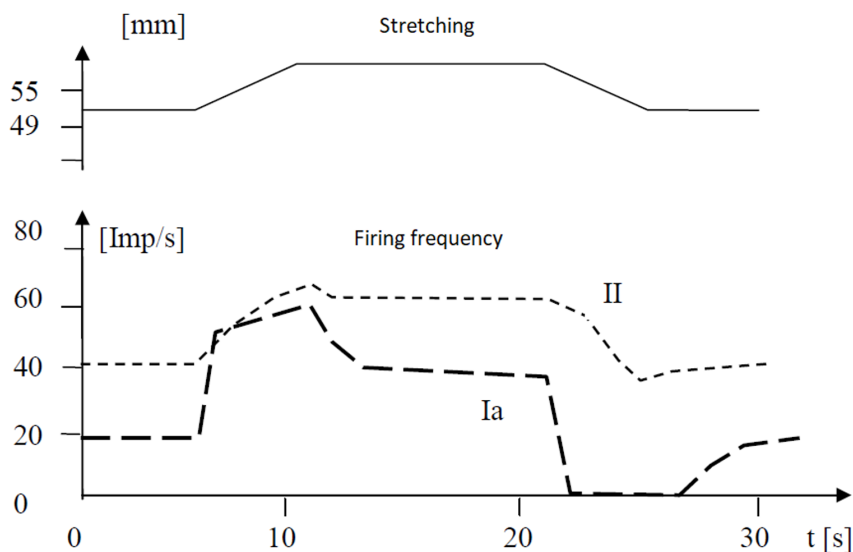


Fig. 3.3. Muscle spindle - comparison between fibers Ia and II dynamics

Comparison between fibers of type Ia and II performed on the nerve fibers of the same spindle belonging to the 'tenuissimus' muscle of the cat. The small dynamic phase that is observed in II is probably due to the readjustment of the length of the muscle fibers themselves after the lengthening they have undergone. Image taken from "BIOINGEGNERIA DEL SISTEMA MOTORIO"

is considered as the instantaneous frequency relating to the impulse under examination.

Fibers II are distinguished from Ia by their smaller diameter and slower conduction speed, as well as by a higher excitation threshold. The most important features that distinguish them from Ia are the lack of the dynamic phase and the period of silence in the shortening.

A comparison between the two types of fibers is provided by the experiments of Besson and La Porte (fig.??) performed on the nerve fibers of the same spindle belonging to the 'tenuissimus' muscle of the cat. The small dynamic phase that is observed in II is probably due to the readjustment of the length of the muscle fibers themselves after the lengthening they have undergone.

3.1.3 Spindle dynamics

Regarding the effect of the stimulation of the γ fibers, some microscopic observations performed by Boyd (1966) showed that a stimulation of the γ_S fibers produces a contraction of the NC fibers, with consequent lightening of the load on the equatorial zone of the NB fibers.

Following this principle it can be assumed that instead the efferents γ_D with nerve endings on the polar zones of the NB fibers act by making these portions contract, so as to overload the sensitive equatorial zone.

With this mechanism it is possible to attenuate or revive the activity of Ia by exciting the first or second type of γ fibers.

The typical behavior of the Ia response to an elongation ramp can be schematized as follows:

- **Dynamic index:** the difference between the firing frequency at the end of the ramp and that at which it settles in steady state;
- **Static sensitivity:** the ratio between the frequency variations before and after the elongation and the elongation itself;
- **Dynamic sensitivity:** the relationship between the dynamic index and the elongation speed
- **Polarization:** the initial frequency.

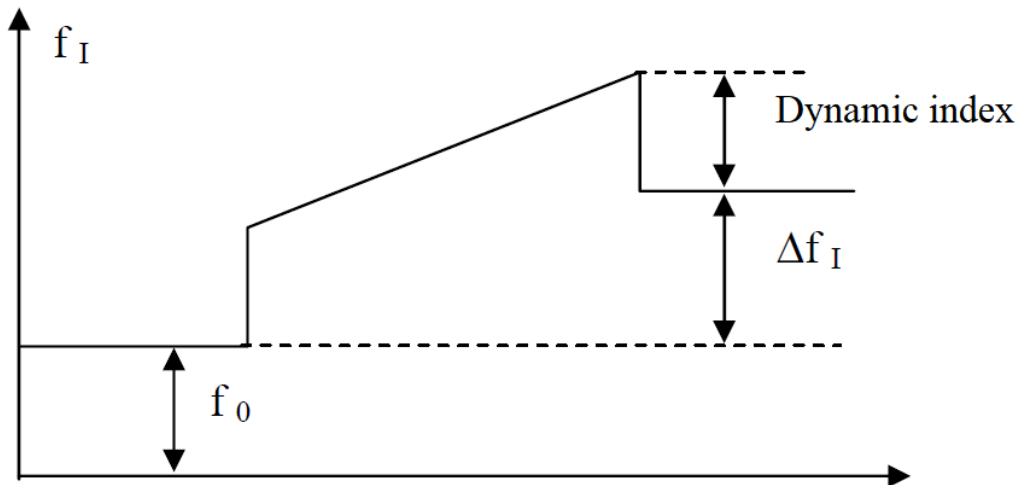


Fig. 3.4. Muscle spindle - comparison between fibers Ia and II dynamics

Illustrative diagram indicating the various phases of spindle activation. Showing the frequency on the ordinate axis and time on the abscissa axis, it shows:

- **Dynamic index:** the difference between the firing frequency at the end of the ramp and that at which it settles in steady state;
- **Static sensitivity:** the ratio between the frequency variations before and after the elongation and the elongation itself;
- **Dynamic sensitivity:** the relationship between the dynamic index and the elongation speed.
- **Polarization:** the initial frequency f_0 .

Image taken from "BIOINGEGNERIA DEL SISTEMA MOTORIO"

It can be said that a stimulation of the γ_D increases the dynamic index and dynamic sensitivity, while leaving the static sensitivity and polarization unchanged or almost unchanged.

A stimulation of the γ_S instead decreases the dynamic index and increases the static sensitivity and polarization.

It can therefore be concluded that qualitatively the fibers γ_D influence the response of Ia to elongation, such as to enhance the dynamic characteristics (depending on the elongation speed), while they have no influence on the static ones (depending on the elongation).

The γ_S fibers, on the other hand, have a depressing effect on the sensitivity to the stretching speed, but exhilarating on the sensitivity to the stretch.

It should be noted that in case of shortening there is no longer the silence of the Ia, but a simple decrease in frequency: very abrupt if the stimulation is

γ_D , continuous and regular if the stimulation is γ_S .

On the other hand, studying the influence of stimulation γ on afferent fibers II, it is noted that the γ_S have an effect similar to that which they have on Ia, while the γ_D have absolutely no effect.

This is evidently in relation to the fact that the fibers II have terminations only on the fibers at NC, while the γ_D act only on the fibers at NB.

However, it should be added that physiological experiments to stimulate these small nerve fibers are extremely delicate, as it is not easy to isolate them safely and totally exclude uncontrollable effects.

3.2 Golgi Tendon Organ

Given the arrangement in series with the muscle fibers, in the muscle-tendon junction, the Golgi Tendon Organ (GTO) is subjected to a portion of the force generated by the entire muscle, and can therefore detect its extent. The afferent fibers Ib encode the force applied to the muscle in firing frequency, and have an inhibitory effect on the alpha motor neuron. In practice, the operation is highly non-linear, with threshold and saturation, and the most evident effect is that of inhibition of contraction in the presence of high forces. It therefore has a protective function for the muscle.

3.3 Spindle reaction to contraction

Fig.3.5 shows how the spindle reacts to muscle contraction. As can be seen, the response to an externally imposed elongation can be strongly controlled (modulated) by the signals coming from the system γ . The shortening of the muscle due to the contraction produces a lowering of the spindle discharge. This lowering can be avoided by the simultaneous contraction of the intrafusal fibers, which keep the central part sensitive to elongation in tension. This is an example of alpha-gamma linkage (alpha-gamma co-activation).

Fig.3.6 shows the GTO structure and how it is affected by the contraction.

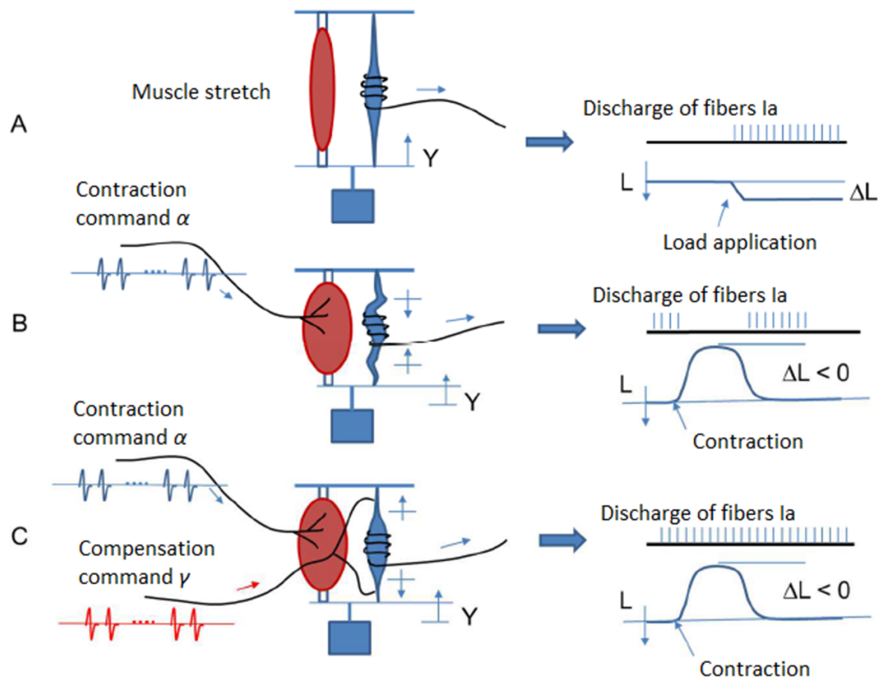


Fig. 3.5. Spindle reaction

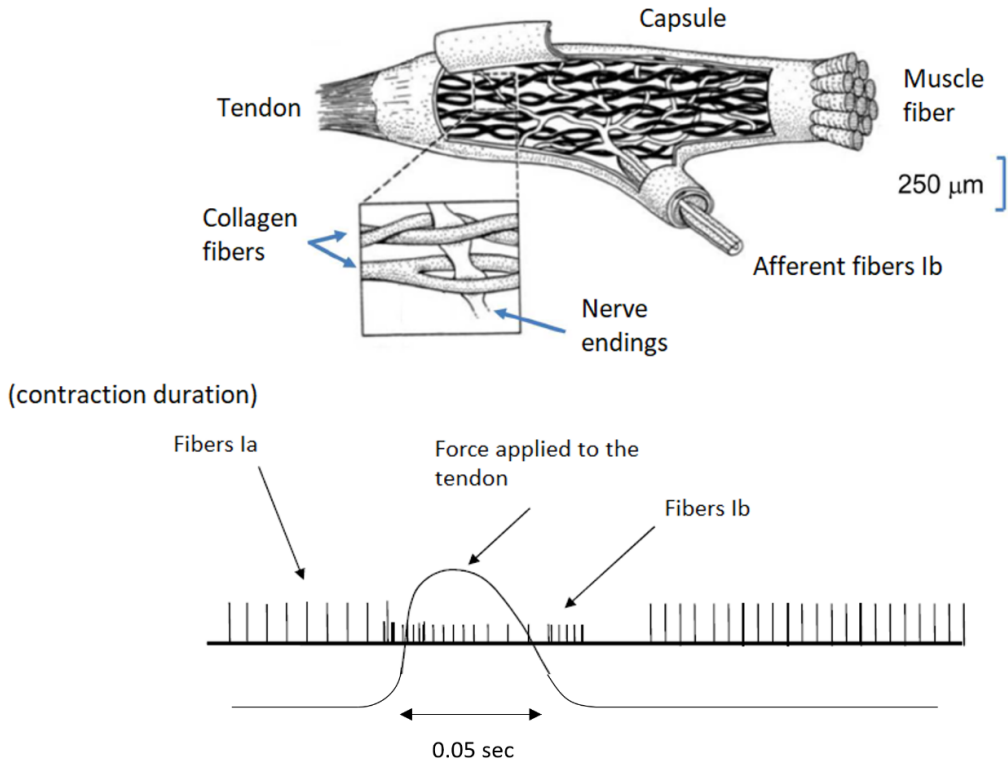
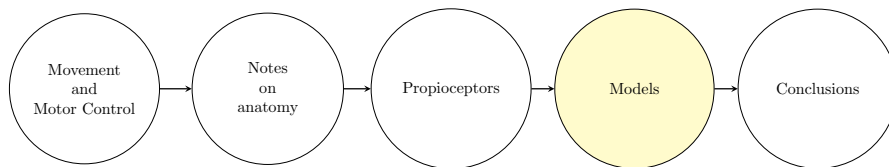


Fig. 3.6. GTO structure and reaction

Images taken from "BIOINGEGNERIA DEL SISTEMA MOTORIO"

Chapter 4

Mathematical model of the neuromuscular system



The objective of the proposed model, consisting of a mathematical model biologically inspired by the neuromuscular system and a representative model of the afferent system, is to:

- Generate a realistic model that is able to provide a qualitative description of an MN pool with the presence of the afferents fibers and the MN controller;
- Check if high frequency signals can control force generation.

In order to do so, a mathematical model biologically inspired by the neuromuscular system was created and two different representative models of the afferent system were connected to it:

- The first is a complete model that tries to be as realistic as possible in its structure, simulating the activity of the muscle spindle and the GTO, and of all the nerve connections and synapses that bring the signal back to the spine;

- The second model, on the other hand, reduces the realism of the first model to mathematical formulas that are in any case able to represent, in a qualitative way, the behavior of the afferences in the motor neuron loop: its purpose is to react to changes in muscle dynamics and consequently modulate the excitability of NM using physiological-inspired positive and negative feedback loops.

The idea is to test which system is best able to simulate what happens during a contraction: for this reason, a series of tests (5.2) have been carried out in order to see how the models react to different types of inputs and what is the "message" that is returned to the MN pool and then to the control unit. To see how high-frequency signals adapt to motor neuron control and compare their behavior to low- and high-frequency signals, an analysis of the behavior of the models at frequencies $0Hz$ (no modulation), $5Hz$, $15Hz$ and $20Hz$ is performed.

4.1 Descending run model

The following model is used to simulate the descending circuit that connects the motor cortex to the motoneuron (MN) pool. The structure of the model that simulates the descending run is well described in (Watanabe, Kohn; 2015) and is shown in the fig.4.1.

The model describes all the various sections that form the descending circuit.

Cortical common input The input from the cortex is described by 4000 descending axons; each of these 4000 axons connect to $\sim 30\%$ of the MNs, randomly chosen for each simulation run (each MN will roughly receive a similar number of synaptic inputs).

The spike trains of descending axons were modeled as independent renewal point processes with interspike intervals (ISIs) following a Poisson distribution.

Motoneuron Pool Each motor unit encompasses a MN and a muscle unit (MU). The input to the MN pool is the combination of the common synaptic inputs (**CSI**) and a different independent noise (**IN**) source input in the

form of a Poisson point process, with the ISIs following a Poisson distribution.

The MN models follow (Cisi and Kohn, 2008): they are conductance based, with two compartments to represent the MN soma and the dendritic tree, as can be seen in fig.4.2 - 4.3.

The MN pool used in this study is composed of 10 slow MNs, 10 fatigue resistant MNs, and 5 fast-fatiguing MNs (Watanabe et al., 2013), for a total of 25 motor neurons that were representative of crucial properties observed in the cats. All the synapses, from the CSI and the IN inputs, on a given MN act through changes in the dendritic conductances (Watanabe et al., 2013; Destexhe et al., 1993).

The net dendritic synaptic conductance of a randomly chosen MN provides an estimate of the overall CSIs to the MNs since, probabilistically, the MNs have similar net synaptic conductance signals.

Twitch and force generation Following [8], the force produced by a given MU is obtained by the convolution of the respective MN spikes with the impulse response of a second-order critically damped system.

This force signal is then passed through a nonlinear saturation (Watanabe et al., 2013) and summed to the force signals of the other MUs, resulting in the muscle force $F(t)$.

$$a(t) = A_{peak} \frac{t}{t_{peak}} \exp\left(1 - \frac{t}{t_{peak}}\right) u(t) \quad (4.1)$$

$$e(t) = \sum \delta(t - t_{APi}) \quad (4.2)$$

$$f(t) = e(t) \cdot a(t) \quad (4.3)$$

$$(4.4)$$

Where $a(t)$ is the function that models one twitch; A_{peak} and t_{peak} are the peak and time-to-peak (or contraction time) of the twitch; $u(t)$ is the Heaviside step function; $f(t)$ is the force developed by one MU; $e(t)$ is the system input, i.e., the superposition of all MU action potentials occurring at

times t_{AP_i} .

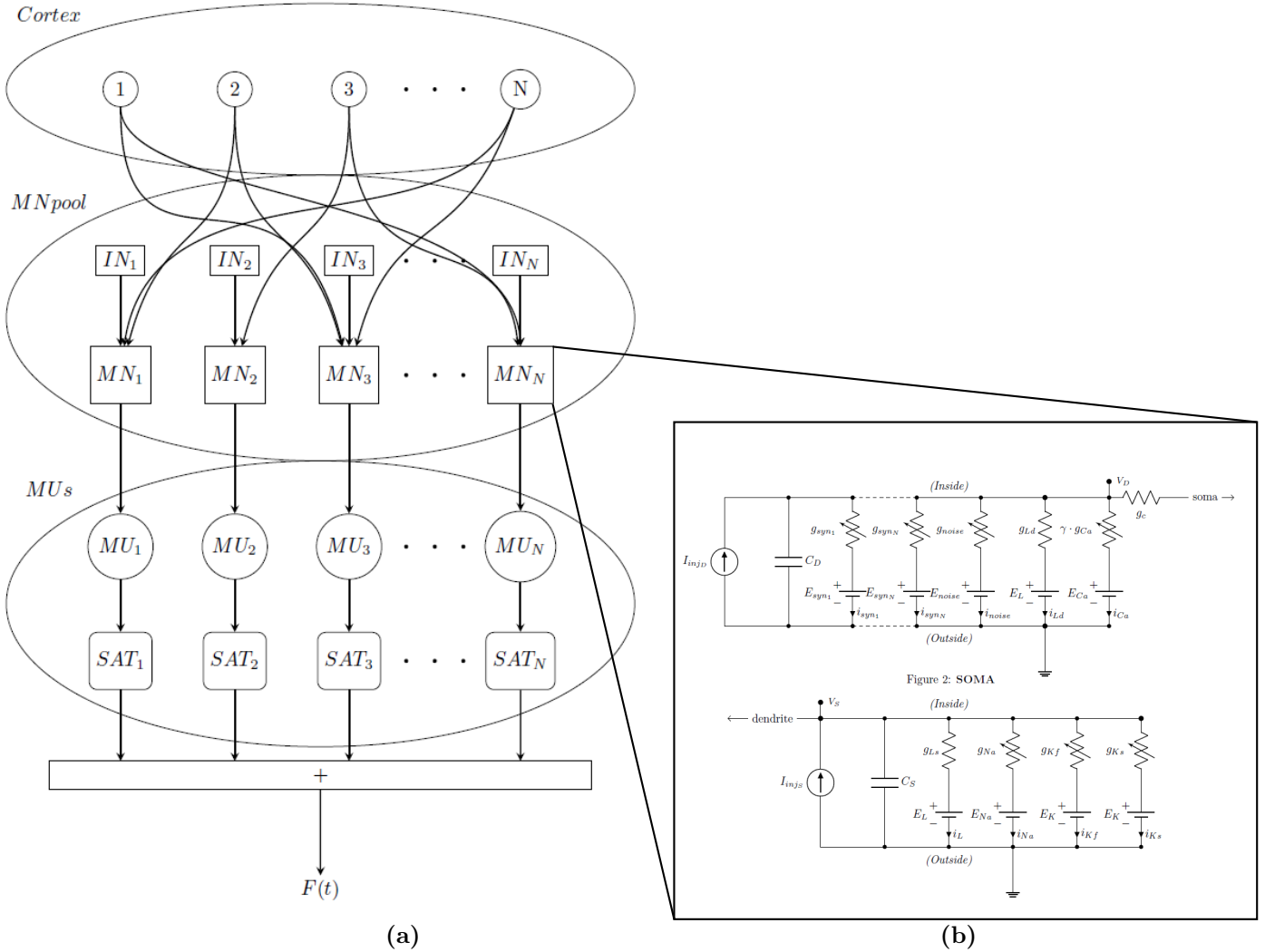


Fig. 4.1. Descending run model

(a) Schematic view of the overall model.

Cortical common input: the input from the cortex is described by 4000 descending axons; each of these 4000 axons connect to $\sim 30\%$ of the MNs, randomly chosen for each simulation run (each MN will roughly receive a similar number of synaptic inputs).

Motoneuron Pool: each motor unit encompasses a MN and a muscle unit (MU). The input to the MN pool is the combination of the descending signal from the cortex and a different independent noise (IN) source input in the form of a Poisson point process, with the ISIs following a Poisson distribution. The MN pool used in this study is composed of 10 slow MNs, 10 fatigue resistant MNs, and 5 fast-fatiguing MNs (Watanabe et al., 2013).

Contraction: following (Cici, Khon - 2008), the force produced by a given MU is obtained by the convolution of the respective MN spikes with the impulse response of a second-order critically damped system.

(b) Equivalent circuit used to represent each MN model.

Neural fibers modeling All the neural fibers are modeled following the studies by Cisi and Kohn (2008).

The parameters are randomly generated, between a given pair of values, for each fibers, making each fiber unique and resulting in different pools every time they are generated (see Appendix A).

The model uses the Hodgkin Huxley equations to calculate the voltage-dependent ionic currents through channels [1]: all the differential equations(4.5 to 4.7) need were solved using a fourth-order Runge - Kutta method with fixed step of 0.05 ms.

Rate constants approximated by short rectangular pulses were used compared to traditional non-linear functions [11]; by using this activation approach is that, it was possible to remove the non-linearities from the rate functions, allowing to use larger time steps when solving the differential equations, thus increasing the computational efficiency [11]. The pulses would be activated when the membrane potential in the compartment crossed the voltage threshold, with a duration of 0.6ms.

The original values for the rate constants were estimated from depolarised and hyperpolarised values from Traub's original formulation.

The somatic compartment contains $Na+$ and fast $K+$ currents, that are responsible for generating somatic spiking, and a slow potassium current that produces an after hyperpolarisation; the dendritic compartment has L-type Ca^{2+} current to make dendrite active [12].

The activation variables m , h , n , p and q represent the state of the sodium activation, sodium inactivation, fast potassium activation, slow potassium inactivation. The value of the activation variable is determined by its associated rate constant. The maximum conductance values were selected to bring the physiological properties of the motoneurons in line with what is plausible based on previous experimental characterisation.

$$C_d \frac{dV_d(t)}{dt} = -I_{syn_d}(t) - g_{ld}(V_d(t) - E_l) - g_c(V_d(t) - V_s(t)) + I_{inj_d}(t) \quad (4.5)$$

$$C_s \frac{dV_s(t)}{dt} = -I_{syn_s}(t) - g_{ls}(V_s(t) - E_l) - g_c(V_s(t) - V_d(t)) + I_{inj_s}(t) \quad (4.6)$$

$$I_{ion}(t) = \bar{g}_{Na} m^3 h (V_s(t) - E_{Na}) + \bar{g}_{Kf} n^4 (V_s(t) - E_K) + \bar{g}_{Ks} q^2 (V_s(t) - E_K) \quad (4.7)$$

$$C_s = 2 \cdot \pi \cdot l_s \cdot r_s \quad (4.8)$$

$$C_s = 2 \cdot \pi \cdot l_s \cdot r_s \quad (4.9)$$

$$C_d = 2 \cdot \pi \cdot l_d \cdot r_d \quad (4.10)$$

$$g_c = \frac{2}{\frac{R_i \cdot l_d}{\pi \cdot r_d^2} + \frac{(R_i \cdot l_s)}{\pi \cdot r_s^2}} \quad (4.11)$$

$$g_{ls} = \frac{2 \cdot \pi \cdot r_s \cdot l_s}{Rm_s} \quad (4.12)$$

$$g_{ld} = \frac{2 \cdot \pi \cdot r_d \cdot l_d}{Rm_d} \quad (4.13)$$

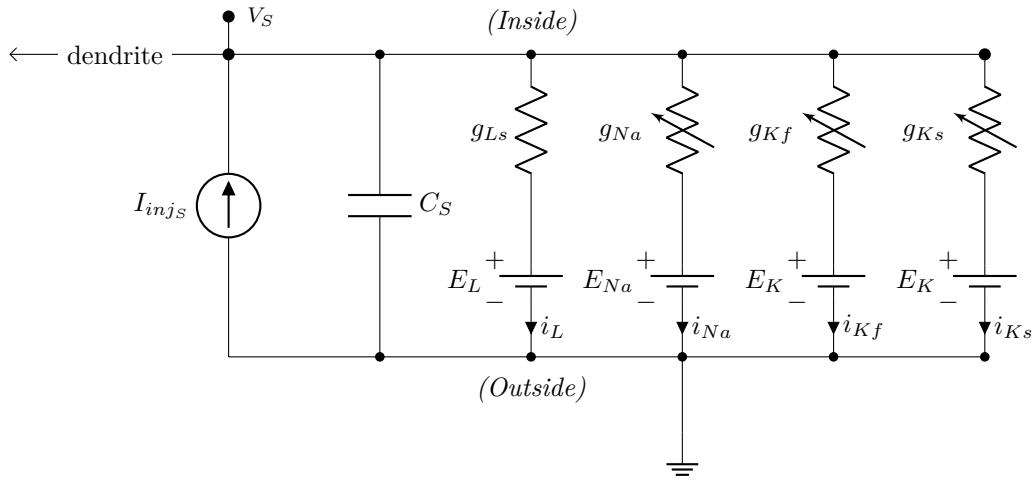
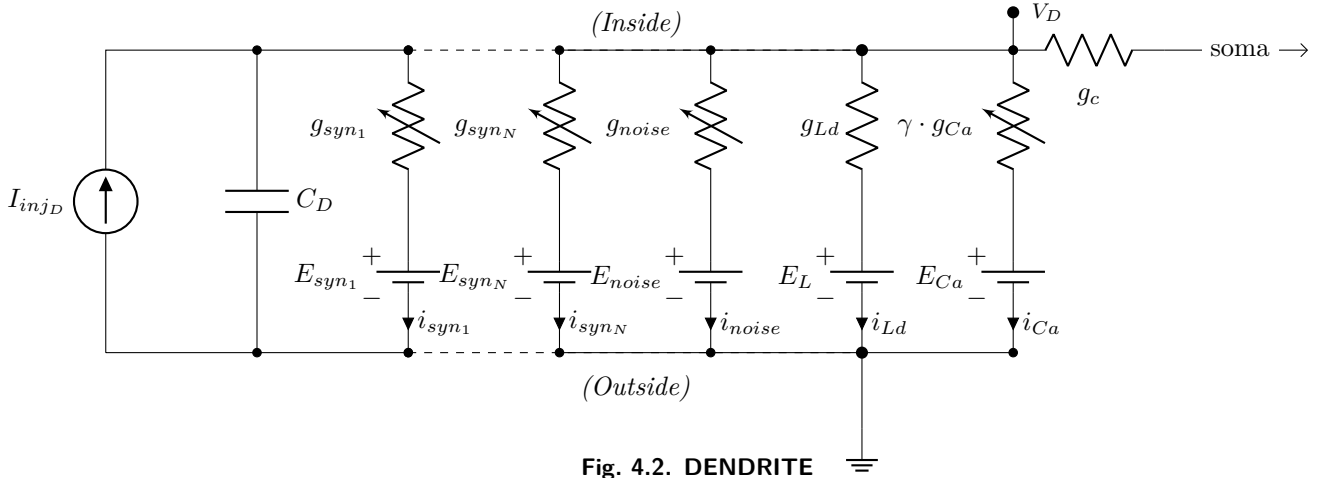
$$Rn = \frac{1}{g_{ls} + \frac{g_{ld} \cdot g_c}{g_{ld} + g_c}} \quad (4.14)$$

$$V_{th} = Rn \cdot I_{rh} \quad (4.15)$$

Equations (4.5), (4.6), (4.7), (4.11), (4.12), (4.13), (4.14), and (4.15) describe the membrane potentials of the dendrite and soma compartments of the motoneuron models.

In these equations, $V_d(t)$ and $V_s(t)$ are the dendritic and somatic membrane potential; E_l is the leak equilibrium potential; g_{ld} and g_{ls} are the leak conductance for dendrite and soma; g_c is the coupling conductance; C_d and C_s are dendritic and somatic membrane capacitances; C_m is the membrane specific capacitance; R_i is the cytoplasm resistivity; Rm_d and Rm_s are den-

dritic and somatic membrane specific resistances; l_d , l_s , r_d and r_s are the dendritic and somatic compartment length and radius; $I_{syn_d}(t)$ and $I_{syn_s}(t)$ are the postsynaptic currents caused by independent synaptic connections on the dendritic or somatic compartment; $I_{inj_d}(t)$ and $I_{inj_s}(t)$ are the injected currents, inside the dendrite and the soma, for test purposes; $I_{ion}(t)$ is the membrane current due to the voltage-dependent ionic conductances (g_{Na} , g_{Kf} and g_{Ks}); m , h , n and q are state variables, whose time evolution depends on voltage-dependent rates (αm , βm , αh , βh , αn , βn , αq and βq); g_{Na} , g_{Kf} and g_{Ks} are the maximal conductances of the sodium, fast potassium and slow potassium currents, with equilibrium potentials of $E_{Na} = 120mV$ and $E_K = -10mV$. The leakage Nernst voltage was $E_l = 0mV$.



Equivalent circuit used to represent each MN model: g_{syn1} to g_{synM} , synaptic conductances of a dendrite activated by synapses 1 to M, respectively; g_c , coupling conductance; g_{Ld} and g_{Ls} , dendritic and somatic leakage conductances, respectively; g_{Na} , g_{Kf} , and g_{Ks} , conductances of Na^+ , fast K^+ , and slow K^+ , respectively; E_L , leakage potential; E_{Na} and E_K , Na^+ and K^+ equilibrium potentials, respectively; E_{syn1} to E_{synM} , reversal potentials for synapses 1 to M, respectively; C_S and C_D , somatic and dendritic capacitances, respectively; V_S and V_D , somatic and dendritic membrane potentials, respectively.

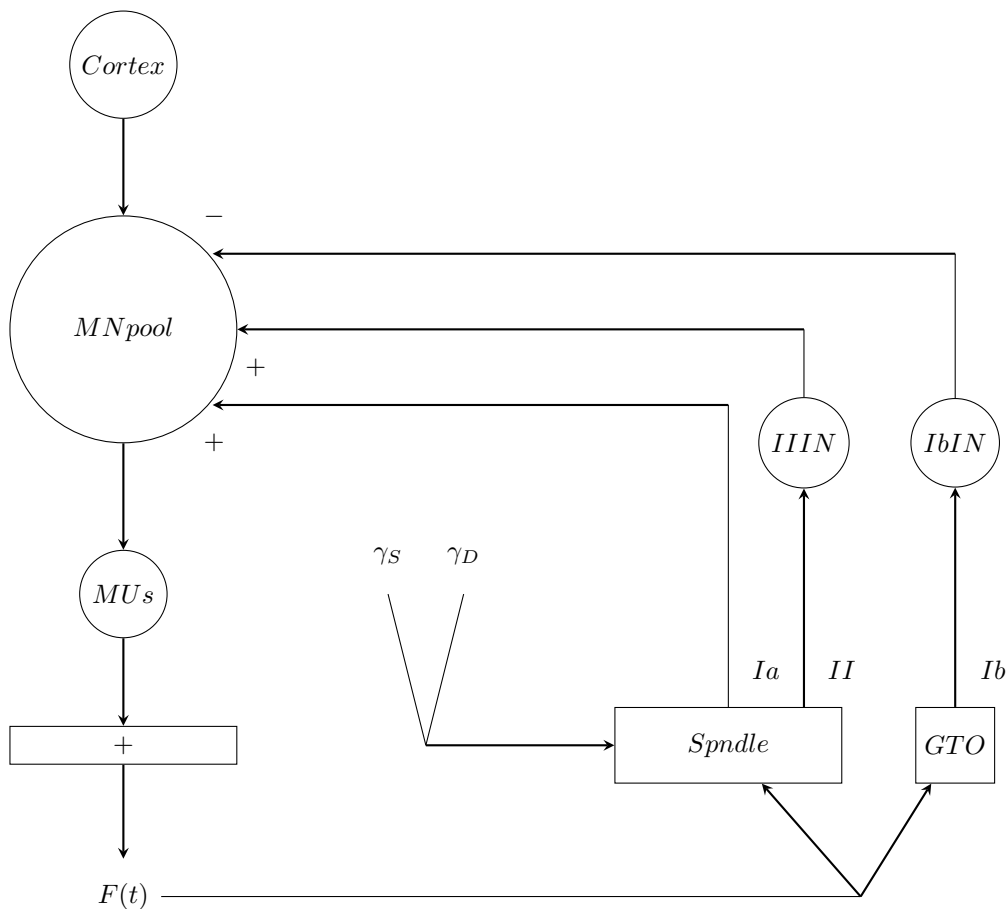


Fig. 4.4. Afferent run

Structure of the afferent feed-back model used in this study: The force generated by the twitches of the motor units is used to calculate the speed of contraction and the elongation/shortening vectors of the spindle and GTO fibers.

Inside the spindle, the combined action of the efferent fibers γ_D and γ_S and the fibers Ia and II takes place for the generation of the response to the force examined in that particular time window; when the muscle contracts, fibers Ia and II, internal to the spindle, shorten, while fibers Ib, internal to the tendon, lengthen; vice versa, when the muscle relaxes, fibers Ia and II will lengthen while fibers Ib will shorten. The Ia fibers are therefore responsible for the perception of both the speed of elongation and the displacement of the muscle fibers during the elongation phase; fibers II are responsible for perceiving only the displacement of the fibers in the elongation phase; the Ib fibers are responsible for perceiving only the displacement of the fibers in the shortening phase.

The response of the three types of fibers is sent back to the MN pool: fibers Ia enter directly into the MN pool, fibers II and Ib pass through the corresponding interneurons which act as relay cells.

4.2 Afferent run

Once the force generated by the MN pool during contraction has been calculated, we move on to the analysis of the afferent signal that reports the feedback to the spine and, in turn, to the cortex.

The afferent signals are generated by the proprioceptors, the muscle spindles and the GTO; the models of these two organs are made following the studies by (Vaughan G. et al., 2018), (James Day et al., 2017), (T. P. Knellwolf et al, 2018) and (Milana P. Mileusnic et al, 2006).

The afferent run structure can be seen in fig.4.4

4.2.1 Feed-back response

The force generated by the twitches of the motor units is used to calculate the speed of contraction and the elongation/shortening vectors of the spindle and GTO fibers.

Inside the spindle, the combined action of the efferent fibers γ_D and γ_S and the fibers Ia and II takes place for the generation of the response to the force examined in that particular time window: as the muscle contracts, fibers Ia and II, internal to the spindle, shorten, while fibers Ib, internal to the tendon, lengthen; vice versa, when the muscle relaxes, fibers Ia and II will lengthen while fibers Ib will shorten.

Following what is the natural behavior of the spindle and the GTO, the afferences are structured as follows:

- Spindle
 - Ia fibers are responsible for perceiving both the speed of lengthening and the displacement of the muscle fibers;
 - II fibers are responsible for perceiving only the displacement of the fibers in the elongation phase;
- GTO
 - Ib fibers: Ib fibers are responsible for perceiving only the displacement of the fibers in the shortening phase.

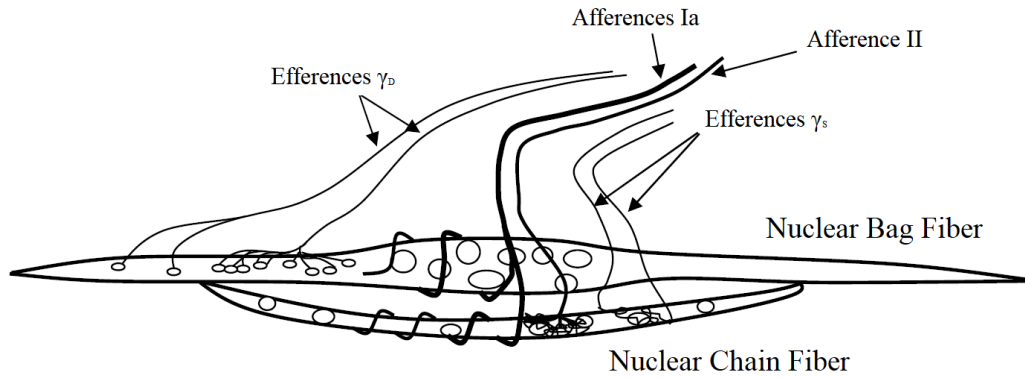


Fig. 4.5. Spindle structure

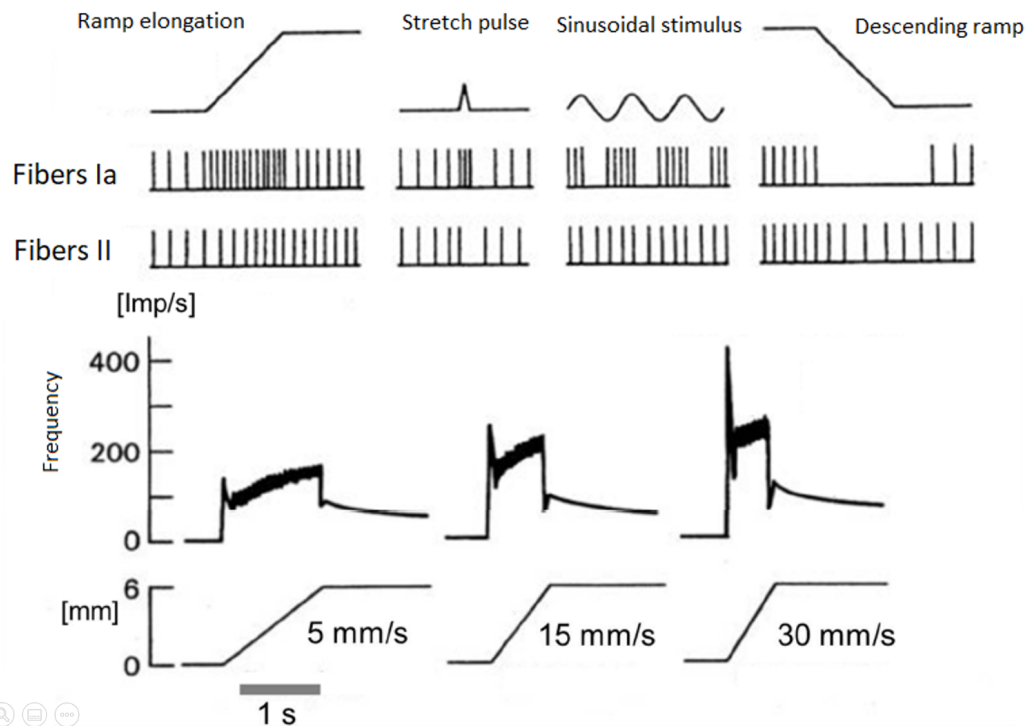


Fig. 4.6. Spindle behavior

Structure of a spindle taken as a basis for the model used: Ia fibers bind to both Nuclear Bag and Nuclear Chain fibers, II fibers only bind to Nuclear Chain fibers; the γ_D fibers bind to the Nuclear Bag fibers, the γ_S fibers bind to the nuclear chain fibers.

Images taken from "BIOINGEGNERIA DEL SISTEMA MOTORIO"

4.2.2 Full afferent model

The idea of the complete model proposed here is to simulate, in the most realistic way possible, the activity of the muscle spindle, the GTO and the entire afferent circuit during an isotonic contraction.

Models that simulate the behavior of the spindle already exist, but all them are based on the mechanics of the fibers: in this the calculation of the response of the afferents will start directly from the force generated during the twitch of the muscle.

Structure

The structure of this model tries to faithfully follow that of the corresponding anatomical system, fig.4.5-4.6 shows the structure used as the basis for the spindle and the intended behavior.

As can be seen, the afferent fibers coming from the spindle and the GTO reinsert themselves into the motor circuit in different ways. Ia fibers return directly into the MN pool, with an excitatory contribution, while Ib and II enter their respective interneurons first and then are relaid to the MN pool with an inhibitory and an excitatory contribution respectively.

Similar to how descending axons are connected to the MN pool, where each of these axons connect to $\sim 30\%$ of the MNs, also for the Ia fibers and the IbIN and IIIN outputs connectivity matrices have been built in order to randomly chose the percentage with which the fibers are connected to each other for each simulation run (each MN will roughly receive a similar number of afferent inputs).

Behavior

Response to force The model exploits the physiological functioning of the spindle and the GTO to produce the response to the contraction. The response depends on the force produced in the time window under consideration and follows the following concept:

- if $F(t) > F_{mean}(t)$ a contraction is occurring:
 - The muscle fibers are shortening;

- The tendon fibers are stretching;
- Ia and II fibers go silent
- Ib fibers start shooting
- if $F(t) < F_{mean}(t)$ a relaxation is occurring:
 - The muscle fibers are stretching;
 - The tendon fibers are shortening;
 - Ia and II fibers start shooting
 - Ib fibers go silent

Newton's second law of motion is used to calculate the speed of contraction. By dividing the force $F(t)$ by the mass m , the acceleration $a(t)$ is obtained. By integrating the acceleration, just found, over time, we obtain the displacement speed $v(t) - v(t_0)$ and by integrating again we obtain the displacement $x(t) - x(t_0)$:

$$F(t) = m \cdot a(t) \quad (4.16)$$

$$\int_{t_0}^t \frac{F(t)}{m} dt = \int_{t_0}^t a(t) dt = v(t) - v(t_0) \quad (4.17)$$

$$\int_{t_0}^t \left(\int_{t_0}^t \frac{F(t)}{m} dt \right) dt = \int_{t_0}^t (v(t) - v(t_0)) dt = x(t) - x(t_0) - v(t_0)(x - x_0) \quad (4.18)$$

$$\text{Assuming } v(t_0) = 0 \rightarrow v(t_0)(x - x_0) = 0 \quad (4.19)$$

$$\int_{t_0}^t \left(\int_{t_0}^t \frac{F(t)}{m} dt \right) dt = \int_{t_0}^t (v(t) - v(t_0)) dt = x(t) - x(t_0) \quad (4.20)$$

Once the phase in which the muscle is found has been established, the difference between the force generated during contraction and the average force, calculated in the time window considered, is integrated with respect to time; the muscle mass taken into consideration is adjustable.

With a first integral of this new force it is possible to find the speed of shortening/elongation, with a second integral it is possible to find the displacement of the fibers.

Based on this concept the speed of contraction of the fibers and their displacement are calculated as follows:

$$\text{contraction speed}(t) = \int_{t_0}^t \frac{F_{mean}(t) - F(t)}{m} dt \quad (4.21)$$

$$\text{fibers displacement}(t) = \int_{t_0}^t \left(\int_{t_0}^t \frac{F_{mean}(t) - F(t)}{m} dt \right) dt \quad (4.22)$$

These are in the form of vectors that represent speed and displacement at any instant of time.

Newton's law and Hill model Newton's law, however, is not suitable for fully representing the behavior of the muscle, resulting in speeds and lengths well above those physiologically possible: Newton's law $F(t) = m \cdot a(t)$ is a linear formula where as the parameters increase, the force involved increases, even at infinite levels.

This cannot happen in the muscle, for obvious reasons: the muscle force does not have a linear trend while in fact, following the Hill model, it has a paraboloid trend with concavitus downwards, with asymptotes representing the maximum force and speed that it can achieve.

Hill's model, however, is based on the length of the fibers and how they are lengthened or shortened during muscle activity: in order to use this model it would have been necessary to build a muscle model that simulates the contraction with mechanical displacement of the fibers; instead a time window is used within which the integrals used for the force analysis are carried out To overcome this problem, limits have been imposed on the maximum possible speed and the maximum length of the fibers.

Fibers activation The action of the γ s efferences, which should come from the cortex, are calculated on the basis of the velocity and displacement just calculated.

The average speed of contraction (AS) and the average displacement of the fibers (AD) are found:

$$AS(t) = \sum \frac{\text{contraction speed}(t)}{T} \quad (4.23)$$

$$AD(t) = \sum \frac{\text{fibers displacement}(t)}{T} \quad (4.24)$$

Where $T = 50ms$ is the length of the time window under exam, see 4.3.3.

The problem of the time window The consequence of using the force with respect to the instantaneous elongation is that, to analyze the response, it is necessary to use a predetermined time window, in our case $50ms$, thus losing the memory of which is the "rest" length of the fibers with respect to when they are stretched or contracted and, consequently, losing the instantaneity of the response, which in this case will depend on the level of strength with respect to the average of the values within the time window taken into consideration at that moment.

To overcome the memory problem, the time window of $50ms$ is analyzed $1ms$ at a time and the average of the force is calculated and updated with each new $1ms$ examined up to $10ms$: in this way a sort of fictitious "memory" is created inside the window itself, which takes into account how the dynamics of the fibers evolved in those $50ms$, the downside of this, however, is that the response depends entirely on the average: the response to an impulse or a contraction ramp will be offset from the average value, as seen in fig.5.4(d-e). Another problem of this approach is that there is no answer if the force has a constant value, which can be very problematic.

The main limitation that this model therefore has is the time window to which it is bound, resulting in the lack of firing at constant force values, due to the lack of memory of the "resting" length of the fibers, and a poorer response for high frequency inputs.

This is mainly a computational problem, due to the use of the Hole to find the length and speed parameters: in other models, based on the muscle fibers mechanics, the spindle would respond to the instantaneous elongation and to the elongation speed of the fibers; in this case, however, what is taken into consideration is the force $F(t)$ from which the parameters that we would have wanted from the ideal case are calculated backwards.

Impulse trains generation Now the the γ_D and the γ_S can be calculated as follows:

$$\gamma_D = \omega \cdot AS(t) \quad (4.25)$$

$$\gamma_S = \omega \cdot AD(t) \quad (4.26)$$

Where ω represents the weight associated with the single fiber, it is generated randomly from a uniform distribution between 0 and 1.

Following [2], the activation levels of the fibers are calculated as follows:

$$f_{dynamic} = \left[1 - \exp\left(\frac{t_{dynamic}}{\tau_{bag1}}\right) \cdot \frac{\gamma_{dynamic}}{\gamma_{dynamic} + freq_{bag1}} \right] \quad (4.27)$$

$$f_{static} = \left[1 - \exp\left(\frac{t_{static}}{\tau_{bag2}}\right) \cdot \frac{\gamma_{static}}{\gamma_{static} + freq_{bag2}} \right] \quad (4.28)$$

At this point, two conditions must be guaranteed for the pulse train generation:

- $\rho < \delta t \cdot f_{dynamic/static}$
- at least $1ms$ has passed since the previous pulse

Where ρ is a randomly generated decimal number.

When the conditions are met, a pulse is generated for that particular fiber (or fibers), the pulses last $1ms$ and have a refractory period of $1ms$.

Due to the non-linear behavior of the spindle [2], once the pulse trains have been generated, a check is made on the response level of fibers Ia and II to see which of the two generates the greater response: the response of the fiber with the lower response is set to 0.

Transport The trains of spikes thus generated are then used to generate the occupancy of the synapses, distinguishing them between excitatory and inhibitory according to the following formulas (Destexhe et al., 1994):

Letting r represent the fraction of bound receptors, the forward and backward rate for transmitter binding are described by the equation:

$$\frac{dr}{dt} = \alpha[T](1 - r) - \beta r \quad (4.29)$$

During a pulse ($t_0 < t < t_1$), $[T] = T_{max}$ and r is given by:

$$r(t - t_0) = r_\infty + (r(t_0) - r) \exp\left(\frac{-(t - t_0)}{\tau_r}\right) \quad (4.30)$$

where

$$r_\infty = \frac{\alpha \cdot T_{max}}{\alpha \cdot T_{max} + \beta} \quad (4.31)$$

$$\tau_r = \frac{1}{\alpha \cdot T_{max} + \beta} \quad (4.32)$$

After a pulse ($t > t_1$), $[T] = 0$ and r is given by: (4.33)

$$r(t - t_1) = r(t_1) \exp(-\beta(t - t_1)) \quad (4.34)$$

These equations simulate the opening and closing of synaptic channels, allowing their modeling and the simulation of the passage of current between two synapses: a single transmitter pulse can evoke a fast, excitatory conductance or a slower, inhibitory, synaptic current, parameters can be seen in

A; response saturation occurs naturally as r approaches 1 (all channels reach the open state).

In this way the signal is transformed into volts inside the fibers, which in turn will follow again the model of motor neurons already seen in fig??-??. The interneurons, at this point, will act as a relay to carry the message towards the MN pool, in particular, the fibers Ia and II will have an excitatory influence, the Ib fibers an inhibitory one.

Their model still follows that of the previous fibers with a difference in the parameters which are recovered from the Remote Project [13].

Once the afferent response has been calculated, this is added as an external input to the MNpool for the PID processing cycle, see 4.3.3.

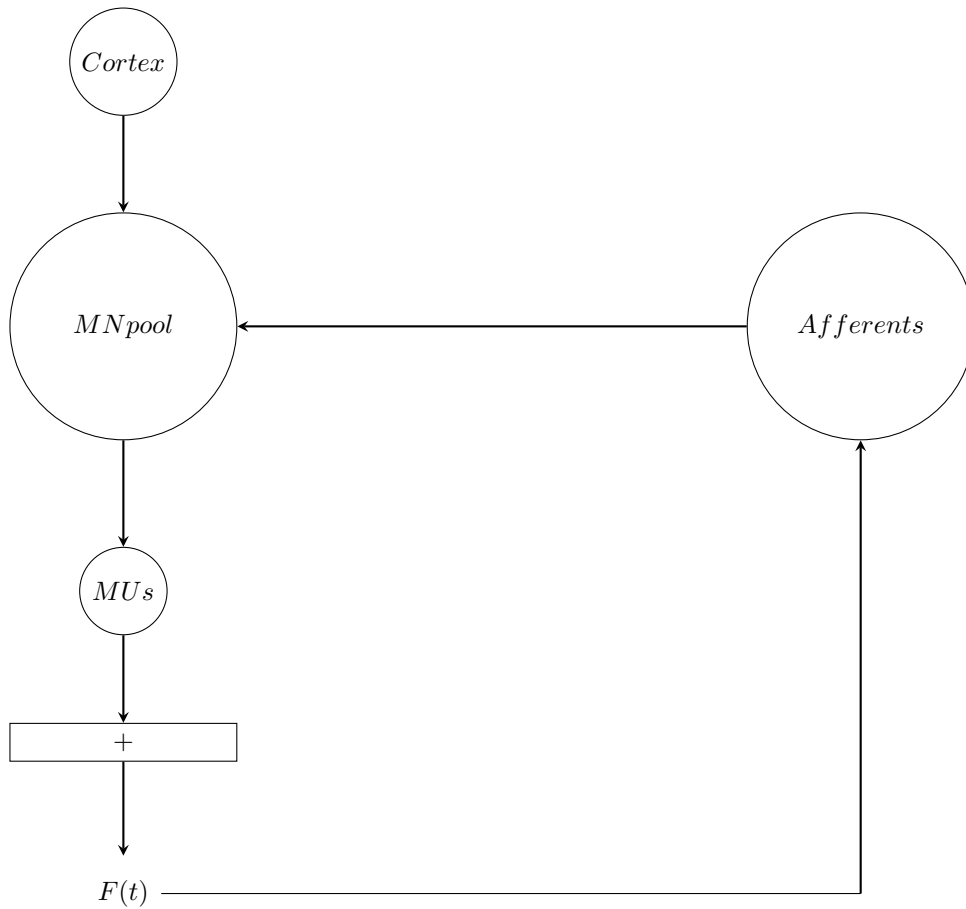


Fig. 4.7. Simplified model

Structure of the simplified afferent feed-back model used in this study: The force generated by the twitches of the motor units is used to calculate the speed of contraction and the elongation/shortening vectors of the spindle and GTO fibers.

Inside the "Afferents" block, the combined action of the efferent fibers γ_D and γ_S and the fibers Ia and II is simulated for the generation of the response to the force examined in that particular time window.

The response of the three types of fibers is combined and sent back to the MN pool where it is used to modulate the descending command.

4.2.3 Simplified mathematical model

We now move on to the simplified mathematical model.

The goal of this model is to give an afferent response given the contraction of the muscle, it is not designed to be as realistic as the complete one.

The idea of using a simplified model is to bypass the complexity of the afferent nervous system using mathematical formulas that are still able to represent the "essence" of afferences in the motor neuron loop: it reacts to changes in muscle dynamics and modulates excitability of MNs accordingly using physiologically-inspired positive and negative feedback loops.

A complexity problem During the muscular contraction numerous circuits are involved starting from the spinal cord: there are signals directed to the muscle directly involved in the contraction; signals directed to the antagonist muscle; afferent signals that report information on the just happened contraction, these are also divided between the excitatory and inhibitory ones. To all this we must also add the physical and geometric complexity of a system that is still widely studied: there is a real difficulty in obtaining in vitro results from patients due to the position, within the muscle and spine, of these circuits and due to their size.

From all these difficulties arises the need to use a simplified model that is able to give a plausible idea of what happens, within this complex system, during the activation of the muscle.

Response to force The response to force of this model remains unchanged from the previous one.

The main difference is that in this model, instead of generating impulses that will then pass to the nerve fibers, a parametric response of the afferents is generated.

More specifically:

$$\begin{aligned} \text{Spindle output Ia} &= f_{dynamic} \cdot \left(\int_{t_0}^t \frac{F_{mean}(t) - F(t)}{m} dt - \int_{t_0}^t \left(\int_{t_0}^t \frac{F_{mean}(t) - F(t)}{m} dt \right) dt \right) = \\ & f_{dynamic} \cdot (AS(t) - AD(t)) \end{aligned} \quad (4.35)$$

$$\text{Spindle output II} = f_{static} \cdot \left(\int_{t_0}^t \frac{F_{mean}(t) - F(t)}{m} dt \right) = \gamma_{static} \cdot AD(t) \quad (4.36)$$

$$\text{GTO output Ib} = \int_{t_0}^t \frac{F(t) - F_{mean}(t)}{m} dt = GTO_{AD}(t) \quad (4.37)$$

Also in this model, the integrals are unable to fully represent the behavior of the muscle, resulting in speeds and lengths well above those physiologically possible. To overcome this problem, limits have been imposed on the maximum possible speed and the maximum length of the fibers.

Fibers activation Also in this model, the γ s which manages the reaction level of the single fibers are automatically as follows:

$$\gamma_D = \omega \cdot AS(t) \quad (4.38)$$

$$\gamma_S = \omega \cdot AD(t) \quad (4.39)$$

Where ω represents the weight associated with the single fiber, it is generated randomly from a uniform distribution between 0 and 1;

Following [2], the activation levels of the fibers are calculated as follows:

$$f_{dynamic} = \left[1 - \exp\left(\frac{t_{dynamic}}{\tau_{bag1}}\right) \cdot \frac{\gamma_{dynamic}}{\gamma_{dynamic} + freq_{bag1}} \right] \quad (4.40)$$

$$f_{static} = \left[1 - \exp\left(\frac{t_{static}}{\tau_{bag2}}\right) \cdot \frac{\gamma_{static}}{\gamma_{static} + freq_{bag2}} \right] \quad (4.41)$$

Also in this model a check is made to see which fiber Ia and II has the greatest response: the response of the fiber with the lowest response is set to 0.

Once the response is generated, the information is transferred along the afferent path up to the spinal column.

Feedback transport The model simulates the passage along the fibers from the proprioceptive organs to the interneurons and then back into the NM pool.

The number of fibers is user adjustable.

More specifically:

- The Ia fibers enter directly into the MNpool;

- Fibers II enter first the interneuron IIIN then into the MNpool;

- Fibers Ib enter first the interneuron IbIN then into the MNpool.

Each passage through a nerve fiber or an interneuron was simulated as a derivative in time and finally summed as follows:

$$Ia = \frac{dSpindle\ output\ Ia}{dt} \quad (4.42)$$

$$II = \frac{dSpindle\ output\ II}{dt} \quad (4.43)$$

$$Ib = \frac{dGTO\ output\ Ib}{dt} \quad (4.44)$$

$$IIIN_{output} = \frac{dII}{dt} \quad (4.45)$$

$$IbIN_{output} = \frac{dIb}{dt} \quad (4.46)$$

$$Afferents = Ia - IbIN_{output} + IIIN_{output} \quad (4.47)$$

Given the tools used for the calculation, to avoid saturation at still low quantities of afferent fibers, the magnitude of the afferent feedback was limited to 100, changeable by the user, using the scale:

$$Afferent\ Feedback = \frac{Afferents(t) - Afferents_{min}}{Afferents_{max} - Afferents_{min}} \quad (4.48)$$

During the tests done, $Afferents_{max} = 100$ and $Afferents_{min} = 0$. Once the afferent response has been calculated, this is used to modulate the descending command for the new control cycle.

4.3 Tests run with the mdoels

In this section all the tests performed will be explained, the results are visible and will be commented in Chapter 5

4.3.1 Descending run model

We start by testing the descending model for proper functioning.

The tests carried out were:

- Force generation from input signals at different frequencies: with this tests we want to check the correct functioning of the MUs; the inputs used are signals in which the first half of the time series does not contain the sinusoid, the second half contains sinusoids at different frequencies, namely $0Hz$, $5Hz$, $15Hz$ and $20Hz$;
- Force controlled with the PID directly driving the conductance of the MNs without sinusoid modulation: this is done to better compare the effect of sinusoidal input at different frequencies.
- Force controlled with the PID directly driving the conductance of the MNs without the contribution of the afferents: this is done to better compare the results of the two afferent models.

4.3.2 Spindle model

With this tests we want to check the correct functioning of the spindle model for both the full and the simplified model: The tests used are:

- sinusoidal stimuli with frequencies of $5Hz$ and $15Hz$;
- ramp elongation;
- stretch pulse;
- descending ramp;

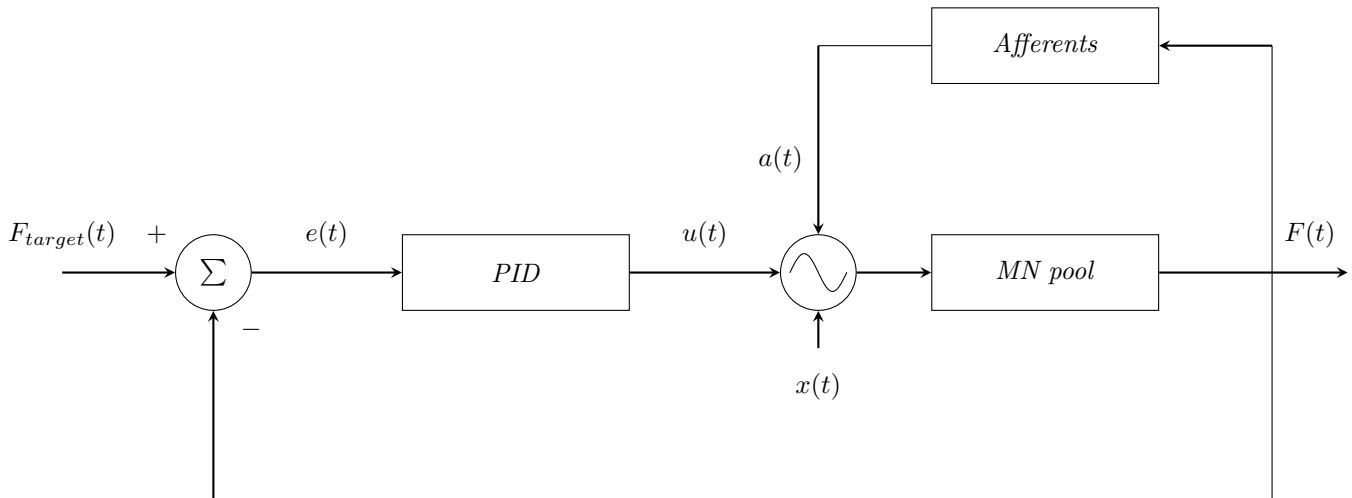
4.3.3 Control cycle structure

The control unit of the model is a PID controller which compares the force generated to the chosen target force and la cui uscita viene usata per modulare il segnale in ingresso alla MN pool.

The control structure can be seen in fig.4.8. The full simulation duration is $10s$, the sampling time is $50ms$, for a total of 200 cycles.

The choice of the sampling time is due to the fact that, for a correct use

Fig. 4.8. Control cycle



Cycle structure: $F_{target}(t)$ represents the target force, $e(t)$ is the error between the target force and the force $F(t)$ generated at each cycle, $x(t)$ is the descending command, $u(t)$ is the output signal of the PID controller, $a(t)$ is the afferent feed-back signal. $u(t)$ and $a(t)$ modulate $x(t)$ and the new signal is used as input of the MN pool for the generation of the force $F(t)$.

of the controller in the analysis of the input signal and in the generation of the correction signal, it is necessary to take the complete cycle of the input signal: in the case of a sinusoidal input at $20Hz$, the cycle is completed every $50ms$.

The input signal is given by the target force the system must reach. The target force is $F_{target}(t) = 210gf$, which represent 10% of the maximal voluntary contraction (MVC) and is expressed in gram-force (gf), defined as the force per unit mass due to gravity at the Earth's surface and representing the standard gravity.

In order to reach the target, a sinusoid, which enters the MN pool, is modulated at each cycle: the sinusoid used for the tests has different frequencies, so to see how these affect the generation of the force, the frequencies suate are again: $0Hz$, $5Hz$, $15Hz$ and $20Hz$.

Cycle At each cycle I have the following steps:

1. target force sampling;
2. modulation of the input sine wave based on the PID output of previous

- cycle;
3. generation of the afferent response based on the force generated in the previous cycle;
 4. combination of the sine wave and afferent feedback as input for the MN pool;
 5. simulation of the MN pool reaction to the new input;
 6. force calculation starting from the generated spikes;
 7. calculation of the error as the difference between the generated force and the target force;
 8. generation of the new amplitude of the input sine wave using the PID.

The way in which point 4 is approached changes between the two models:

- Full model: the responses of the single fibers, together with the sinusoid in input, are inserted separately, each with its own synapse, and separately pass through the respective connectivity matrices;
- Simplified model: the complete response of the afferent circuit is added to the input sinusoid and it is only this sum that enters the MN pool as input.

4.3.4 PID

A Proportional-Integral-Derivative controller (PID controller or three-term controller), is a feed-back control mechanism that continuously calculates an error value $e(t)$ as the difference between a desired setpoint and a measured process variable and applies a correction based on proportional, integral, and derivative terms (denoted \mathbf{P} , \mathbf{I} , and \mathbf{D} respectively), hence the name.

This system continuously calculates an error value $e(t)$ as the difference between the desired setpoint $r(t)$ and a measured process variable $y(t)$:

$$e(t) = r(t) - y(t) \tag{4.49}$$

and applies a correction based on proportional, integral, and derivative terms. The controller attempts to minimize the error over time by adjustment of a control variable $u(t)$ to a new value determined by a weighted sum of the control terms.

- Term **P** is proportional to the current value of the error $e(t)$: if the error is large and positive, the control output will be proportionately large and positive, taking into account the gain factor K ;
- Term **I** accounts for past values of the error $e(t)$ and integrates them over time to produce the I term: if there is a residual error after the application of proportional control, the integral term seeks to eliminate the residual error by adding a control effect due to the historic cumulative value of the error;
- Term **D** is a best estimate of the future trend of the of the error $e(t)$, based on its current rate of change: it seeks to reduce the effect of the error by exerting a control influence generated by the rate of error change. The more rapid the change, the greater the controlling or damping effect.

4.3.5 Tuning

The search for the correct values of the PID's K s is entrusted to a Particle Swarm Optimization (**PSO**) algorithm. A possible tuning method for the PID is to do it manually: first, you set the K_i and K_d values to zero, after which you increase the K value until the loop output oscillates; K_p is usually set to about half this value.

At this point, K_i is increased until any offset is corrected in sufficient time for the process. However, too much K_i will cause instability.

Finally, K_d is increased, if necessary, until the ring is fast enough to reach its reference after a load disturbance. However, too much K_d causes excessive response and overshoot.

In the particular case studied in this thesis, given the high instability and

complexity of the system under consideration, we preferred to use an auto-tuning method that was able to set the Ks at the best possible values.

PSO

The algorithm iteratively tries to improve a candidate solution with regard to a given measure of quality. It solves a problem by having a population of particles, chosen by the user, moving around in the search-space according to the particle's position and velocity. Each particle's movement is influenced by its local best known position, but is also guided toward the best known positions in the search-space, which are updated as better positions are found by other particles.

At each cycle the swarm moves towards the new global minimum and updates the values of the Ks parameters used by the PID:

$$v_k^{t+1} = \omega v_k^{t+1} + \phi_1 \beta_1 (pbest_k^t - x_k^t) + \phi_2 \beta_2 (gbest_k^t - x_k^t) \quad (4.50)$$

for each condition, individually using the linearly decreasing inertia weight approach:

$$\omega = \frac{0.9 - 0.4}{T} t \quad (4.51)$$

introduced by Shi and Eberhart [3].

This was combined with time-varying acceleration coefficients (TVAC):

$$\phi_1 = \frac{2.5 - 0.5}{T} t + 0.5 \quad (4.52)$$

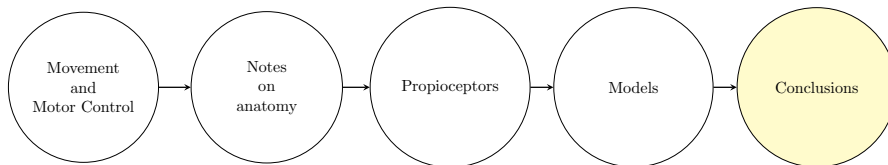
$$\phi_2 = \frac{0.5 - 2.5}{T} t + 2.5 \quad (4.53)$$

It starts with a high ϕ_1 cognitive weight, so it can focus on a local area, then the social weight increases ϕ_2 [4], [5]. β_1 and β_2 represent random numbers which are used in the computation to update the velocity v of each particle, p_{best} (the best position of the particle), g_{best} (the best global position) and to calculate the integral of time-weighted absolute error (ITAE) $e(t)$, which reflect the degree to which absolute error and steady-state error effect performance assessment [6]. The number of particles is defined outside

the function; each particle is represented by a dictionary representing the best position achieved by that particle, its velocity and its current position. The "search area" of the particle is defined by a lower and an upper bound for the positions achievable by the particle. The parameters used for the PSO can be seen in A.5

Chapter 5

Results



In this chapter the results of the tests done in the previous chapter will be analyzed, starting from the descending run model up to the final results.

5.1 Descending model

Fig.5.1 and fig.5.2 show the results of the tests done with the descending model.

Fig.5.2a shows the force generated by the descending run model when the inputs are signals in which the first half of the time series does not contain the sinusoid, the second half contains sinusoids at different frequencies, namely $0Hz$, $5Hz$, $15Hz$ and $20Hz$; this test was done following [7].

This results are perfectly in line with the ones seen in [7] and [8], they shows the nonlinear behavior of the MN pool and how high frequencies actively contributes to the generation of forces.

Fig.5.2b shows the behavior of the model while being controlled by the PID directly driving the conductance of the MNs without any sinusoid modulation.

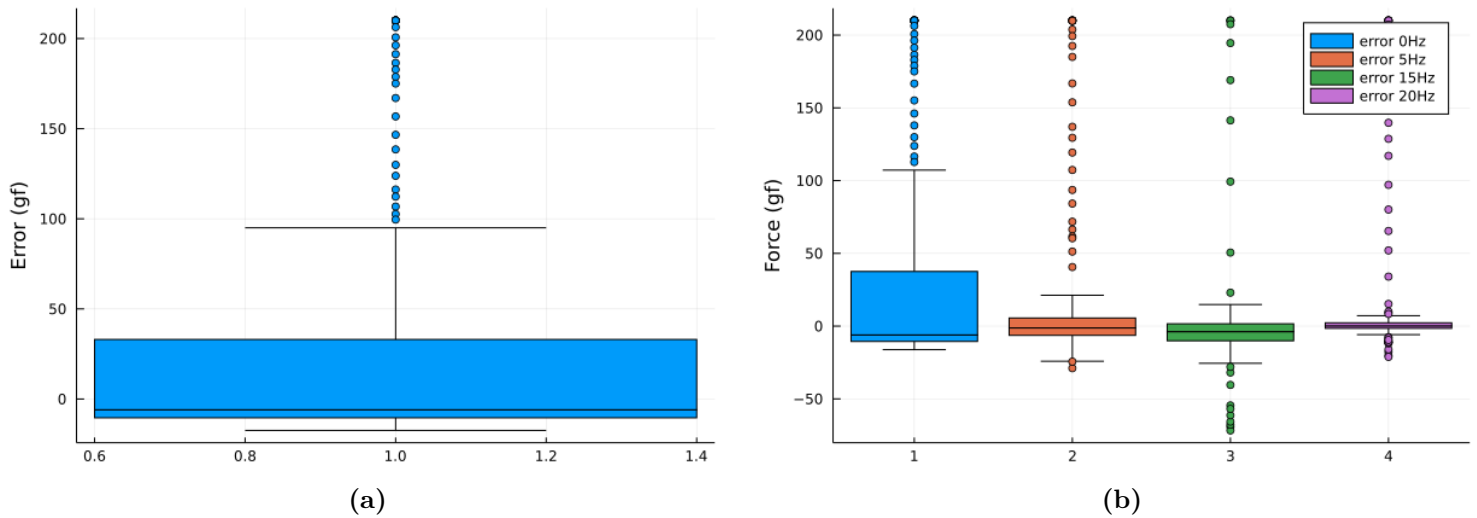


Fig. 5.1. Average model error when no afferent inputs are used

Boxplots of the average errors of the descending run model: **a)** Average errors of the model while being controlled by the PID directly driving the conductance of the MNs without any sinusoid modulation, at different values of the K_s parameters; **b)** Average errors of the model while being controlled by the PID directly driving the conductance of the MNs, without the contribution of the afferents, with a sinusoid at different frequencies, namely $0Hz$, $5Hz$, $15Hz$ and $20Hz$.

Fig.5.2c shows the behavior of the model while being controlled by the PID directly driving the conductance of the MNs, without the contribution of the afferents, with a sinusoid at different frequencies, namely $0Hz$, $5Hz$, $15Hz$ and $20Hz$.

These results are important to see how the control circuit behaves with and without the presence of the contribution of the afferents. The results show that in both control cases, with and without the presence of a signal modulated by the PID, the system exhibits different behaviors in the initial part of the transient, according to which frequency of the signal, PID modulation case, and which K_s parameters were used: what is most striking is the initial part of the rise, for different K_s there are different rise times, higher in the case of K_s found at $0Hz$, lower in the case of K_s found at $15Hz$; what is noticed is also the overshoot, very large in the case of $15Hz$, which could lead to instabilities and yet manages to become stable right after it, much lower in the other cases. In all the cases examined, however, the steady state

value is quickly reached and the signal remains stable at all the frequencies analyzed.

Fig.5.1 shows the boxplot of the average errors for this two cases.

Given this results, the Ks parameters which lead to the minimum average error, for this model, will be used every time the input input signal is at 0Hz, no modulation, during the next tests with afferents.

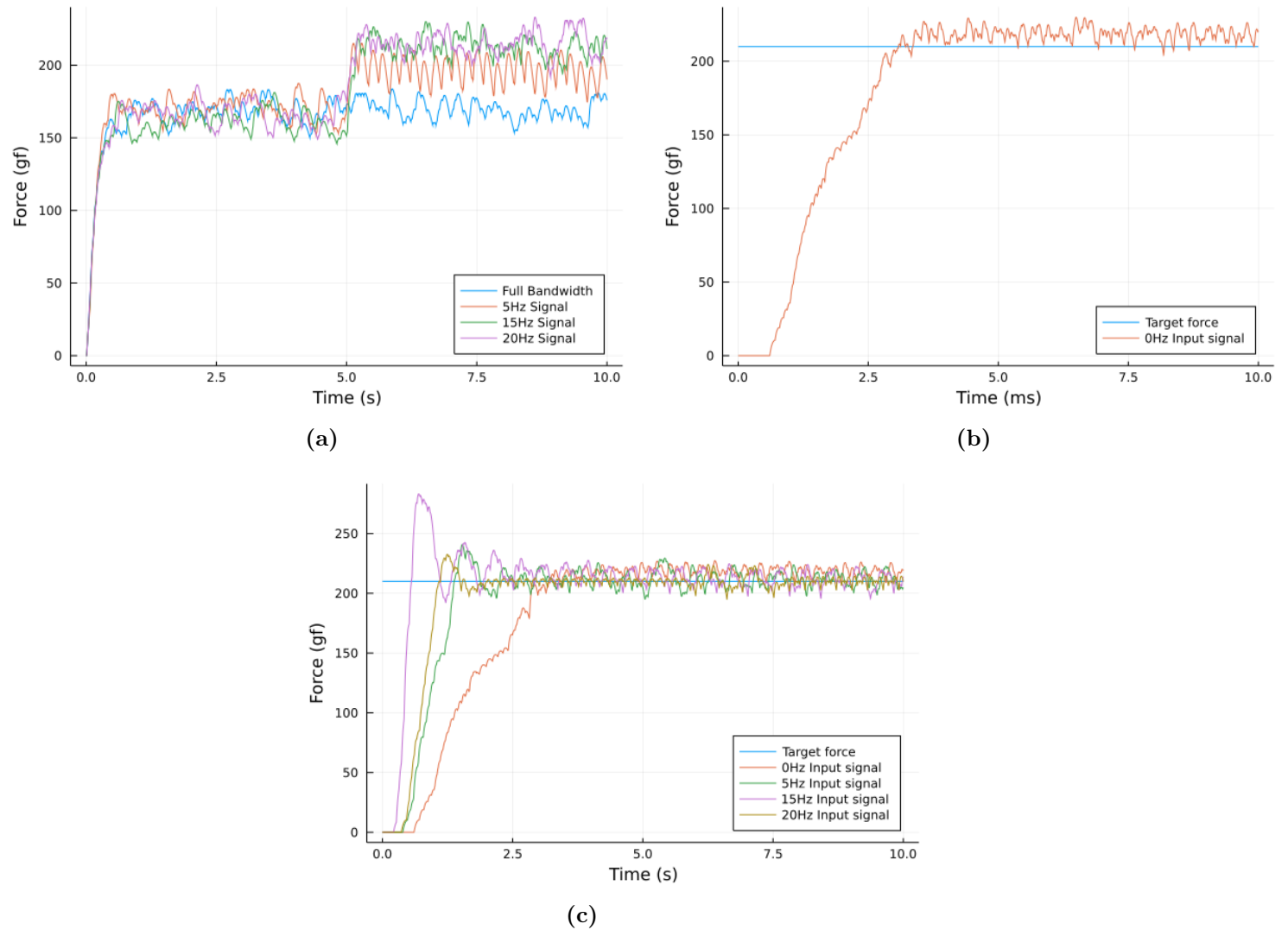


Fig. 5.2. Descending model test results

Results for different tests on the descending run model: **a)** Force generated by the descending run model when the inputs are signals in which the first half of the time series does not contain the sinusoid, the second half contains sinusoids at different frequencies, namely $0Hz$, $5Hz$, $15Hz$ and $20Hz$; **b)** Behavior of the model while being controlled by the PID directly driving the conductance of the MNs without any sinusoid modulation; **c)** Behavior of the model while being controlled by the PID directly driving the conductance of the MNs, without the contribution of the afferents, with a sinusoid at different frequencies, namely $0Hz$, $5Hz$, $15Hz$ and $20Hz$.

5.2 Afferent model analysis

5.2.1 Full spindle model results

Fig.5.4 shows the results of the tests done for the complete muscle spindle model. The results show that the spindle model responds better to certain stimuli than to others, especially as regards the Ia fibers.

Following the idea that an increase in force corresponds to an increase in the contraction of the fibers, while a decrease would correspond to an elongation, the figure shows how the fibers Ia are able to follow both the ramps and the sinusoidal inputs at different frequencies.

This is a very good result given the nature of the quantities with which this response is being calculated: in this case what is taken into consideration is the force $F(t)$ from which the parameters that we need are calculated backwards.

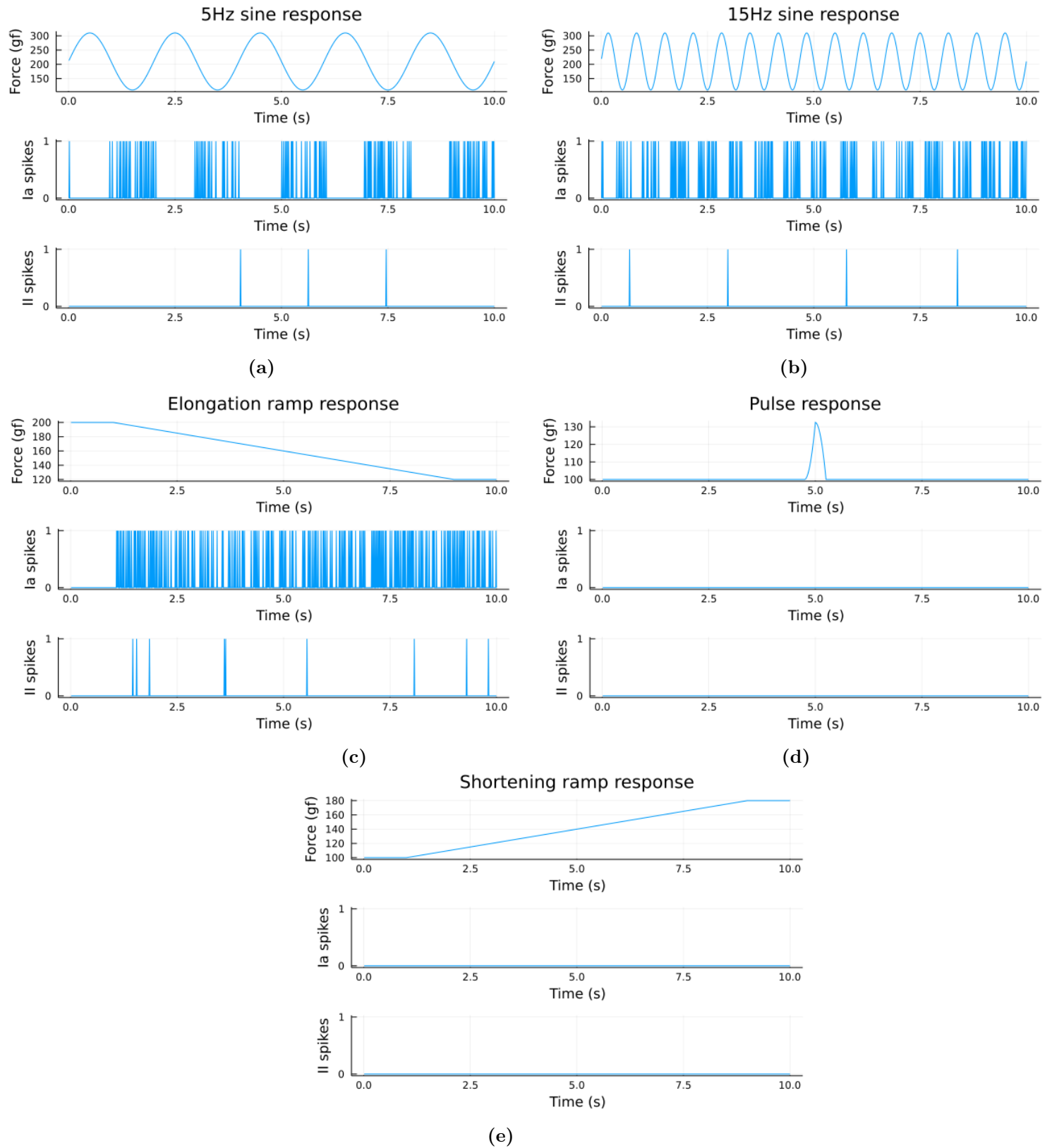


Fig. 5.3. Full spindle model behavior

Behavior of the full spindle model for: **(a)** Sinusoidal stimulus at $5Hz$, **(b)** Sinusoidal stimulus at $15Hz$, **(c)** Ramp down, **(d)** Stretch pulse, **(e)** Ramp up

Analysis of the spindle reaction of to high frequency stimuli It should be noted that the ability to respond to different inputs depends on the frequency with which the oscillations occur, if too high, therefore too narrow, the model is not able to follow them adequately: this is physiologically realistic with what happens in the muscle.

The cause of this is the use of the time window to analyze the force response. If the peaks are too close together, the response of the fibers is so high that it saturates: the time available to the spindle is limited to $50ms$ and each pulse lasts $1ms$ with a subsequent wait of $1ms$. As the elongation increases the response of the fiber increases, therefore the generation of peaks increases, but if the peaks of the sine wave are within the $2ms$ already used by a spike, that peak is lost and the possibility of a response becomes more sparse precisely because immediately after the peak there is a rise in force, corresponding to a contraction, which results in a decrease in the response of the fiber.

Fibers II, on the other hand, are unable to follow the trend of the force in the same way as fibers Ia, this is an expected result of this model, in fact the action of fibers II is very limited by the presence of Ia, as explained for both models, due to the non linearity of the spindle, when the response of Ia is higher than that of II, the response of the latter is reset to 0 and vice versa.

Limitations From these results it can be said that, given the function that the spindle has in the control cycle, the major limit that the model has is the time window to which it is bound, resulting in the lack of firing at constant force values, due to the lack of memory of the "resting" length of the fibers, and a poorer response for high frequency inputs. Added to this, is the problem of the complexity of the model: it is necessary to set all the various components and variables of a structure that is still widely studied and the results still are not able to follow properly what should happen, generally speaking, inside this complex circuit of different types of fibers.

5.2.2 Simplified spindle model results

For a matter of comparison between the two models, here is reported the response of the fibers Ia and II of the simplified model, subjected to the same tests as in the previous case. In fig.5.6 you can see the results.

In this case the answer is much more generic and what is obtained is a generic activation in view of the contraction.

Results In fig.5.6 is shown the total action of the afferents of the simplified model, that is what arrives at the input of the MN pool and which modifies the descending command.

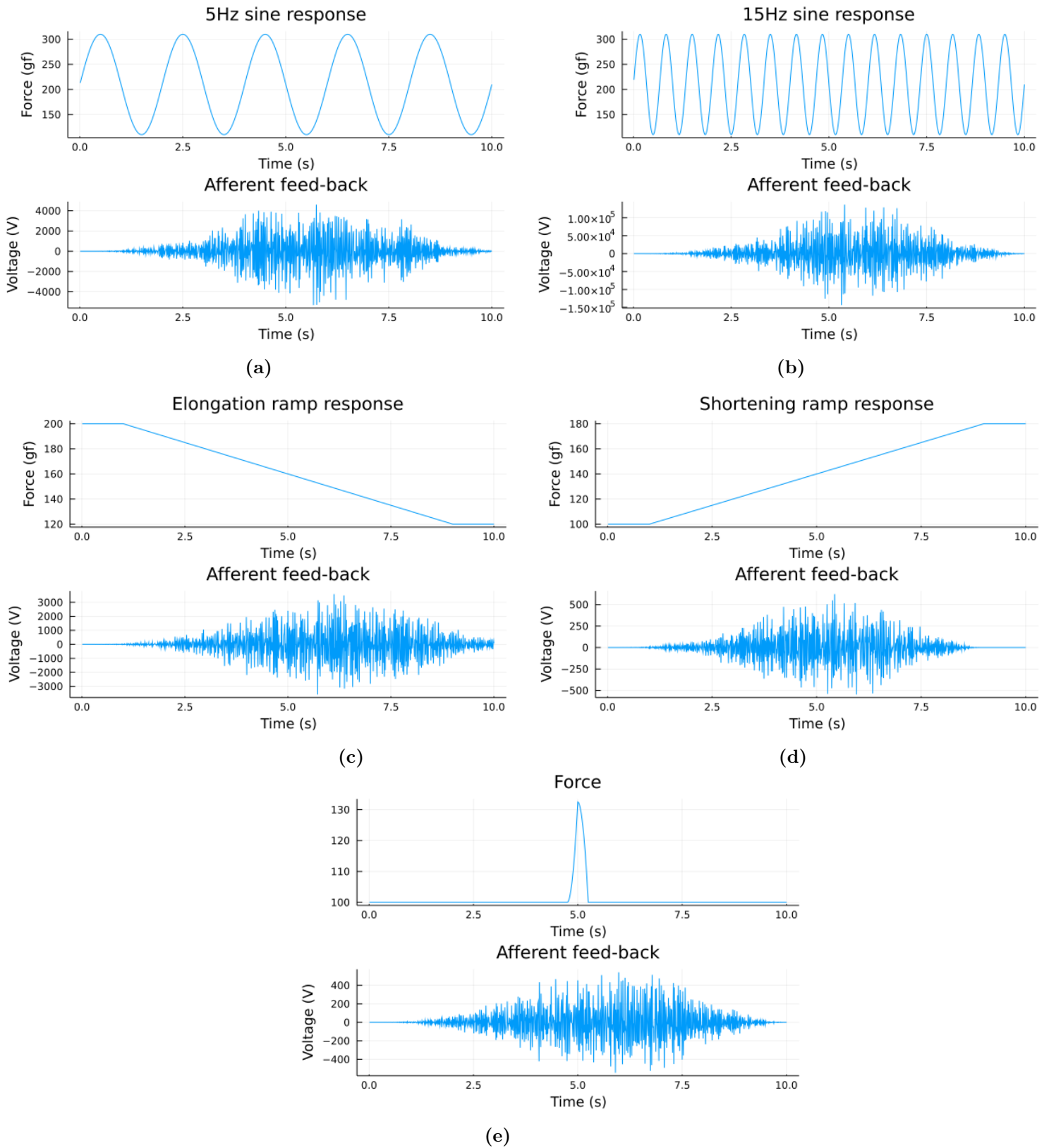


Fig. 5.4. Full spindle model behavior

Behavior of the full spindle model for: (a) Sinusoidal stimulus at $5Hz$, (b) Sinusoidal stimulus at $15Hz$, (c) Ramp down, (d) Stretch pulse, (e) Ramp up.

For each panel the force trace and the voltage (V) generated by the afferents are shown.

Full and simple model afferent feed-back comparison

The action of the afferents, as explained in Chapter 4, is given by the sum of the three afferents according to the formula:

$$\text{Afferent feed-back} = I_a + IIIIN - IbIN$$

Where the action of IbIN is calculated by the GTO whose behavior, in the model, is equal and opposite to that of the Ia fibers, remember that when the muscle stretches the tendon fibers relax, vice versa when the muscle contracts the fibers tendon stretch; the negative values of the afferents are given precisely by the contribution of this factor.

Fig.5.5 shows the total afferent feedback from the full model, while fig.5.6 shows the total afferent feedback from the simplified model.

The tests used are again those listed above.

The results show how the complete model remains very close, even too much, to the single outputs of the spindle of the GTO, it is not able to simulate the whole complex set of contributions intended for the excitation/inhibition of the muscle fibers.

The simplified model, on the other hand, as already mentioned before, manages to give a good representation of the "essence" of the afferent feedback in the motor neuron loop.

For this reason the final tests will be covered using only the simplified control model.

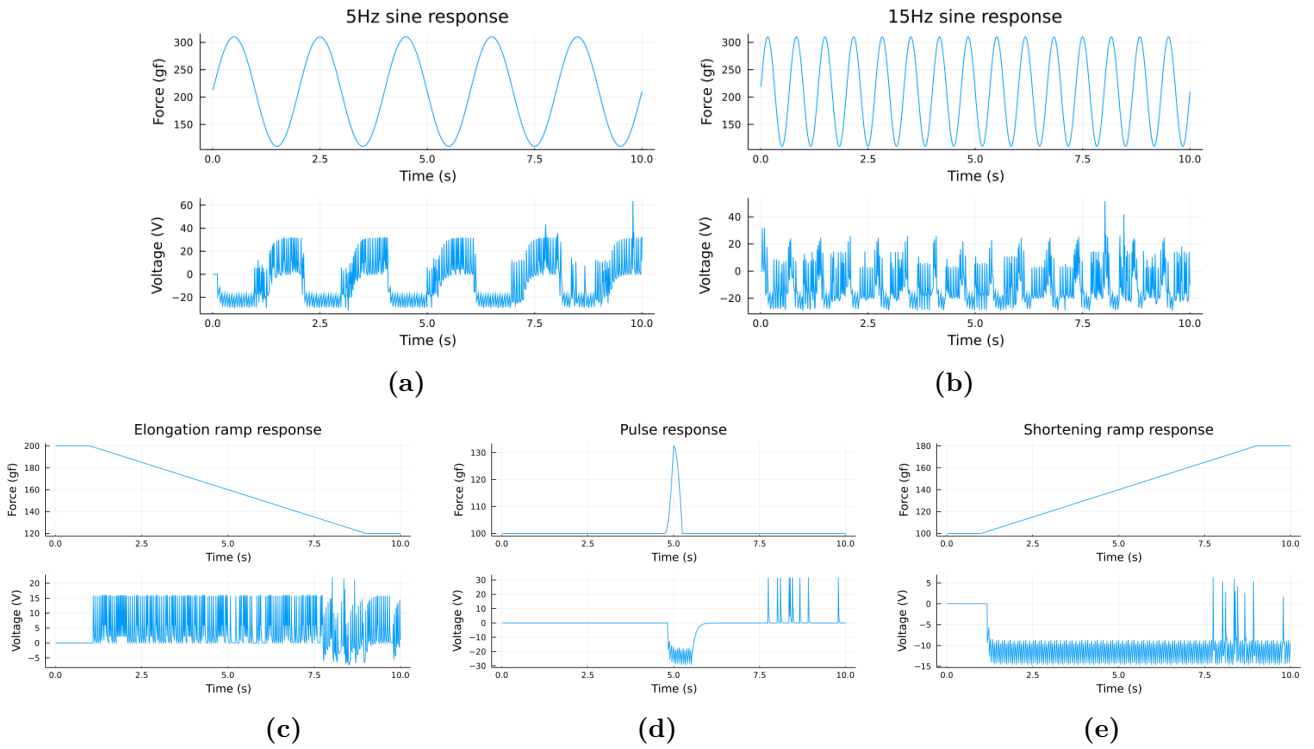


Fig. 5.5. Full spindle model afferent feed-back

Complete afferent feed-back of the full spindle model for: (a) Sinusoidal stimulus at $5Hz$, (b) Sinusoidal stimulus at $15Hz$, (c) Ramp down, (d) Stretch pulse, (e) Ramp up. For each panel the force trace and the voltage (V) generated by the afferents are shown.

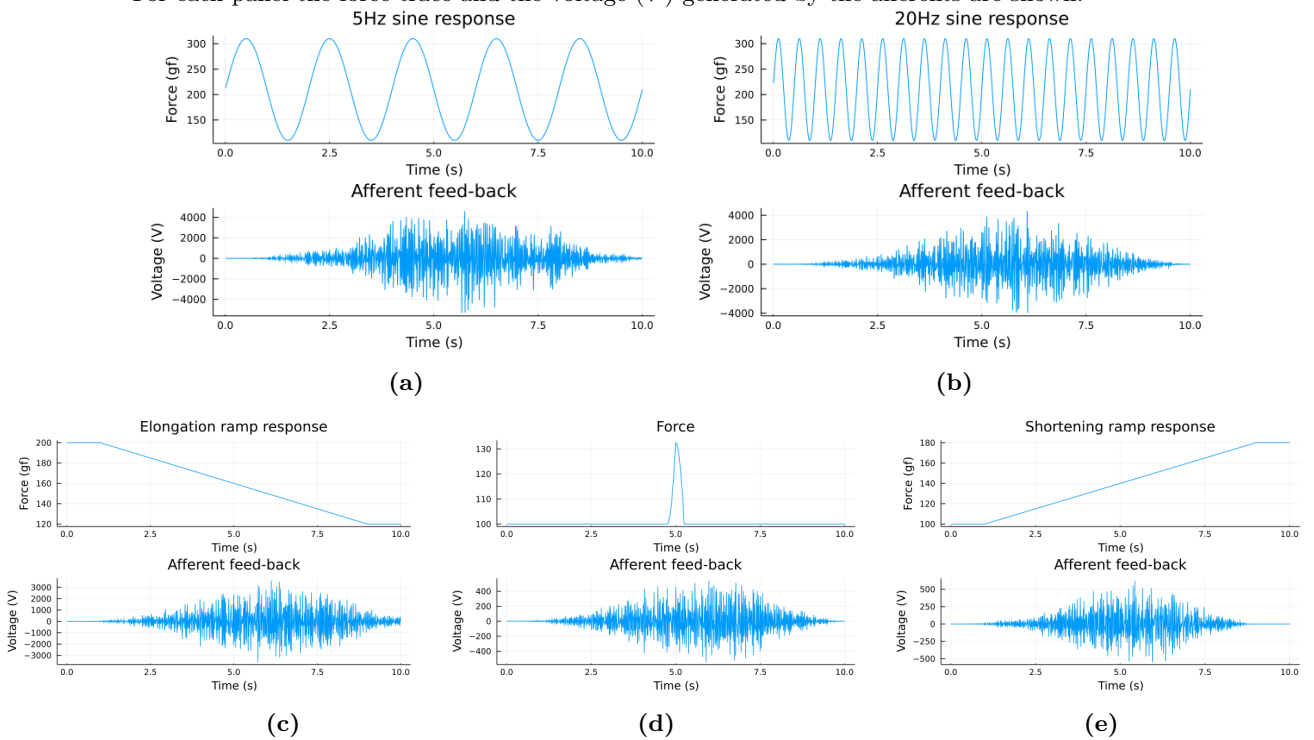


Fig. 5.6. Simplified model afferent feed-back

Complete afferent feed-back of the simplified model for: (a) Sinusoidal stimulus at $5Hz$, (b) Sinusoidal stimulus at $15Hz$, (c) Ramp down, (d) Stretch pulse, (e) Ramp up. For each panel the force trace and the voltage (V) generated by the afferents are shown.

5.3 Results of the simplified afferent feed-back model tests

First, a low frequency test is done, frequency 0 so without modulation; the test is done in order to:

- see how the model behaves with respect to when the afferents were not present;
- how many afferent fibers can be used before the model loses control;
- whether the number of fibers used is plausible with reality.

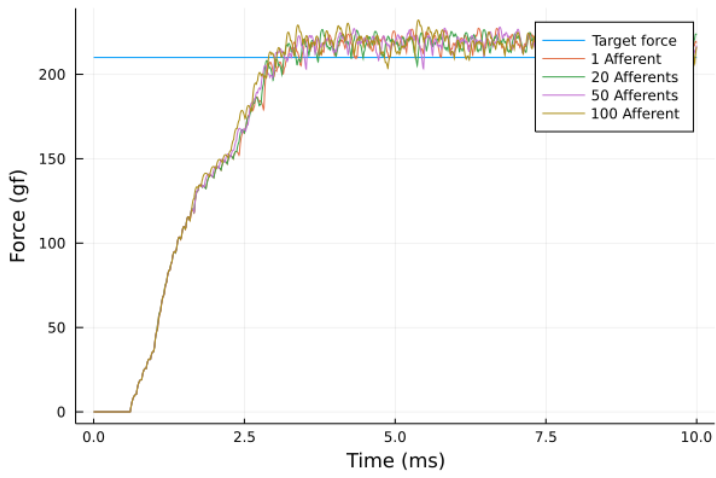
From the fig.5.7a we can see how the model is very stable up to the use of 100 afferent fibers, while at 150 the saturated force entering into tetanic contraction.

Fig.5.7b shows the boxplots of the average errors for this test: also from here, it can be seen from an error point of view how this increases dramatically when more than 100 fibers are used.

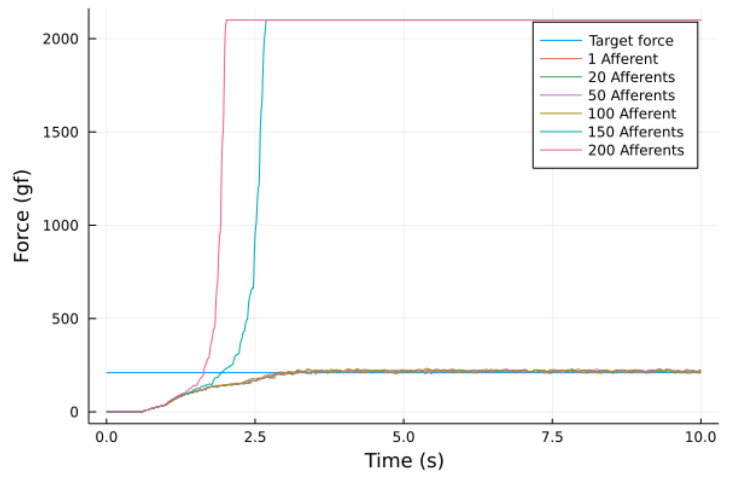
In the studies done on real patients muscle spindles, [14] - [15], on the tibialis anterior muscle and the foot, there were recordings from a number of afferent fibers that varied between 12 and 26.

The model is able to control up to 100 fibers which means it is able to be used in studies with a more realistic number of fibers.

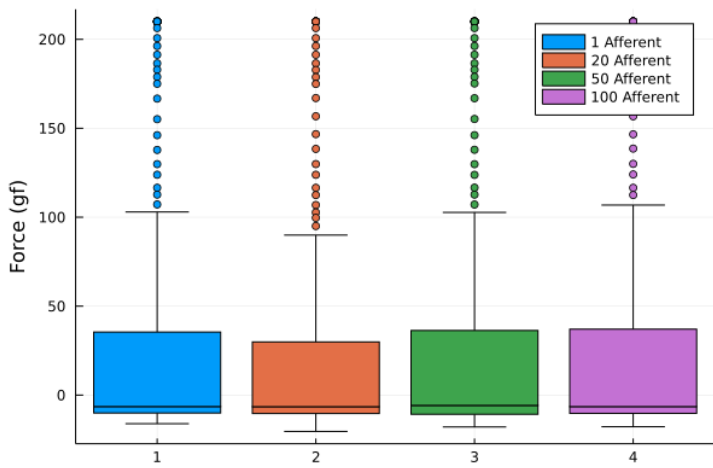
The subsequent tests will then be carried out with a maximum number of fibers equal to 100 and with input signals to the MN pool modulated by the PID at different frequencies.



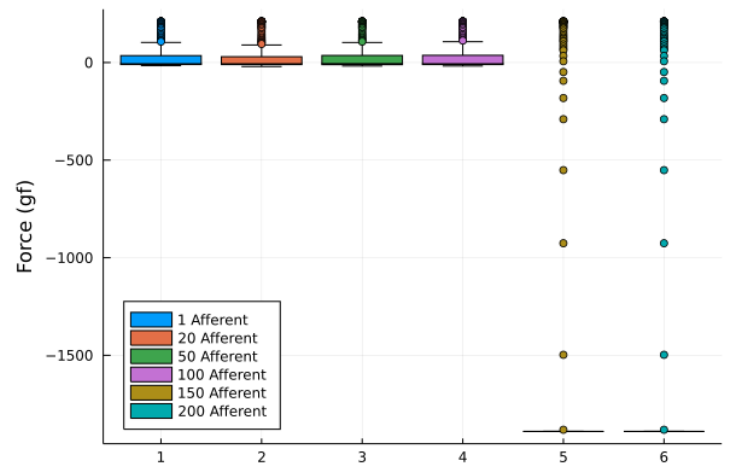
(a)



(b)



(c)



(d)

Fig. 5.7. Simplified afferent feed-back model test results at 0Hz

Results for the simplified afferent feed-back model when the input signal is modulated by the PID with frequency equal to 0Hz, no modulation, with different numbers of afferent fibers: **a)** Number of afferent fibers used up to 100; **b)** Number of afferent fibers used up to 200; **c - d)** Average errors of the model with using different numbers of fibers.

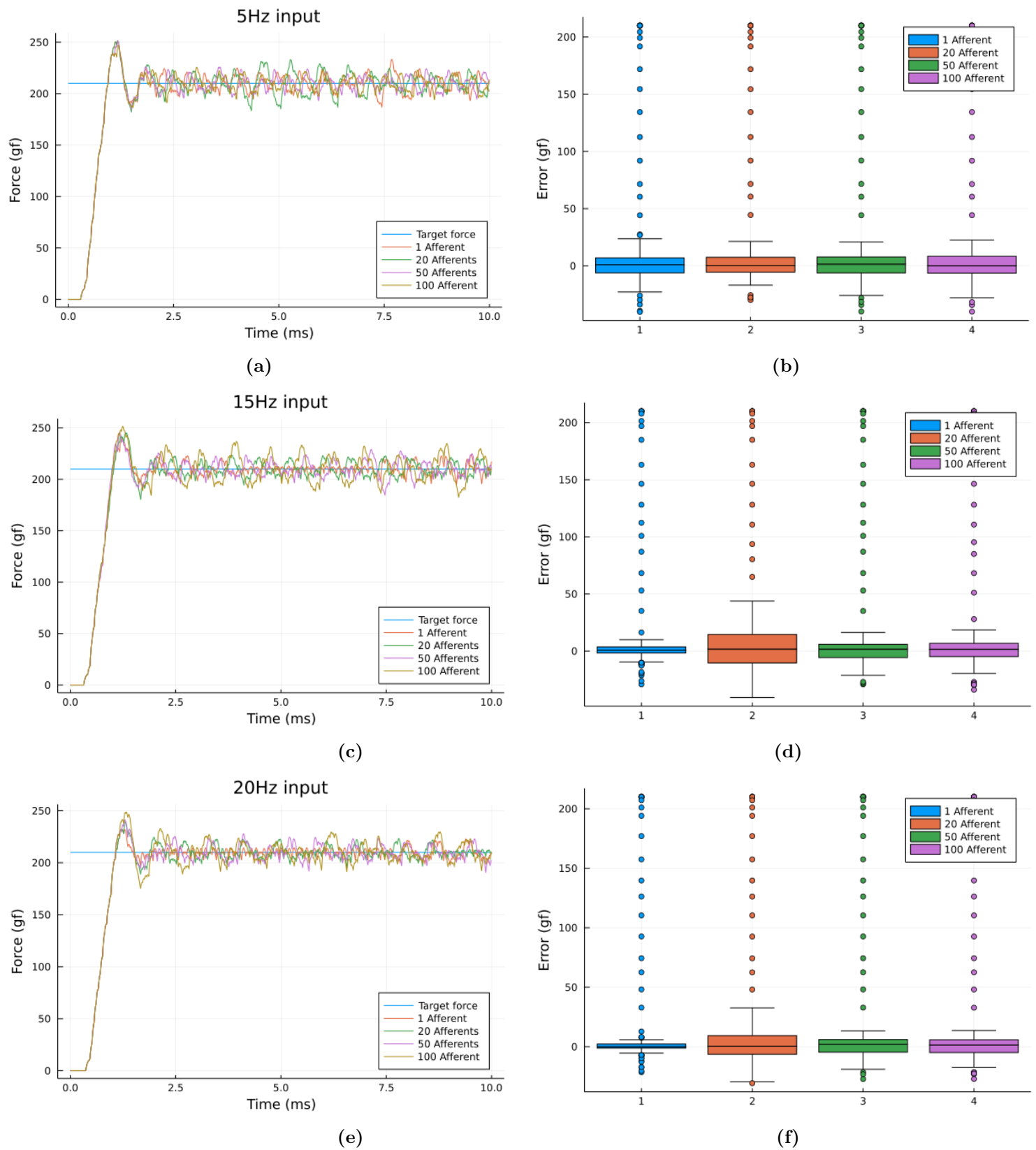


Fig. 5.8. Simplified afferent feed-back model test results at $0Hz$

Results for the simplified afferent feed-back model when the input signal is modulated by the PID with different frequencies: **a - b**) input signal modulated at a frequency equal to $5Hz$, with different numbers of afferent fibers and boxplots of the average errors; **c - d**) input signal modulated at a frequency equal to $15Hz$, with different numbers of afferent fibers and boxplots of the average errors; **e - f**) input signal modulated at a frequency equal to $20Hz$, with different numbers of afferent fibers and boxplots of the average errors;

Results Fig.5.8 shows the results of the tests made with the model, when in input it has a signal modulated by the PID at frequencies 5, 15 and 20.

5.4 Conclusions

The goal of the thesis was to build two possible models for afferent feedback in motor control and compare them to see which of the two best suited the study of the contribution of high frequencies in motor control.

The results obtained show how the complete model tries to play its role but is limited by the above problems.

On the contrary, the simplified model, although much more generic in its function, is able to perfectly follow the control command, adapting to the force generated at all the frequencies considered.

Comparing the boxplots of fig.5.8 with the one of fig.5.7, in which the input signal to the MN pool is not modulated, it is also noted how the presence of the modulation, at whatever frequency it is, decreases the average error.

Following are some tests that test the model used as it tries to follow different force traces to see if it is able to follow them or it becomes unstable.

Fig.5.9 shows how the model remains stable even for different force traces; the model presents delays and strong fluctuations in the critical points, these mainly due to the problem of the time window mentioned above and from which the simplified model also suffers.

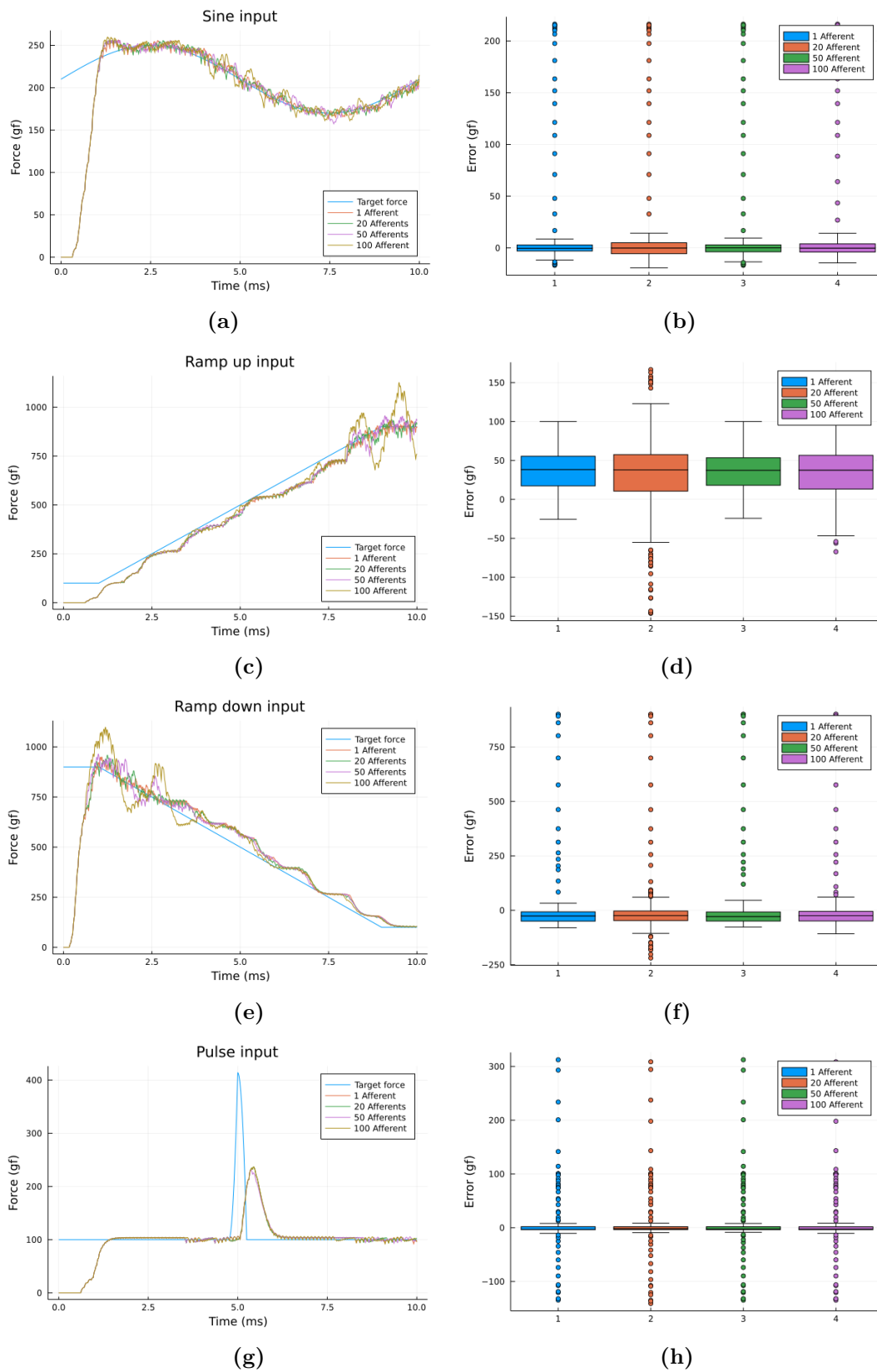


Fig. 5.9. Simplified afferent feed-back model test results with different force traces

Results for the simplified afferent feed-back model during different force traces: **a - b)** sinusoidal target force modulated at a frequency equal to 0.1Hz , with different numbers of afferent fibers and boxplots of the average errors; **c - d)** Ramp up target force, with different numbers of afferent fibers and boxplots of the average errors; **e - f)** Ramp down target force, with different numbers of afferent fibers and boxplots of the average errors; **g - h)** Pulse target force, with different numbers of afferent fibers and boxplots of the average errors;

Appendix A

Appendix A

A.1 Motor neurons parameters

Number of S type fibers = Number of FR type fibers = Number of FF type fibers = Excitatory synaptic opening rate = $2 \frac{1}{ms}$ Excitatory synaptic closing rate = $1 \frac{1}{ms}$ Inhibitory synaptic opening rate = $0.5 \frac{1}{ms}$ Inhibitory synaptic closing rate = $0.1 \frac{1}{ms}$

A.1.1 S-type

$$A_{peak} = [10.50, 12.50] \text{ gf}$$

$$t_{peak} = [100.0, 110.0] \text{ ms}$$

$$Tetanic = [40.0, 50.0] \text{ gf}$$

$$g_{Na} = [5.7, 6.4] \mu s$$

$$g_{Kf} = [0.8, 0.9] \mu s$$

$$r_s = [0.00388, 0.00413] \text{ cm}$$

$$l_s = [0.00775, 0.00825] \text{ cm}$$

$$r_d = [0.0021, 0.00312] \text{ cm}$$

$$l_d = [0.55, 0.68] \text{ cm}$$

$$Rm_s = [1.05, 1.15] \text{ K}\Omega \cdot \text{cm}^2$$

$$Rm_d = [10.7, 14.4] \text{ } K\Omega \cdot \text{cm}^2$$

$$I_{rh} = [3.5, 6.5] \text{ } nA$$

A.1.2 FR-type

$$A_{peak} = [12.50, 30.00] \text{ } gf$$

$$t_{peak} = [55.5, 73.5] \text{ } ms$$

$$Tetanic = [50.0, 120.0] \text{ } gf$$

$$g_{Na} = [6.4, 7.2] \text{ } \mu s$$

$$g_{Kf} = [0.5, 0.9] \text{ } \mu s$$

$$r_s = [0.00412, 0.00438] \text{ } cm$$

$$l_s = [0.00825, 0.00875] \text{ } cm$$

$$r_d = [0.00312, 0.00418] \text{ } cm$$

$$l_d = [0.68, 0.81] \text{ } cm$$

$$Rm_s = [0.95, 1.05] \text{ } K\Omega \cdot \text{cm}^2$$

$$Rm_d = [6.95, 10.7] \text{ } K\Omega \cdot \text{cm}^2$$

$$I_{rh} = [6.5, 17.5] \text{ } nA$$

A.1.3 FF-type

$$A_{peak} = [30.00, 50.00] \text{ } gf$$

$$t_{peak} = [56.9, 82.3] \text{ } ms$$

$$Tetanic = [120.0, 200.0] \text{ } gf$$

$$g_{Na} = [3.6, 6.0] \text{ } \mu s$$

$$g_{Kf} = [0.1, 0.3] \text{ } \mu s$$

$$r_s = [0.00438, 0.00568] \text{ } cm$$

$$l_s = [0.00875, 0.01135] \text{ } cm$$

$$r_d = [0.00418, 0.00463] \text{ cm}$$

$$l_d = [0.81, 1.06] \text{ cm}$$

$$Rm_s = [0.65, 0.95] \text{ K}\Omega \cdot \text{cm}^2$$

$$Rm_d = [6.05, 6.95] \text{ K}\Omega \cdot \text{cm}^2$$

$$I_{rh} = [17.5, 25.1] \text{ nA}$$

A.2 Afferent fibers parameters

A.2.1 Ia-type

$$g_{Na} = [5.7, 6.4] \mu\text{s}$$

$$g_{Kf} = [0.8, 0.9] \mu\text{s}$$

$$r_s = [0.00388, 0.00413] \text{ cm}$$

$$l_s = [0.00775, 0.00825] \text{ cm}$$

$$r_d = [0.0021, 0.00312] \text{ cm}$$

$$l_d = [0.55, 0.68] \text{ cm}$$

$$Rm_s = [1.05, 1.15] \text{ K}\Omega \cdot \text{cm}^2$$

$$Rm_d = [10.7, 14.4] \text{ K}\Omega \cdot \text{cm}^2$$

$$I_{rh} = 1 \text{ nA}$$

A.2.2 II-type

$$g_{Na} = [5.7, 6.4] \mu\text{s}$$

$$g_{Kf} = [0.8, 0.9] \mu\text{s}$$

$$r_s = [0.00388, 0.00413] \text{ cm}$$

$$l_s = [0.00775, 0.00825] \text{ cm}$$

$$r_d = [0.0021, 0.00312] \text{ cm}$$

$$l_d = [0.55, 0.68] \text{ cm}$$

$$Rm_s = [1.05, 1.15] \text{ K}\Omega \cdot \text{cm}^2$$

$$Rm_d = [10.7, 14.4] \text{ K}\Omega \cdot \text{cm}^2$$

$$I_{rh} = 1 \text{ nA}$$

A.2.3 Ib-type

$$g_{Na} = [5.7, 6.4] \mu\text{s}$$

$$g_{Kf} = [0.8, 0.9] \mu\text{s}$$

$$r_s = [0.00388, 0.00413] \text{ cm}$$

$$l_s = [0.00775, 0.00825] \text{ cm}$$

$$r_d = [0.0021, 0.00312] \text{ cm}$$

$$l_d = [0.55, 0.68] \text{ cm}$$

$$Rm_s = [1.05, 1.15] \text{ K}\Omega \cdot \text{cm}^2$$

$$Rm_d = [10.7, 14.4] \text{ K}\Omega \cdot \text{cm}^2$$

$$I_{rh} = 1 \text{ nA}$$

A.3 Interneurons parameters

A.3.1 IIIN-type

$$g_{Na} = [5.7, 6.4] \mu\text{s}$$

$$g_{Kf} = [0.8, 0.9] \mu\text{s}$$

$$r_s = [0.00388, 0.00413] \text{ cm}$$

$$l_s = [0.00775, 0.00825] \text{ cm}$$

$$r_d = [0.0021, 0.00312] \text{ cm}$$

$$l_d = [0.55, 0.68] \text{ cm}$$

$$Rm_s = [1.05, 1.15] K\Omega \cdot cm^2$$

$$Rm_d = [10.7, 14.4] K\Omega \cdot cm^2$$

$$I_{rh} = [0.80, 0.81] nA$$

A.3.2 IbIN-type

$$g_{Na} = [5.7, 6.4] \mu s$$

$$g_{Kf} = [0.8, 0.9] \mu s$$

$$r_s = [0.00388, 0.00413] cm$$

$$l_s = [0.00775, 0.00825] cm$$

$$r_d = [0.0021, 0.00312] cm$$

$$l_d = [0.55, 0.68] cm$$

$$Rm_s = [1.05, 1.15] K\Omega \cdot cm^2$$

$$Rm_d = [10.7, 14.4] K\Omega \cdot cm^2$$

$$I_{rh} = [0.80, 0.81] nA$$

A.4 PID Ks paramters

A.4.1 Descending model

$$\text{Full band} = [0.000766813, 6.82018e - 6, 7.79695e - 5]$$

$$\text{Cut-off frequency at } 5Hz = [0.0010539, 1.5e - 9, 7.60907e - 5]$$

$$\text{Cut-off frequency at } 15Hz = [0.00216939, 2.67121e - 9, 1.85938e - 5]$$

$$\text{Cut-off frequency at } 20Hz = [0.00127122, 8.87367e - 8, 9.79138e - 5]$$

A.4.2 Full afferent model

$$\text{full afferent model full band} = [0.000448678, 1.5e - 9, 2.42776e - 6]$$

$$\text{Cut-off frequency at } 5Hz = [0.000703866, 1.5e - 9, 4.79114e - 5]$$

$$\text{Cut-off frequency at } 15Hz = [0.00301316, 4.66734e - 6, 1.31137e - 5]$$

$$\text{Cut-off frequency at } 20Hz = [0.00145949, 1.5e - 9, 9.93976e - 5]$$

A.4.3 Simplified afferent model

simplified afferent model full band = $[0.00112588, 1.5e - 9, 0.0001]$

Cut-off frequency at $5Hz$ = $[1.0e - 6, 1.5e - 9, 0.0001]$

Cut-off frequency at $15Hz$ = $[1.0e - 6, 1.5e - 9, 1.0e - 8]$

Cut-off frequency at $20Hz$ = $[0.000126537, 5.18358e - 6, 0.0001]$

A.5 PSO parameters

Number of particles = 20

Number of particles = 10

Lower bound = previous best position $\cdot 0.01$

Upper bound = previous best position $\cdot 100$

Bibliography

- [1] M. R. Traub RD, Wong RK and M. H., “A model of a ca3 hippocampal pyramidal neuron incorporating voltage-clamp data on intrinsic conductances,” *J Neurophysiol.*, vol. 66, no. 2, pp. 635–650, 1991.
- [2] L. N. Mileusnic MP, Brown IE and L. GE., “Mathematical models of proprioceptors. i. control and transduction in the muscle spindle,” *J Neurophysiol.*, vol. 96, no. 4, pp. 1772–1788, 2006.
- [3] Y. Shi and R. Eberhart, “Empirical study of particle swarm optimization,” *Proceedings of the 1999 Congress on Evolutionary Computation-CEC99 (Cat. No. 99TH8406)*, vol. 3, no. , pp. 1945–1950, 1999.
- [4] S. K. P. Praveen Kumar Tripathi, Sanghamitra Bandyopadhyay, “Multi-objective particle swarm optimization with time variant inertia and acceleration coefficients,” *Information Sciences*, vol. 177, no. 22, pp. 5033–5049, 2007.
- [5] S. M. . L. B. Pornsing, C., “Novel self-adaptive particle swarm optimization methods,” *Soft Comput*, vol. 20, no. , pp. 3579–3593, 2016.
- [6] A. E. A. Awouda and R. B. Mamat, “Refine pid tuning rule using itae criteria,” *2010 The 2nd International Conference on Computer and Automation Engineering (ICCAE)*, vol. 5, no. , pp. 171–176, 2010.
- [7] R. N. Watanabe and A. F. Kohn, “Fast oscillatory commands from the motor cortex can be decoded by the spinal cord for force control,” *J Neurosci.*, vol. 35, no. 40, pp. 13 687–13 697, 2015.

- [8] R. R. L. Cisi and A. F. Kohn, "Simulation system of spinal cord motor nuclei and associated nerves and muscles, in a web-based architecture," *J Comput Neurosci*, vol. 25, no. 3, pp. 520–542, 2008.
- [9] C. Frigo, *BIOINGEGNERIA DEL SISTEMA MOTORIO*. Aracnee (24 luglio 2018), 2018.
- [10] Eric R. Kandel, James H. Schwartz and Thomas M. Jessell, *Principles of Neural Science (third edition)*. Appleton Lange; 3rd edition (1 october 1992), 1992.
- [11] Z. F. M. F. M. Alain Destexhe and T. Sejnowski, "An efficient method for computing synaptic conductances based on a kinetic model of receptor binding," *Neural Computation*, vol. 6, no. 1, pp. 14–18, 1994.
- [12] K. H., "Impact of the localization of dendritic calcium persistent inward current on the input-output properties of spinal motoneuron pool: a computational study," *J Appl Physiol (1985)*, vol. 123, no. 5, pp. 1166–1187, 2017.
- [13] Cisi and Kohn, "Remoto - remote motoneuron network simulator." [Online]. Available: <http://remoto.leb.usp.br/remoto/index.html>
- [14] B. I. M. V. Day J, Bent LR and C. AG., "Muscle spindles in human tibialis anterior encode muscle fascicle length changes," *J Neurophysiol.*, vol. 117, no. 4, pp. 1489–1498, 2017.
- [15] H. E. Knellwolf TP, Burton AR and M. VG., "Firing properties of muscle spindles supplying the intrinsic foot muscles of humans in unloaded and freestanding conditions," *J Neurophysiol.*, vol. 121, no. 1, pp. 74–84, 2019.
- [16] R. N. W. Leonardo Abdala Elias and A. F. Kohn, "Spinal mechanisms may provide a combination of intermittent and continuous control of human posture: predictions from a biologically based neuromusculoskeletal model," *PLoS Comput Biol.*, vol. 10, no. 11, p. e1003944, 2014.
- [17] W. ER and B. SN, "Circuits generating corticomuscular coherence investigated using a biophysically based computational model. i. descending systems," *J Neurophysiol.*, vol. 101, no. 1, pp. 31–41, 2009.

-
- [18] F. Negro and D. Farina, “Decorrelation of cortical inputs and motoneuron output,” *J Neurophysiol.*, vol. 106, no. 5, pp. 2688–2697, 2011.
- [19] L. A. E. V. M. C. E. M. M. Renato N Watanabe, Fernando H Magalhães and A. F. Kohn, “Influences of premotoneuronal command statistics on the scaling of motor output variability during isometric plantar flexion,” *J Neurophysiol.*, vol. 110, no. 11, pp. 2592–2606, 2013.
- [20] H. A. I. J. G. V. R. J. B.-L. J. P. J. Gallego JA, Dideriksen JL and F. D. Rocon E, “The phase difference between neural drives to antagonist muscles in essential tremor is associated with the relative strength of supraspinal and afferent input. j neurosci,” *J Neurosci.*, vol. 35, no. 23, pp. 8925–8937, 2015.